



Particle Measurement Programme (PMP) Heavy-Duty (HD) Inter-laboratory Exercise

Exploratory work at JRC (Oct'07 – Feb'08)

B. Giechaskiel, S. Alessandrini, F. Forni, P. Martinez-Lozano, D. Lesueur,
M. Carriero, G. Martini

Transport and Air Quality Unit, Institute for Environment and Sustainability
European Commission Joint Research Centre, Ispra

EUR 23426 EN - 2008

The mission of the Institute for Environment and Sustainability is to provide scientific-technical support to the European Union's Policies for the protection and sustainable development of the European and global environment.

European Commission
Joint Research Centre
Institute for Environment and Sustainability

Contact information

Name: Giorgio Martini

Address: Transport and Air Quality Unit, Institute for Environment and Sustainability, Joint Research Centre, Via E. Fermi, I-21020 Ispra (VA), Italy

E-mail: giorgio.martini@jrc.it

Tel.: +39-0332-789293

Fax: +39-0332-785869

<http://ies.jrc.ec.europa.eu>

<http://www.jrc.ec.europa.eu>

Legal Notice

Neither the European Commission nor any person acting on behalf of the Commission is responsible for the use which might be made of this publication.

A great deal of additional information on the European Union is available on the Internet.

It can be accessed through the Europa server:

<http://europa.eu/>

**Europe Direct is a service to help you find answers
to your questions about the European Union**

**Freephone number (*):
00 800 6 7 8 9 10 11**

(*) Certain mobile telephone operators do not allow access to 00 800 numbers or these calls may be billed

JRC 46524

Catalogue number LB-NA-23426-EN-C

EUR 23426 EN

ISBN 978-92-79-09485-9

ISSN 1018-5593

DOI 10.2788/83175

Luxembourg: Office for Official Publications of the European Communities

© European Communities, 2008

Reproduction is authorized provided the source is acknowledged

Printed in Italy

Contents

Contents	3
List of Figures	5
List of Tables	7
Acknowledgements	8
1. INTRODUCTION	1
2. EXPERIMENTAL FACILITIES	3
PARTICLE GENERATORS	3
TEST ENGINE	4
FUEL AND LUBE OIL	5
SAMPLING SYSTEMS AND CONDITIONS	5
Dilution air	5
Primary Full Dilution tunnel	5
Secondary dilution tunnel (PTS) and Particulate Mass (PM) sampling	6
Particle Number (PN) sampling	7
PARTIAL FLOW SYSTEMS	7
AVL Smart Sampler SPC-472.....	11
Control Sistem PSS-20	11
PN measurement from partial flow systems	12
TEST PROTOCOL	12
Cycles.....	12
Weighting procedure	12
Test matrix of exploratory work.....	12
3. RESULTS	13
BACKGROUND TESTS	13
Partial Flow system: AVL Smart Sampler SPC-472	13
Partial Flow System: Control Sistem PSS-20	13
Primary full dilution tunnel (CVS).....	14
Secondary dilution tunnel (PTS).....	15
FILTER TESTS	18
CHARACTERISATION OF PARTICLE NUMBER SYSTEMS	19
CPCs comparisons	23
Volatile Removal Efficiency	26
Volatile Removal Efficiency with diesel engine exhaust gas	27
Dilution Ratios	29
Penetrations.....	33
Particle Reduction Factors (PRF).....	34
Further SPCS investigation	35
COMPARISON OF PARTICLE NUMBER SYSTEMS	40
Comparison of SPCSs	40
Hot-cold dilution	42
Comparison of SPCSs at the same partial flow system.....	42
Comparison of SPCSs at different partial flow systems.....	44
Comparisons of PMP systems at CVS	46

SAMPLING PARAMETERS	49
Cyclone effect.....	49
Heated line.....	49
PRE-CONDITIONING TESTS	53
CONTINUITY PROTOCOL	57
REAL TIME EMISSIONS	58
Cold WHTC.....	58
Hot WHTC.....	60
WHSC.....	62
ETC.....	62
ESC.....	64
Steady states.....	66
DMM	69
4. CONCLUSIONS.....	72
Facilities	72
Mass and number background	72
Filter (PM) tests.....	73
Characterization of particle counting and sampling systems	73
Comparison of particle number systems	74
Conclusions about the set up.....	74
Pre-conditioning	75
Continuity protocol.....	75
Real time emissions (engine with CRT)	75
Parameters	76
REFERENCES.....	77
DEFINITIONS, ACRONYMS, ABBREVIATIONS.....	79
ANNEXES.....	81
Annex A. Test fuel specifications for the exploratory work and the validation exercise.....	81
Annex B: Experimental set up details	82
Annex C: Cyclone cut-points (URG-2000-30EP, 91 lpm 2.5 µm).....	83
Annex D: Operation of SPCS.....	84

List of Figures

Figure 1: Particle generators: a) Horiba NaCl b) Horiba C40 c) JRC NaCl.	3
Figure 2: a) Golden Engine (IVECO CURSOR 8) b) CRT c) open filter d) no after-treatment.....	4
Figure 3: Schematic of the set up.	6
Figure 4: Partial flow systems (Control Sistem PSS-20 and AVL Smart Sampler SPC-472)	8
Figure 5: Background tests with the SPC-472 system a) no modification b) with HEPA filter at the dilution air line c) heated PM holder d) with carbon filter at the dilution air line.....	14
Figure 6: Set up for background tests from the full dilution tunnel (CVS).....	15
Figure 7: Background mass levels when sampling from the full dilution tunnel (blue points). Mass when sampling directly from HEPA filters are shown (rest colors).....	15
Figure 8: PN and PM background measurements (a) without and (b) with HEPA filter at the dilution air line.	16
Figure 9: PN and PM background measurements (a) with 47 mm and (b) 70 mm filters. Numbers in parenthesis indicate the mass on the backup filter.....	17
Figure 10: PN and PM background measurements without any flow (a) with 47 mm and (b) 70 mm filters. Numbers in parenthesis indicate the mass on the backup filter.....	17
Figure 11: Filter tests results.	18
Figure 12: Schematic set up for the comparison of SPCSs' CPCs.....	23
Figure 13: Comparison of the two SPCSs CPCs.....	24
Figure 14: Comparison between SPCSs CPCs and the 3790 CPC.....	24
Figure 15: Comparison of the CPC 3010D (old golden) with the CPC 3790.....	24
Figure 16: Comparison of the Nanomet 3790n with the 3790.....	25
Figure 17: Comparison of the Nanomet 3790n with GRIMM PMP.....	25
Figure 18: Setup for calibration tests (volatile removal and penetration) a) polydisperse aerosol b) monodisperse aerosol.....	26
Figure 19: Volatile removal efficiency of various systems sampling polydisperse C40 particles (peak 35 nm).....	27
Figure 20: Volatile removal efficiency of various systems sampling polydisperse C40 particles (peak 171 nm).....	28
Figure 21: Volatile removal efficiency of various systems sampling polydisperse C40 particles (peaks at 35 and 171 nm).....	28
Figure 22: Schematic set up for the removal efficiency evaluation.....	28
Figure 23: a) Total (EEPS) and non volatile (SPCS, TD+CPC) emissions during the preconditioning phase. Numbers indicate the time moments of the size distribution of the next panel b) Total particle size distribution (from EEPS).....	30
Figure 24: Set up for the measurement of the sample flow rate for different pressures.....	32
Figure 25: Effect of under-pressure on SPCS's sample flow rate.....	32
Figure 26: Old Nanomet's penetrations at JRC. AEA's results during the light duty PMP programme are also shown.	33
Figure 27: SPCS's penetrations at JRC.....	34
Figure 28: Comparison of SPCS-20 (at a partial flow system with constant DR) and SPCS-19 (at CVS with different DRs).....	36
Figure 29: SPCSs ratio (DR 10x15 reference value) by changing a) the primary dilution ratio (PDR) and b) the secondary dilution ratio (SDR). The gas measurements from Table 10 are also shown.....	36
Figure 30: Particle number flux during a part of the ETC cycle 3 different days with different dilution ratio settings (SPCS-19 at the CVS).....	38
Figure 31: Particle number flux during a part of the ETC cycle 3 different days with different dilution ratio settings (SPCS-20 at the PSS-20).	38
Figure 32: Effect of bypass on the instability	38
Figure 33: Particle flux for different dilution settings.....	39
Figure 34: Summary of the emissions with the SPCS (SPCS-19 at CVS, SPCS-20 at PSS-20).....	39
Figure 35: Schematic set up for the comparison of SPCSs at the primary dilution tunnel.....	40
Figure 36: Comparison o SPCSs sampling from the primary dilution tunnel over a cold WHTC.....	41
Figure 37: Comparison of the two SPCSs.	41
Figure 38: Comparison of SPCS with a 3790 CPC.....	41

Figure 39: Comparison of SPCSs from the same sampling point using different dilution temperatures (SPCS-20 cold).....	42
Figure 40: Schematic set up for the comparison of SPCSs at partial flow systems.....	43
Figure 41: Steady state tests with both SPCS sampling from PSS-20.....	43
Figure 42: Cold WHTC with both SPCS sampling from PSS-20.....	44
Figure 43: Schematic set up for the comparison of SPCSs at different partial flow systems.....	44
Figure 44: Comparison of full flow and partial flow systems (high emissions cold WHTC).....	45
Figure 45: Comparison of full flow and partial flow systems (low emissions hot WHTC).....	45
Figure 46: Schematic set up for the comparison of different particle number systems.....	46
Figure 47: Comparison of different particle number systems over a cold WHTC.....	47
Figure 48: Comparison of different particle number systems over steady states.....	48
Figure 49: Comparison of different particle number systems over steady states.....	48
Figure 50: Comparison of different particle number systems over steady states.....	48
Figure 51: Schematic set up for the effect of cyclone.....	50
Figure 52: Effect of cyclone on SPCS results during a transient test (SPCS-19 was used downstream of a cyclone).....	50
Figure 53: Effect of cyclone on SPCS results during steady states (SPCS-19 was used downstream of a cyclone).....	51
Figure 54: Schematic set up for the effect of the heated line.....	51
Figure 55: Effect of a 4 m heated line (at 47°C) on SPCS results.....	52
Figure 56: Effect of sampling parameters on SPCS-19 emissions (difference compared to a 3790 CPC downstream of a thermodenuder).....	52
Figure 57: Schematic set up for the pre-conditioning tests.....	53
Figure 58: Pre-conditioning effect on particle emissions of a “mini cycle” consisting of modes #2, #8, #3 and #1 of ESC. Modes #7, #9, #11 are low temperature modes (the CRT loads), while mode #10 is high temperature mode (the CRT regenerates).....	54
Figure 59: Pre-conditioning of 10 min (mode #10 ESC) and 20 min (mode #7 ESC).....	55
Figure 60: Pre-conditioning of 15 min (mode #10 ESC) and 30 min (mode #7 ESC).....	55
Figure 61: Total and non-volatile particles during the pre-conditioning.....	55
Figure 62: Emissions during mode #10 (ESC).....	56
Figure 63: Continuity protocol at mode 4 and 7. Mode 4 emissions increase over time.....	57
Figure 64: Emissions during a cold WHTC.....	58
Figure 65: a) Beginning of a cold WHTC. Arrows indicate the times that the size distributions of the second figure correspond. b) Size distributions during a cold WHTC. The times for each distribution are indicated with an arrow at the first figure.....	59
Figure 66: Cold WHTC emissions.....	60
Figure 67: Comparison of a 3010D and a 3025A downstream of SPCS.....	60
Figure 68: Emissions (>23 nm) during a hot WHTC.....	61
Figure 69: Emissions downstream of a TD.....	61
Figure 70: Comparison of a 3010D and a 3025A downstream of SPCS.....	61
Figure 71: WHSC emissions.....	62
Figure 72: Comparison of a 3010D and a 3025A downstream of SPCS.....	62
Figure 73: ETC emissions with EEPS and SPCS.....	63
Figure 74: Total (>3 nm) and non-volatile (>23 nm) particles over an ETC.....	63
Figure 75: Non-volatile particles >3 and >23 nm over an ETC.....	63
Figure 76: Emissions over an ESC.....	64
Figure 77: Size distributions.....	65
Figure 78: Particle emissions over an ESC and exhaust gas temperature.....	65
Figure 79: Non-volatile (>3 and >23) nm emissions over an ESC.....	65
Figure 80: Particle emissions during steady states.....	66
Figure 81: Size distributions at mode #10 (ESC).....	67
Figure 82: Size distributions at mode #7 (ESC).....	67
Figure 83: Size distributions with nano-SMPS downstream of a TD.....	67
Figure 84: Non-volatile (>3 and >23 nm) during mode #10 (ESC).....	68
Figure 85: Difference of mass emissions between DMM and filter PM at CVS.....	69
Figure 86: Difference of number emissions between DMM and SPCS at CVS.....	69
Figure 87: Comparison of DMM with SPCS and 3025A over a cold WHTC (Engine out).....	70
Figure 88: Comparison of DMM with SPCS and 3025A over an ESC (Engine out).....	70

Figure 89: Comparison of DMM with SPCS and 3025A over a cold WHTC (Engine with CRT)..... 71
 Figure 90: Comparison of DMM with SPCS and 3025A over an ESC (Engine with CRT). 71
 Figure 91: Comparison of DMM with SPCS and 3025A over an ETC (Engine with CRT)..... 71

List of Tables

Table 1: Expected time schedule 2
 Table 2: Golden Engine Information..... 5
 Table 3: Theoretical corrections for the dilution ratio of ejector dilutors according to Giechaskiel et al. (2004)..... 20
 Table 6: Slopes and final correction at this report for various CPCs. Numbers in parenthesis are calculated indirectly. 25
 Table 7: Summary of volatile removal efficiency results 27
 Table 8: Measured DRs and comparison with manufacturer’s value for ambient pressure and underpresre. 30
 Table 9: Measured DRs and comparison with model’s value for ambient pressure, overpressure and underpresre..... 31
 Table 10: Measured DRs and comparison with manufacturer’s value for different DR settings. 31
 Table 11: Measured DRs and comparison with manufacturer’s value for ambient pressure and underpressure 32
 Table 12: Average penetrations and standard deviation of the penetrations. 33
 Table 13: Average penetrations and standard deviation of the penetrations 34
 Table 14: Average PRF and standard deviation of the PRF 35
 Table 15: Average PRF and standard deviation of the PRF 35
 Table 16: Particle number results during a cold (left) and hot WHTC (right). 45
 Table 17: Difference between DMM (downstream of a TD) and PM from CVS. 69

Acknowledgements

The authors would like to gratefully acknowledge J. Andersson from Ricardo, who acts as the Golden Engineer for the PMP Inter-comparison exercise, for his helpful advice throughout and following the testing. We would also like to thank Dekati Ltd. for providing the thermodenuder and the evaporation chamber, TSI for providing a PMP compliant counter and Horiba for providing the Golden instruments.

Special acknowledgements to A. Brunella, J. Boch and M. Akard from Horiba for the assistance during the setup of the golden instruments and Q. Wei and L. Hill from Horiba for their helpful comments and corrections concerning the operation of the golden instruments. Finally, D. Scheder from Horiba for his support during the particle systems characterization measurements and his helpful comments on the manuscript.

1. INTRODUCTION

The mandate given to the Particle Measurement Programme (PMP) Working Group by the UN-ECE GRPE (Working Party on Pollution and Energy) was to develop new particle measurement techniques to complement or replace the existing filter-based particulate mass measurement method, with special consideration given to measuring particle emissions at very low levels. These techniques should include a detailed specification of test procedures and equipment, be suitable for Light-Duty Vehicle and Heavy-Duty Engine type approval testing, and be suitable for use in transient testing. Since, within the European Union (EU), type approval testing to demonstrate compliance with emissions standards involves a limited number of tests which could take place at one of many laboratories, good repeatability, and reproducibility from laboratory-to-laboratory are key requirements for regulatory measurement techniques. PMP has therefore sought to investigate and demonstrate the repeatability and reproducibility of the proposed techniques. PMP was also tasked with accumulating data on the particle emissions performance of a range of engine and vehicle technologies when tested according to the proposed procedures.

The Light-Duty and Heavy-Duty inter-laboratory correlation exercises of the PMP were designed to enable an evaluation of the repeatability and reproducibility of particle number and mass measurements made with the systems recommended following the PMP Phase 1 and Phase 2 studies. The two recommended systems were (PMP 2003):

- A filter mass method (PM) based broadly upon those currently used in Europe and the US and that proposed for the United States for 2007 type approvals (CFR 2001).
- A particle number method (PN) using a particle counter, a defined size range and sample pre-conditioning to exclude semi-volatile particles.

The Light-Duty exercise preceded that for Heavy-Duty and circulated a Euro 4 Diesel vehicle with DPF plus a reference particle measurement system between laboratories. In addition, each lab was invited to employ its own particle measurement system and to test other Euro 4 vehicles. The results of the Light-Duty inter-laboratory exercise were reported during 2007 (Andersson et al. 2007, Giechaskiel et al. 2008a, b, Giechaskiel et al. 2007b).

The Heavy-Duty exercise consists of three parts:

- The *exploratory work* at JRC for the definition of the measurement protocol.
- The *validation exercise* for the evaluation of the particle number repeatability and reproducibility using the same systems at all labs (Golden Systems). In the validation, exercise an engine (Golden Engine) will be circulated along with two Golden Systems which will be used at the full and partial flow systems respectively. The Golden Engineer with the project manager will ensure that the participating labs will follow precisely the measurement protocol. Low sulfur fuel and lubricant from the same batch will be used from all labs. The participating labs, in addition to JRC are, AVL_MTC, RICARDO, UTAC, and EMPA (they work for their governments). JRC will measure again at the end of the exercise to ensure that nothing has changed at the engine during the exercise.
- The *round robin exercise* for the evaluation of the particle number repeatability and reproducibility using different systems. In the round robin, a reference engine will circulate, but each lab will use its own particle number systems at the full flow dilution tunnel and optionally at the partial flow systems. All labs will use fuel and lubricant of the

same type (but not of the same batch). The participating labs are from EU, Japan Korea, and Canada (to be confirmed).

The validation and the round robin exercises will start as soon as the exploratory work in JRC has been finalized and they will run in parallel. The expected timetable is given in Table 1:

Table 1: Expected time schedule

<i>Date</i>	<i>Validation Exercise</i>	<i>Round Robin</i>
Oct – Feb 2008	JRC (exploratory work)	
Jan – Feb 2008	JRC (Phase A)	
Mar – Apr 2008	AVL_MTC	
May – Jun 2008	JRC (Phase B)	TUV
Jul – Aug 2008	RICARDO	RICARDO
Sep – Oct 2008	UTAC	VOLVO
Dec – Jan 2009	EMPA	Japan (NTSEL, JARI)
Feb – Mar 2009	JRC	Korea (NIER)
Jul – Aug 2009		JRC
Sep – Oct 2009		UTAC
Nov – Dec 2009		TNO
Jan – Feb 2010		VTT
Mar – Apr 2010		SCANIA
May – Jun 2010		Environment Canada (?)
Jul – Aug 2010		Daimler Chrysler

This document reports the results of the exploratory work during the PMP Heavy-Duty inter-laboratory exercise – from Oct. '07 to Feb. '08 - conducted at the Vehicles Emissions Laboratory (VELA-5) in the Transport and Air Quality Unit of the European Commission's Joint Research Centre (JRC, Ispra). This report presents the results of the work undertaken on an IVECO Cursor 8 Heavy-Duty engine equipped with a Continuous Regenerating Trap (CRT), i.e. the Golden Engine. Main objective of these tests were to finalize the measurement protocol that will be used in the validation exercise and the round robin. These tests included background tests, filter media effect, filter face velocity, preconditioning effect, comparisons of different particle number systems, and investigation of the golden instruments.

2. EXPERIMENTAL FACILITIES

In the following sections, the experimental details for the measurements conducted in the JRC facilities will be described.

PARTICLE GENERATORS

For the estimation of the particle number measurement systems' penetrations and volatile removal efficiencies the following generators were used:

Salt generator: A JRC prototype salt generator was used. This generator is similar to the one AEA used for their experiments during the Light-Duty laboratory exercise (evaporation-condensation technique). The salt aerosol generator consisted of a ceramic crucible heated via an electric Bunsen. The bulk material (NaCl) was placed in the ceramic crucible and heated to near its boiling point. A small flow (N_2) was introduced into the crucible to displace vapor from the surface of the bulk material to a cooler region of the generator where condensation occurred. Particle diameters and/or concentrations could be varied by controlling the rate of vapor transport from the crucible (via the crucible air flow) and/or the subsequent cooling rate of the vapor (via the carrier air flow).

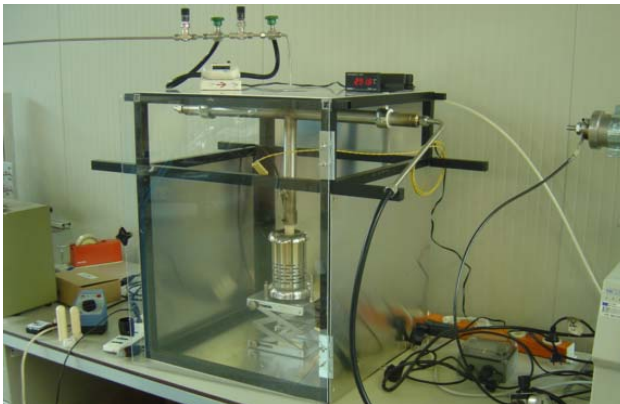


Figure 1: Particle generators: a) Horiba NaCl b) Horiba C40 c) JRC NaCl.

Salt generator: A Horiba prototype salt generator based on the nebulisation technique was used. This generator produced particles with mean diameter >70 nm.

C40 generator: A Horiba C40 generator based on the evaporation-condensation technique was used.

TEST ENGINE

The engine used in this study (Figure 2) was the PMP “Golden Engine”, i.e. an IVECO Cursor 8 Euro 3 engine with a Continuous Regenerating Trap (CRT) (Table 2). The Golden Engine was provided by the UK Department for Transport which signed a contract with Ricardo to this respect. Ricardo provided the technical assistance to install the engine on the test bench. The distance between the engine and the after treatment device was 270 cm (internal diameter 15 cm). Exhaust gas temperatures and pressures were recorded upstream and downstream of the after treatment device. Engine coolant and intercooler temperatures were controlled respectively at 75 and 40-45°C.

The engine was also tested with a partial (open) filter from EMITEC and without any after-treatment device (Engine out). For the last case the engine was not throttled to simulate the pressure drop of the after-treatment devices.

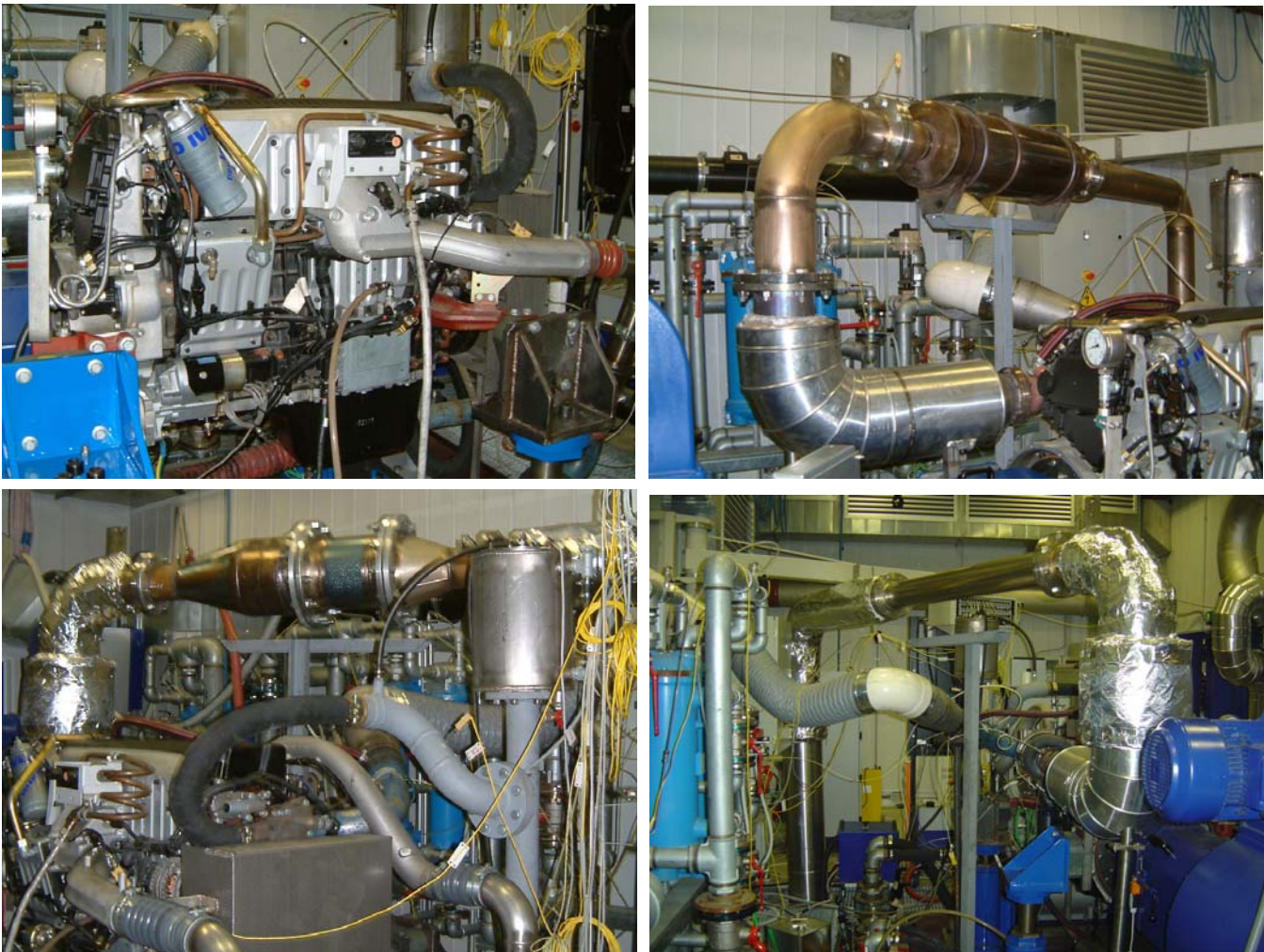


Figure 2: a) Golden Engine (IVECO CURSOR 8) b) CRT c) open filter d) no after-treatment

Table 2: Golden Engine Information

Make and model	IVECO Cursor 8 (Euro 3)
Engine configuration and capacity	7.8 l, 6 cylinder, 4 valves/cylinder
Compression ratio	17:1
Maximum power	260 kW @ 1900 to 2400 rpm
Maximum torque	1280 Nm @ 1000 to 1900 rpm
After-treatment	Continuous Regenerating Trap (CRT)

FUEL AND LUBE OIL

The test lubricant was a BP Vanellus E8 fully synthetic, 5W/30 PAO (polyalphaolefin) based oil with <0.2% sulfur content. The lubricant was added to the engine following the procedure described in the inter-laboratory guide (Andersson and Clarke 2008). The exploratory tests were conducted without conditioning of the fresh lubricant, as the target was to investigate differences among different protocols and different parameters and not the absolute levels of the engine.

The fuel used in this engine (RF06-03 PMP) complied with Annexes 3 and 4 of Directive 2003/17/EC describing fuel specifications to be employed after 1st January 2009 (i.e. sulfur content of lower than 10 ppm) (Annex A). It was a CEC (Coordinating European Council) certified reference fuel.

SAMPLING SYSTEMS AND CONDITIONS

The measurements were conducted on a test bench at the VELA-5 JRC laboratories (Motor AFA-TL 510/1.9-4, 500 kW, 2500 Nm, 3500 rpm). A general description of the set up follows. As the objective of these measurements was to finalize the measurement protocol, no specific protocol was followed during the tests and for this reason only the general overview of the set up is given. The details for each measurement are given at the corresponding paragraphs. A figure with the most important dimensions of the installation is given in Annex B.

Dilution air

The dilution air line for the full flow tunnel and secondary tunnel had highly efficient dilution air filters for particles and hydrocarbons that reduce particle contributions from the dilution air to near zero (H13 of EN 1822).

Primary Full Dilution tunnel

The exhaust was transported to the primary full dilution tunnel through a 9.5 m long (only the first 2 and last 2 m insulated) stainless steel tube. For the official tests 2 m more will be insulated to comply with the legislation (Reg. 49). The exhaust gas was introduced along the tunnel axis, near an orifice plate that ensured rapid mixing with the dilution air. The flow rate of dilute exhaust gas through the tunnel was controlled by a critical orifice venturi. A flow rate of 80 m³/min at normal reference conditions (0°C and 1 bar) was used for most measurements (unless specified otherwise). This flow rate was selected because it is the maximum that can be achieved by all labs that participate in the validation exercise. Lower flow rate would result to

high diluted exhaust gas temperature in the dilution tunnel (CVS) and consequently to the instruments. Moreover, the temperature in the cell at the end of the day would be very high. This could result at temperatures in the cell $>35^{\circ}\text{C}$ which could affect the operation of the instruments. The tunnel operated in the turbulent flow regime ($\text{Re} = 25000$ depending on the diluted gas temperature). The residence time of the exhaust in the dilution tunnel was in the order of 0.5 s (for $80 \text{ m}^3/\text{min}$). The schematic of the set up can be seen in Figure 2.

Three probes (of inner diameter 12 mm) were used for sampling, placed at the same cross-section of the tunnel and facing upstream the flow. These probes were installed 10 tunnel diameters downstream of the mixing point to ensure complete mixing of the dilution air and the exhaust gas. One probe was used for the secondary dilution tunnel and the particulate mass (PM) measurements and the other two for particle number (PN) measurements. At one of the probes, a URG-2000-EP cyclone was installed (see Appendix C for cut-points).

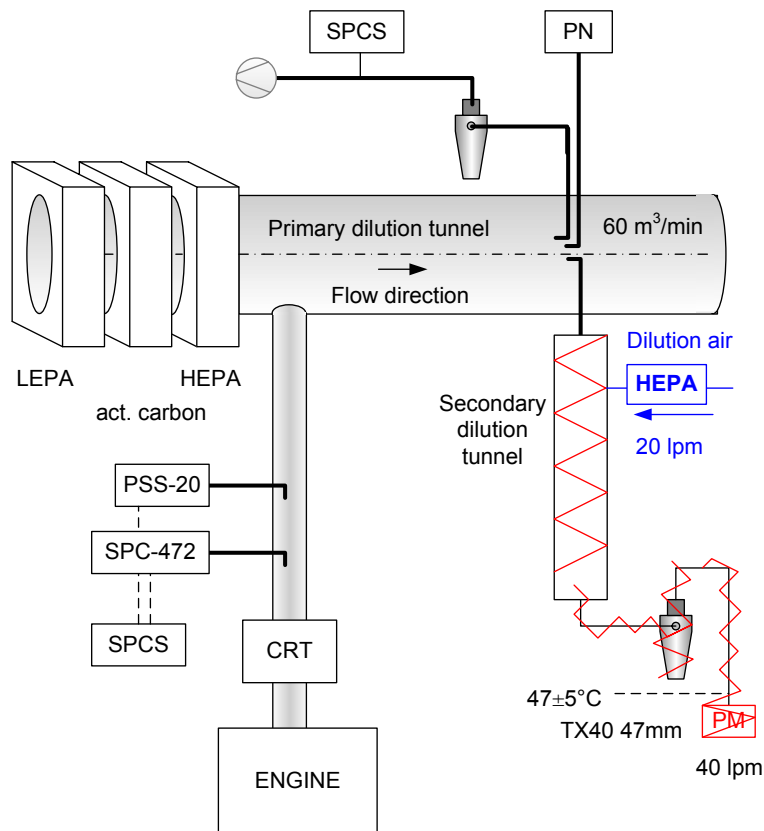


Figure 3: Schematic of the set up.

Secondary dilution tunnel (PTS) and Particulate Mass (PM) sampling

The secondary dilution tunnel used for PM measurements was according to the requirements of Heavy-Duty Engines regulation (Reg. 49). In addition, a cyclone pre-classifier (URG-2000-30EP) was installed to limit the contribution of re-entrained and wear materials to the filter mass. The 50% cut-size of the cyclone for 50 lpm was estimated to be $4 \mu\text{m}$ (see Appendix C). The cyclone, the secondary tunnel and the filter holder were usually externally heated by direct surface heating to permit aerosol stabilization of $>0.2 \text{ s}$ prior to sampling and to ensure close control of the filter face temperature to 47°C ($\pm 5^{\circ}\text{C}$). The temperature was measured 20 cm upstream of the filter. PM samples were collected on 47 or 70 mm Teflon-coated glass-fiber Pallflex® TX40H120-WW filters (TX40). Usually one single 47 mm filter was

used rather than primary and back-up filters to minimize weighing errors and the volatile artifacts of the back-up filter. To quantify this artifact effect some tests were conducted with two filters (main and backup filter). Some extra tests were conducted with 47 mm PALL Teflo, PTFE with polymethylpentene support ring, porous size 2 μm (Teflo) in order to compare the effect of volatile artifact depending on the material of the filter reported by various investigators.

The ratio of dilution air to sample aerosol flow (from the primary tunnel) was usually 1:1 (20-30 lpm sample, 20-30 lpm dilution air, and 40-60 lpm total flow to the filters at normal reference conditions 0°C and 1 bar) so the dilution ratio was 2:1. This range of flowrates (40-60 lpm) resulted in filter face velocities that have been shown to be in the middle of a range where the mass results are not affected by small changes in the filter face velocity (Andersson et al. 2004). The 1:1 ratio of sample and dilution air was chosen as a compromise between the extremely low (1:3) and high (3:1) ratios that the labs usually use. With the 1:1 ratio, it will be possible for all labs to keep a temperature of 47°C at the filter face either by heating the dilution air or externally heating the mixing tunnel. For the JRC case, it was found more difficult to reach the desired temperature by heating the dilution air. The high heat exchange due to the high surface area of the tunnel dropped the diluted gas temperature at ambient levels. For this reason, it was decided to reach the 47°C by heating the secondary tunnel externally (temperature of the heaters ~65°C). A 30 min stabilization time was necessary to reach the desired temperature.

To estimate the filter face velocity surface areas of 11.3 and 27.3 cm^2 were assumed for the 47 and 70 mm filters respectively. The filter face velocity was calculated for 47°C and 101.3 kPa. The flow rates of the mass flow controllers were considered to be given at normal conditions (0°C and 101.3 kPa). The resulting filter face velocities were 69 cm/s for the 47 mm filters at 40 lpm, 103 cm/s for the 47 mm filters at 60 lpm and 43 cm/s for the 70 mm filters at 60 lpm. If the pressure at the filter holder was assumed to be 4-5 kPa lower, then the velocities would have been higher by ~3 cm/s.

Particle Number (PN) sampling

Aerosol samples for particle number measurement were drawn from the primary dilution tunnel. For some tests a cyclone pre-classifier (URG-2000-30EP) with a 50% cut-size at 2.5 μm (for a flow rate of 90 lpm) was used. The following sampling systems were connected to the primary dilution tunnel:

- Particle Number Counters (TSI 3025A, TSI 3010, TSI 3790, TSI 3010D, GRIMM 5.403)
- EEPS (TSI)
- Thermodenuder (Dekati) or evaporation chamber (Dekati)
- Ejector dilutors (Dekati)
- Nanomet (Matter Eng.)
- SPCS (Horiba)

The characteristics of the systems will be given in a separate section.

PARTIAL FLOW SYSTEMS

Two partial flow sampling systems were used: The AVL Smart Sample SPC-472 and the Control Sistem PSS-20. Sampling and measurements with the partial flow sampling systems

were undertaken according to ISO 16183 and the inter-lab guide (Andersson and Clarke 2008). Exhaust gas mass flow was determined by fuel consumption (gravimetrically) and air consumption (hot-wire anemometer). The resulting data were used for controlling the sample flow from the raw exhaust in the partial flow systems.

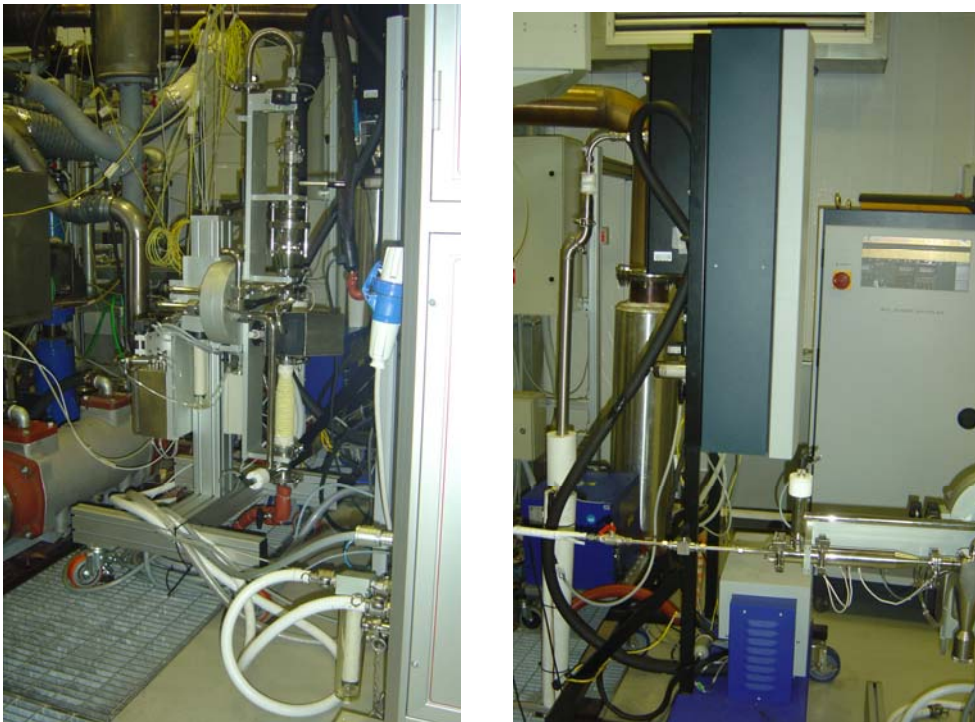


Figure 4: Partial flow systems (Control Sistem PSS-20 and AVL Smart Sampler SPC-472)

Partial flow systems try to simulate the full dilution tunnel. At the dilution tunnel each moment the dilution ratio DR_{CVS} is:

$$DR_{CVS} = \frac{G_{CVS}}{G_{exh}} \quad \text{Eq. 1}$$

Where:

G_{CVS} is the flow rate of the full flow dilution tunnel

G_{exh} is the engine exhaust flow rate

The DR_{PFS} at the partial flow system (PFS) is:

$$DR_{PFS} = \frac{G_{tot}}{G_p} \quad \text{Eq. 2}$$

Where:

G_{tot} is the (total) flow rate through the filter at the partial flow system and

G_p is the exhaust sample flow rate.

As G_{tot} is usually constant, G_p is controlled by changing the dilution air:

$$G_p = G_{tot} - G_{da} \quad \text{Eq. 3}$$

Where

G_{da} is the flow rate of the dilution air at the partial flow system (changing according to the exhaust flowrate).

If a flow is extracted (e.g. with a particle number system) then, the extracted flow must be taken into account in the partial flow systems software (e.g. PSS-20) or an equal flow must be fed back (e.g. SPC-472).

As the dilution ratio at the full dilution tunnel (Eq. 1) and at the partial flow systems (Eq. 2) should be equal (secondary tunnel not considered):

$$\frac{G_{CVS}}{G_{exh}} = \frac{G_{tot}}{G_p} \quad \text{Eq. 4}$$

Introducing the split ratio:

$$r = \frac{G_p}{G_{exh}} \quad \text{Eq. 5a}$$

Rearranging Eq. 4, in order to have equal dilution ratios at the full dilution tunnel and at the partial flow system and using Eq. 5a, the split ratio should take the value:

$$r = \frac{G_p}{G_{exh}} = \frac{G_{tot}}{G_{CVS}} \quad \text{Eq. 5b}$$

The dilution ratio of a partial flow system DR_{PFS} is:

$$DR_{PFS} = \frac{G_{tot}}{G_p} = \frac{G_{tot}}{rG_{exh}} \quad \text{Eq. 6}$$

And dividing Eq. 1 and Eq. 6:

$$\frac{DR_{CVS}}{DR_{PFS}} = \frac{G_{CVS}}{G_{tot}} r \quad \text{Eq. 7}$$

The ratio of DRs of two partial flow systems would be:

$$\frac{DR_{PFS1}}{DR_{PFS2}} = \frac{G_{tot1} r_2}{G_{tot2} r_1} \quad \text{Eq. 8}$$

Note that G_{tot} is set by the user (=1.08 g/s to have a filter face flow rate of 50 lpm at normal conditions) and also the dilution tunnel flow rate G_{CVS} is also defined by the user (80 m³/min). Then the split ratio r is also defined (=0.000626) from Eq. 5b. If the split ratio has a different value than the one from Eq. 5b, then the dilution ratios at the full dilution tunnel and the partial flow system are different and this might affect the volatiles on the filter.

Note that G_{CVS} is referred as G_{edf} in the PSS-20 manual and the exhaust gas flow G_{exh} as F_{exh} . In PSS-20 G_{tot} and G_{edf} are set by the user. Typical values used where $G_{edf} = 80 \text{ m}^3/\text{min} = 4800 \text{ m}^3/\text{h} = 6200 \text{ kg}/\text{h}$ and $G_{tot} = 50 \text{ lpm} = 3000 \text{ nl}/\text{h}$. The split ratio for PSS-20 can also be calculated from Eq. 5 using G_{edf} (and not the real dilution tunnel flow).

If for any reason the split ratio is not constant (e.g. wrong extracted flow setting by the user at PSS-20, or wrong feedback flow at SPC-472) the dilution ratio at the partial flow system is different than at the full dilution tunnel. This error is not a constant ratio and theoretically it can be taken into account only for real time instruments. For example, the real time emissions of PSS-20 can be corrected with the ratio of the real time dilution ratios as follows:

$$\frac{DR_{real}}{DR_{theor}} \quad \text{Eq. 9}$$

Where:

$$DR_{theor} = \frac{G_{tot} + G_{PN}}{G_{tot} + G_{PN} - G_{da}} \quad \text{Eq. 10a}$$

$$DR_{real} = \frac{G_{tot} + G_{PN'}}{G_{tot} + G_{PN'} - G_{da}} \quad \text{Eq. 10b}$$

Where G_{PN} is the set extracted value and $G_{PN'}$ the real extracted value.

It has to be emphasized that the parameters chosen at the CVS and the partial flow system were such as that the dilution ratios are the same at the two systems. However, for PM the total dilution ratio at CVS is higher than at the partial flow system as there is also the secondary dilution.

Labs that use different CVS flow rate can determine the split ratio from equation 5b if they want to have the same dilution ratios at the CVS and at the partial flow systems. However, for the validation exercise all labs will use the values that were given previously irrespective of the CVS flowrates. This was decided in order to be able to compare the partial flow system independently at the end of the exercise.

AVL Smart Sampler SPC-472

The AVL Smart Sampler (SPC-472) is a partial flow system that simulates the operation of the full dilution tunnel by sampling a constant ratio of the exhaust flow (split ratio). This is achieved by changing the dilution air flow rate as the total flow rate remains constant. The SPC-472 was recently upgraded (cyclone installed, 47mm filter holders and controlled temperature of the filters at $47\pm 5^{\circ}\text{C}$ by external heating) to meet the requirements of the PMP protocol (Andersson and Clarke 2008). However extra work from JRC was necessary which included:

- Insulation of the cyclone and the tubes as the temperature couldn't reach 47°C .
- Modification of the system downstream of the cyclone to connect the particle number system.
- Addition of a tube downstream of the filter to feed back a flow equal to the one extracted from the particle number system. A mass flow controller connected at filtered pressurized air was used to feedback the flow rate that the number system was extracting.
- Addition of HEPA and Carbon filters at the dilution air line. As it will be explained in the "Results" section the existing ones were not adequate for particle number measurements. However, the addition of filters at the dilution air line after the unit's MFC reduces the response time (out of the legislation limits) and this might lead to underestimation of the emissions. However, comparison of the real time particle number emissions didn't show any effect. In the future these filters will be removed and a high pressure particle filter will be added upstream the MFC at the dilution air line.

The sampling point of the SPC-472 system was positioned 5 m from the after-treatment device. The sampling probe was sharp-edged and open ended, facing directly into the direction of flow and was provided by the manufacturer. The dilution took part <20 cm from the exhaust tube with filtered air. The mixing tunnel was 63.5 cm long with 3 cm diameter. The residence time of the diluted sample for the flow rate selected (0.862 g/s) was ~ 0.5 s. There was also another (not heated or insulated tube for these experiments but it will be insulated for the official PMP tests) 100 cm (~ 3.5 cm inner diameter) (residence time 1 s). Downstream of the dilution tunnel a URG-2000-30EP cyclone was installed with a 50% cut-size at $4\ \mu\text{m}$ (for a flow rate of 50 lpm, see Appendix C). The extra tube added when the cyclone was installed was around 75 cm (12 mm inner diameter). The filter holder and transfer tubing from the cyclone till the filter were heated to permit aerosol stabilization of only 0.1 s prior to sampling and to ensure close control of the filter face temperature to 47°C ($\pm 5^{\circ}\text{C}$). The temperature was measured 5 cm upstream of the filter. PM samples were collected on 47 mm Teflon-coated glass-fiber Pallflex® TX40H120-WW filters. The estimated filter face velocity for the specific flow rate and 47°C was 69 cm/s.

Control Sistem PSS-20

PSS-20 is a partial flow sampling system which doesn't require compressed air or cooled water. It samples a small quantity of exhaust gas and dilutes it with filtered ambient air. The diluted gas passes through a cyclone and a 47 mm (or 70 mm) filter for the identification of PM emissions (partial flow-total sampling dilution system). The system keeps the temperature of the filter at $47\pm 5^{\circ}\text{C}$ by heating the dilution air. The length of the tube from the exhaust gas tube to the mixing chamber was 75 cm insulated with internal diameter 4 mm. The mixing chamber, which was heated, was 25 cm long with inner diameter 4.5 cm (residence time 0.4 s). For this system the only extra work conducted was to insulate the cyclone. The extracted flow from the system was taken into account with the system's software by adjusting the total flow.

PN measurement from partial flow systems

The systems that were used for PN measurement from the partial flow systems were:

- Particle number counter (3025A from TSI)
- SPCS

The description of these systems was given previously. The only difference is that the sampling line from the partial flow to the SPCS was 1.5 m for the SPC-472 and 20 cm for the PSS-20 (unheated but insulated lines) (internal diameter 4 mm).

TEST PROTOCOL

As the objective of the measurements was to finalize the measurement protocol no specific protocol was followed. However Reg. 49 and ISO 16183 were followed as close as possible. The details of the measurements are given at the respective paragraphs.

Cycles

The European cycles European Transient Cycle (ETC) and European Steady Cycle (ESC) were tested. Emphasis was also given to the World Harmonized Transient (WHTC) and Steady Cycle (WHSC).

Weighting procedure

The filters were conditioned in an open dish (protected from dust) for 1-80 h before the test in an air-conditioned room. The temperature and humidity of the room were $23\pm 2^{\circ}\text{C}$ and $51\pm 2\%$ respectively (within the specification $22\pm 3^{\circ}\text{C}$ and $45\pm 5\%$) (Andersson et al. 2008). Filters were weighted with a Sartorius M5P balance with 10^{-6} g precision as both 47 and 70 mm filters were used. Electrostatic charge effects were minimized by the use of HAUG Type EN SL LC 017782100 neutralizer and grounded conductive surfaces. Each filter was weighted at least three times, and the average of the weightings was used in calculating mass changes.

In parallel two unused (blank) reference filters of the same size and material (47mm TX40) were weighted in order to check the stability of the conditions in the weighting room. The average weight of the reference filters between sample filter weightings was always $\pm 5 \mu\text{g}$.

The weighed filters were used for test within 1 h of their removal of the weighting room. After the tests, the filters were left in the room for 1-80 h for conditioning before being weighted with the same balance, following the same procedure.

Test matrix of exploratory work

The exploratory work conducted in VELA-5 can be divided in the following phases:

- Background tests
- Filter tests
- Particle number systems' characterization
- Comparison of systems
- Sampling parameters
- Pre-conditioning tests
- Real time particle number emissions

The official PMP tests for the validation exercise will be presented elsewhere.

3. RESULTS

In the following sections the results of the exploratory tests are presented. In most figures only one test is reported to improve the readability of the figures, as all other tests showed similar results. Emissions that are reported in [kWh^{-1}] refer to tailpipe conditions and concentrations given in [cm^{-3}] refer to the primary dilution tunnel, unless specified differently. When more than one measurement is reported, then the average value is given. In this case, the ratio of the standard deviation of the measurements to the average value of the measurements, the Coefficient of Variance (CoV), is sometimes referred as repeatability of the measurements. Error bars show one standard deviation.

BACKGROUND TESTS

Objective of these tests was to estimate the contribution of the dilution air on mass (PM) and number (PN) emissions.

Partial Flow system: AVL Smart Sampler SPC-472

The (PN) background levels of the SPC-472 were tested with a TSI 3025A (d_{50} 3 nm) particle number counter connected downstream of the system's cyclone (Figure 5a). The PM background levels were checked using 47 mm TX40 filters (sampling duration of 10 min). The sampling probe was disconnected from the raw exhaust tube and a HEPA filter was connected at the inlet (Figure 5a). The dilution air flow rate was ~20 lpm and the dilution ratio was set constant 5:1 (filtered exhaust flow rate 5 lpm). The results showed that the mass collected on the filter after 10 min sampling of filtered air was ~35 μg and the particle number concentration (particles >3 nm) were 200-4000 cm^{-3} . Their concentration varied with a constant frequency which was associated to the frequency of the compressor for the dilution air. Obviously, the filters of the SPC-472 were not adequate to filter the dilution air. When a HEPA filter was installed at the dilution air line of SPC-472 the PN concentration dropped to below 5 cm^{-3} (Figure 5b). However, the mass concentration remained at the same level (~35 μg for 10 min sampling or ~55 μg for 30 min sampling). Heating the system at 45°C didn't reduce the background levels (~40 μg for 10 min sampling) (Figure 5c). When a carbon filter was installed in addition to the dilution air line the background levels decreased slightly (to 17-39 μg for 30 min sampling) (Figure 5d). Probably these levels would decrease even more if only the dilution air was measured (no sample flow), thus minimizing the contribution of hydrocarbons from the sample line (ambient air).

Partial Flow System: Control Sistem PSS-20

The background mass of the PSS-20 were 23±11 μg for 30 min sampling. The number concentration was 15-50 cm^{-3} .

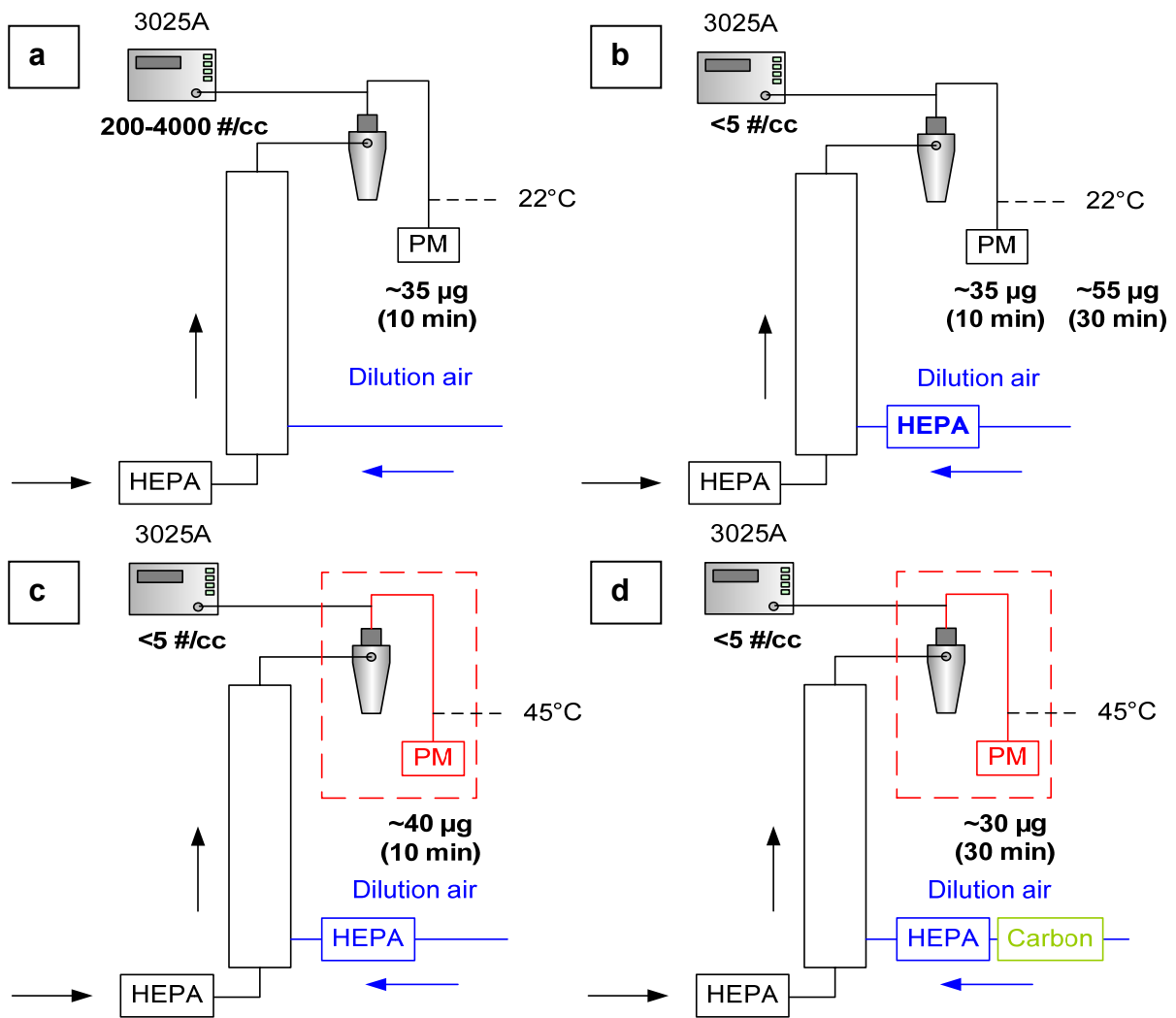


Figure 5: Background tests with the SPC-472 system a) no modification b) with HEPA filter at the dilution air line c) heated PM holder d) with carbon filter at the dilution air line.

Primary full dilution tunnel (CVS)

The PN background levels of the primary full dilution tunnel were tested with a TSI 3010 particle number counter (d_{50} 10 nm) connected directly at the dilution tunnel (Figure 6). The PM background was checked using a filter holder with 47 mm TX40 filters sampling with a flow rate of approximately 25 lpm (through a tygon tube of 50 cm) without any other dilution. The dilution air flow rate of the full dilution tunnel was $80 \text{ m}^3/\text{min}$ and the engine was off (or disconnected at some tests with the tube closed).

The results showed that the mass collected on the filter depended on the sampling time (Figure 7). With 10 min sampling the mass on the filter was $\sim 7.5 \mu\text{g}$ while with 30 min sampling $\sim 20 \mu\text{g}$. The PN emission were around 1 cm^{-3} . It was found that the tygon tube affected the PM emissions. Similar experience has also been reported (Khalek 2005). When no tygon tube was used, the mass on the filter after 30 min of sampling was only $10 \mu\text{g}$. The same figure also shows the mass when sampling directly from a HEPA filter (with or without Carbon filter). The mass in these cases after 30 min are $\sim 5 \mu\text{g}$ (within the uncertainty of the weighting procedure).

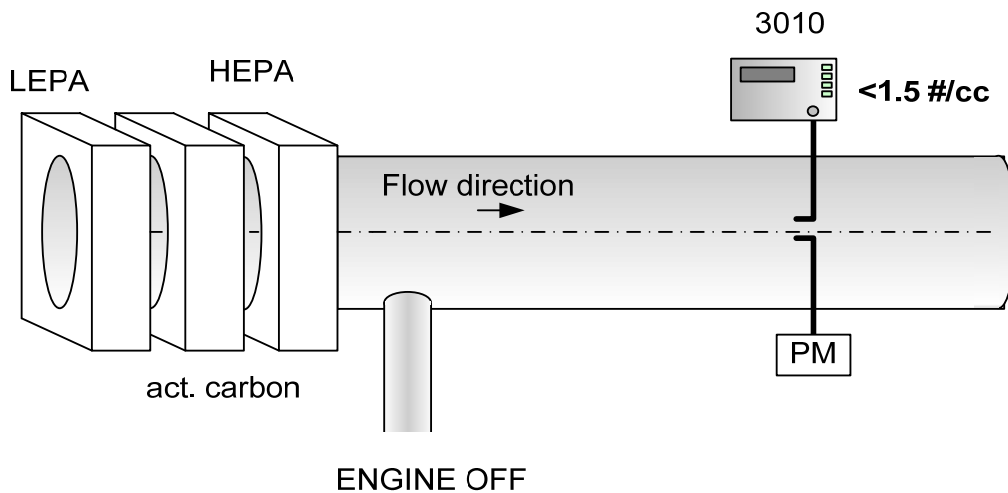


Figure 6: Set up for background tests from the full dilution tunnel (CVS).

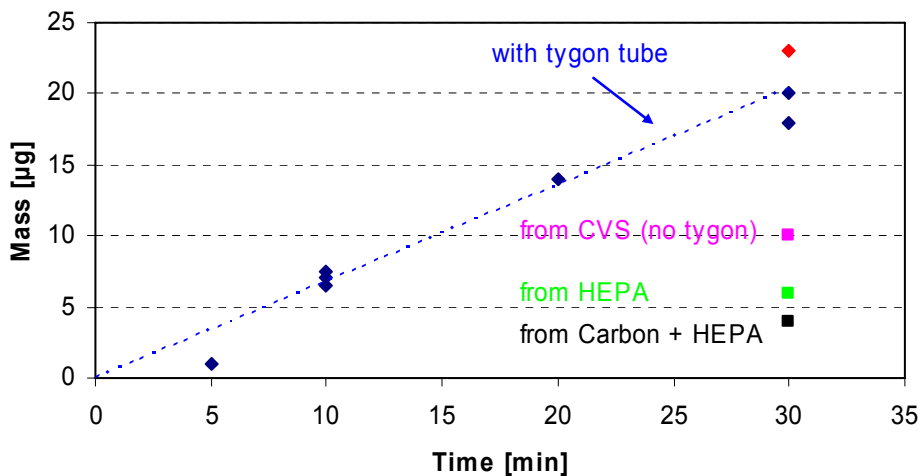


Figure 7: Background mass levels when sampling from the full dilution tunnel (blue points). Mass when sampling directly from HEPA filters are shown (rest colors).

Secondary dilution tunnel (PTS)

The background levels of the secondary dilution tunnel (PTS) were tested with a TSI 3010 particle number counter (d_{50} 10 nm) connected directly at the secondary dilution tunnel (Figure 8-Figure 10). For the PM background 47 mm or 70 mm and TX40 or Teflo filters were used sampling with flow rates between 40 and 60 lpm. The primary tunnel flow rate was 60-80 m^3/min and the engine was off (or disconnected at some tests with the tube closed).

The results showed that the mass collected on the filter (at ambient temperature) was $\sim 20 \mu\text{g}$ with 30 min sampling (TX40, 47 mm, 60 lpm) (Figure 8a). The PN emissions were quite high, around 50 cm^{-3} , although the dilution air for the secondary tunnel is filtered from the same units that filter the air of the primary tunnel (background 1 cm^{-3}). It was found out that the pump installed between the dilution air filtering system and the secondary tunnel produced particles. For this reason a HEPA filter was installed at the line and the levels dropped to $<1 \text{ cm}^{-3}$ (Figure 8b).

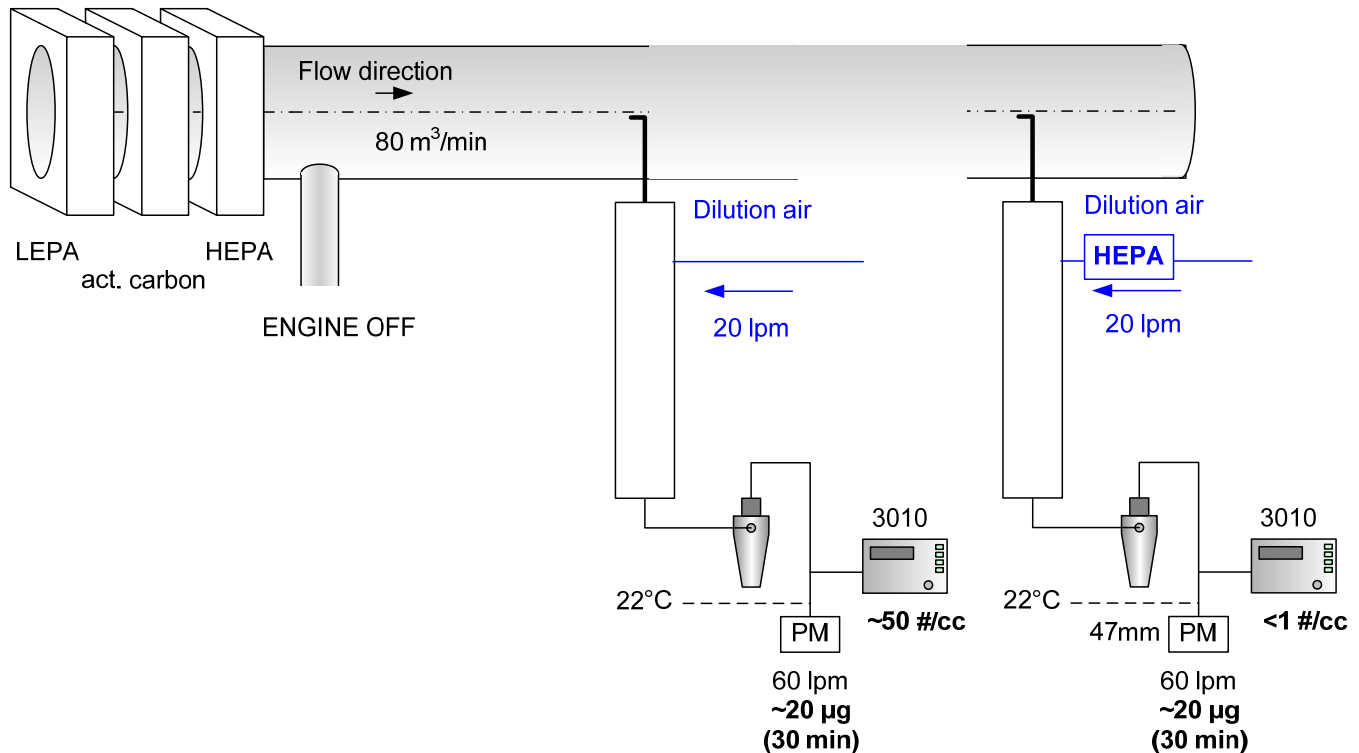


Figure 8: PN and PM background measurements (a) without and (b) with HEPA filter at the dilution air line.

The tests were repeated with heated filter holder at 47°C. Filters of 47 mm (with flow of 40 lpm) and 70 mm (with flow rate of 60 lpm) were used (Figure 9). For these tests backup filters were also installed. The mass collected on the 47 mm filter after 30 min was ~19 µg (and at the backup filter ~4 µg) (Figure 9a). The mass collected on the 70 mm filter after 30 min was ~23 µg (and at the backup filter ~10 µg) (Figure 9b). The loss of mass at the 70 mm backup filter shows that the heating of the filter from ambient temperature (in the weighting room) to 47°C (during the tests) results in evaporation of volatile compounds of the filter. In order to investigate the amount of mass that is evaporated from the filters during the tests, the tests were repeated without any flow at the filter holders (Figure 10). The results showed that the amount desorbed from the 47 and 70 mm filters is within the experimental error ±5 µg.

The tests (without flow) were repeated with 47 mm pre-baked filters (in an oven at 52°C). The mass on the primary was -3 µg and at the backup filter 3 µg. The difference was very small compared to the normal filters (again within experimental uncertainty) suggesting that the pre-baking of the filters is not important (no figure).

Tests were also conducted with 47 mm Teflo filters, which gave similar background (~20 µg for a flow rate of 40 lpm). It must be emphasized that it was impossible to install two Teflo filters. The Teflo filters are thicker and when two filters were installed (main and backup) the filter holder couldn't close tightly and leakage was observed.

Generally the background levels at the secondary tunnel (~20 µg) were higher than at the primary tunnel (~10 µg). It was assumed that the pump in the secondary dilution air line created not only particles but also hydrocarbons. For this reason a carbon filter was also installed in the secondary tunnel dilution air line. The tests were then repeated but the mass collected on the filter was only slightly lower (~17 µg).

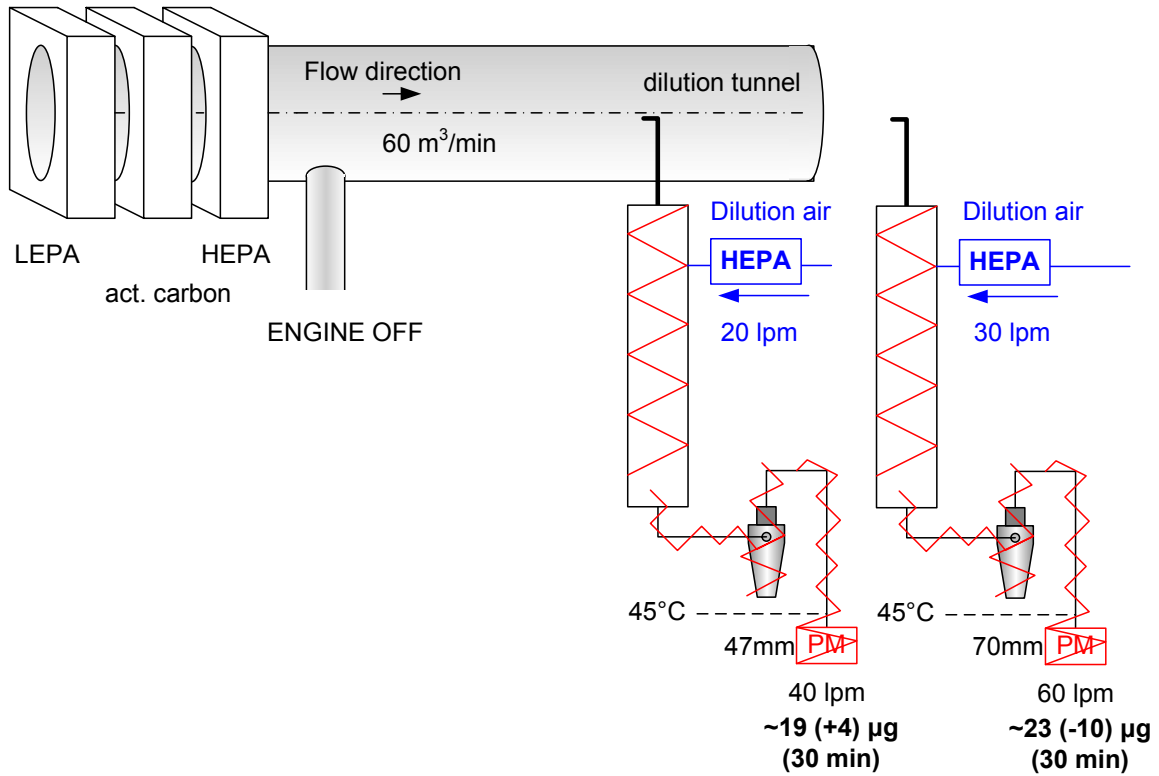


Figure 9: PN and PM background measurements (a) with 47 mm and (b) 70 mm filters. Numbers in parenthesis indicate the mass on the backup filter.

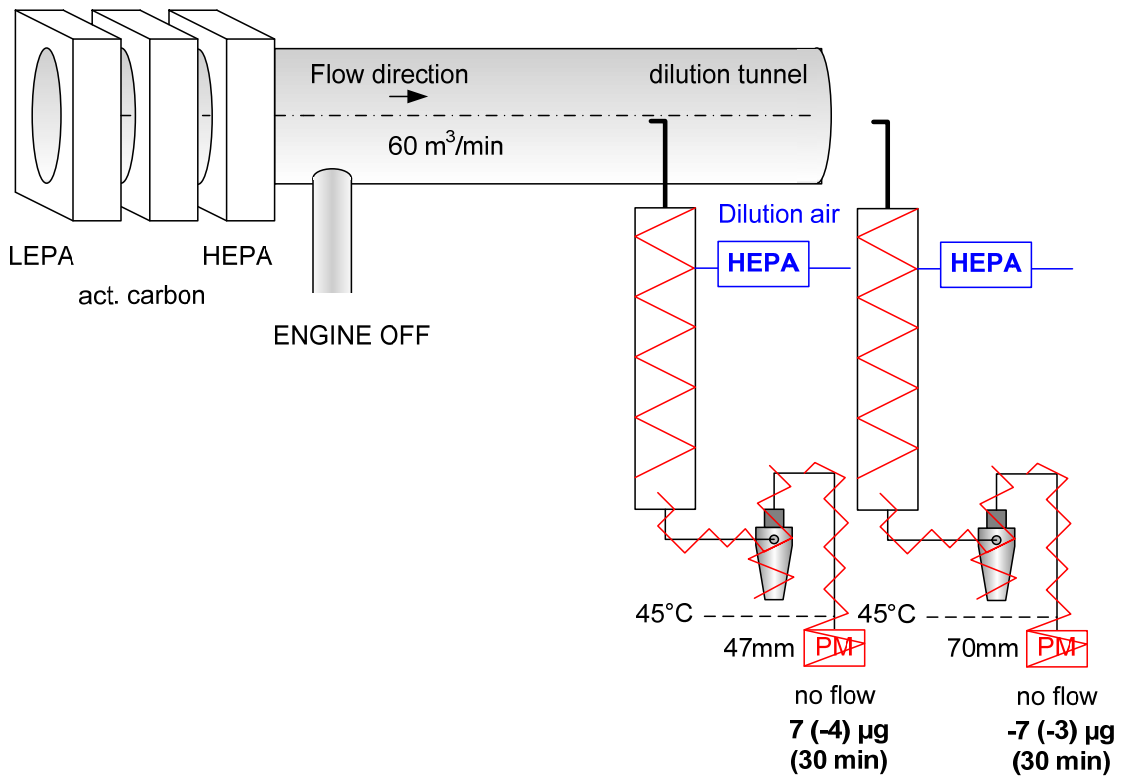


Figure 10: PN and PM background measurements without any flow (a) with 47 mm and (b) 70 mm filters. Numbers in parenthesis indicate the mass on the backup filter.

FILTER TESTS

At a next step the emissions of the engine with different filter media and flow rates were tested for the WHSC (WHSC). The results can be seen in Figure 11. In the same figure the background (BG) levels (as identified from the tests reported in the previous section) are shown.

It is interesting to note that, depending on the filter combination used, the results are different. This has to do with the volatile material collected on the filter (volatile artifact) which depends on parameters like the available surface, the flow rate and the filter material (Andersson et al. 2004, Khalek 2005, 2006, 2007).

The WHSC PM emission levels of the 70 mm filters were 4.5 mg/kWh on the main filter and 2 mg/kWh at the backup filter. The background levels were estimated 1 mg/kWh. It was observed that the emissions with the 70 mm filters were higher than in the rest cases. Probably, this had to do with the low filter face velocity (~43 cm/s calculated for 47°C for 60 lpm). It was not possible to increase the filter face velocity as the maximum flow rate for the secondary dilution tunnel is 60 lpm. The tests with the TX40 filters at 40 and 60 lpm (filter face velocities 69 and 103 cm/s respectively) gave similar emissions (3 at primary and 1.5 mg/kWh at backup filter). This is more or less the filter face velocity range specified in the inter-lab guide. This means that within these limits there shouldn't be observed any differences (of the volatile artifact) on the mass emissions due to different flow rates used. The pre-baked 47 mm TX40 filter gave slightly lower emission for the primary filter but the difference was not statistically significant. The background level of the pre-baked filters was similar with the normal filters suggesting that the pre-baking of the filters is not necessary and does not offer any advantages. Finally, the Teflo filter seemed to give lower emissions but more measurements are necessary to support this. Moreover, as the Teflo background was at similar levels with the rest filters it seemed that again there was no major advantage using these filters. So, for the official PMP tests, it was decided to use a 50 lpm flow with the 47 mm TX40 filters (without pre-baking).

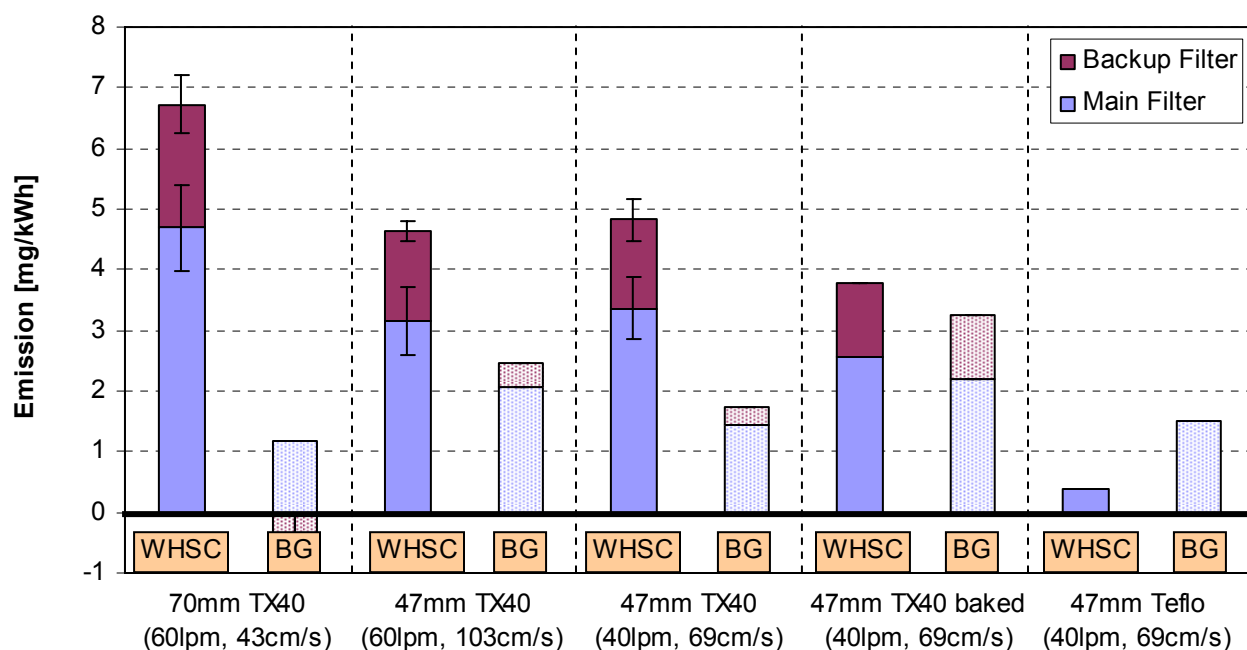


Figure 11: Filter tests results.

CHARACTERISATION OF PARTICLE NUMBER SYSTEMS

The systems used were:

- Particle Number Counters (TSI 3025A, TSI 3010, TSI 3790, TSI 3010D, GRIMM 5.403)
- EEPS (TSI)
- Thermodenuder (Dekati) or evaporation chamber (Dekati)
- Ejector dilutors (Dekati)
- Nanomet (Matter Eng.)
- SPCS (Horiba)

A short description follows:

Particle Number Counters: Various particle number counters were used during the exploratory work. These included the 3025A from TSI (d_{50} at 3 nm, max concentration 10^5), the 3010 from TSI (d_{50} at 10 nm, max concentration 10^4), the 3010D from TSI (d_{50} at 23 nm, max concentration 10^4), the 3790 from TSI (d_{50} at 23 nm, max concentration 10^4) (Liu et al. 2005). A GRIMM 5.403 counter was also used (cutpoint at 3 nm). This counter was upgraded to be able to measure at PMP mode (cutpoint at 23 nm).

Note that, although the PMP requires that the d_{50} should be at 23 nm, particle counters with lower cut-points were also used to identify the contribution of non-volatiles and volatile particles below 23 nm. The results reported here are corrected for coincidence for the 3010 and 3010D counters according to the equation given in their manuals (TSI).

$$N_a = N_i \exp(N_a Q \tau)$$

Where

N_a the actual concentration (cm^{-3})

N_i the indicated concentration (cm^{-3})

Q units transformation $16.67 \text{ cm}^3/\text{s}$

τ effective time each particle resides in the viewing volume

The N_a in the exponent can be approximated by N_i . Three iterations were used for the final result. For the 3010 a reading of 10^4 cm^{-3} needs a 7.4% correction ($\tau=0.4$). For 3010D the correction is +10.6% ($\tau=0.55$). The 3790 uses a continuous, live-time coincidence correction and doesn't need any external correction.

The slope differences were independently investigated (see results below) and their differences will be separately discussed.

EEPS: A 3090 Engine Exhaust Particle Sizer Spectrometer (EEPS) (TSI Inc.) was used for a limited number of tests. EEPS measured particle size distribution with a maximum data rate of 10 size distributions per second (although averages of 1 s were used in the graphs of this study). It measured particle sizes from 5.6 to 560 nm with a sizing resolution of 16 channels per decade (a total of 32 channels). At the instrument's inlet there was a cyclone with a 50% cut-

size at 1 μm (inlet flow rate 10 lpm). By integrating the size distribution the total particle number concentration could be estimated. As the instrument was directly connected to the full dilution tunnel through the particle number sampling probe it was considered that it measured volatiles and non-volatile particles $>5.6\text{ nm}$ (called total particles by convention).

Ejector dilutors: Dekati ejector diluter (EJ) with dry, filtered dilution air at ambient temperature were used. The dilution ratio of the ejector dilutors was determined by measuring sample and total flow rates at ambient temperature and pressure with a 4040 TSI flow meter (Giechaskiel et al. 2004). The first dilutor (#1, 60242) had a dilution ratio of 10.2:1 at ambient conditions, while the second dilutor (#2, 60244) had a dilution ratio of 11.4:1.

For most tests, the dilution air was heated at 150°C and a blanket at 150°C was also used to heat the dilutor's body. The theoretical corrections that should be applied for the different sample and/or dilution air temperatures are shown in Table 3. A correction factor of 0.98 should be applied for the blanket, a correction factor of 0.94 should be applied for the dilution air (the dilution air heats also the sample). A correction of 1.19 to 1.38 should be applied to the second diluter downstream of the evaporation tube due to the high sample temperature. A pressure correction should also be applied to the primary diluter (EJ#1) due to the under-pressure at the sampling point (due to CVS and the 90 lpm pump). For 5 kPa under-pressure the correction should be 1.14 and for 3 kPa (e.g without the 90 lpm, only the CVS under-pressure) 1.08. These number translate to 1.05 (0.94x0.98x1.14) correction for the first diluter and 1.19 to 1.38 for the second (depending how close to the evaporation tube is connected). In these experiments a correction of 1.3 was used as the measured temperature upstream of the secondary diluter was assumed to be 250°C.

Table 3: Theoretical corrections for the dilution ratio of ejector dilutors according to Giechaskiel et al. (2004).

<i>P</i> (s)	<i>T</i> (s)	<i>T</i> (da)	<i>T</i> (m)	<i>Corr</i>	<i>Meas</i>	<i>Comments</i>
100	17	17	(17)	1.00		Normal conditions
100	100	17	(24)	1.12		At CVS (high temperature modes)
100	150	17	(27)	1.19		Downstream evaporation tube (cooled)
100	300	17	(36)	1.38		Downstream evaporation tube
100	17	150	(136)	0.84		Heating of dilution air
100	100	150	(145)	0.94	0.93	Heating of dilution air, effect on sample
97	17	17	(17)	1.08		CVS, under-pressure
95	17	17	(17)	1.14	1.16	CVS, 90 lpm pump under-pressure
100	17	17	150	0.98	0.98	Blanket heating

s Sample

da Dilution air

m Mixture

P Pressure [kPa]

T Temperature [°C]

Numbers in parenthesis are estimations from the model.

No correction for particle losses was applied since according to Ntziachristos et al. (2004), who measured light duty diesel particles, the losses should be less than 5% for particle in the range of 23 to 300 nm.

The filtration system of the manufacturer was not adequate and a HEPA filter was added to the ejector dilution air line to decrease the background levels to $<0.2 \text{ cm}^{-3}$.

Thermodenuder: A thermodenuder (TD) from Dekati Ltd. was used for some measurements to remove volatile particles. The temperature of the heater was set to 275°C (residence time 0.3 s for 10 lpm flow rate). The carbon section had an annular design, i.e. the carbon was placed at both sides of the sample flow. The inner cylinder is cooled by forced convection (air in these experiments) and the outer by natural convection. The residence time in this section was 2.7 s (for a flow rate of 10 lpm). The particle losses L are given by the equations (Ntziachristos et al. 2004) (for 250°C):

$$L = -9.7 \ln D_p - 0.5Q + 68 \quad \text{for } 30 < D_p < 70 \text{ nm}$$

$$L = -0.5Q + 28.7 \quad \text{for } 70 < D_p < 500 \text{ nm}$$

Where

D_p is the particle size [nm] and

Q is the flow rate through the thermodenuder [lpm] (10-20 lpm).

These equations were used to estimate the losses when the particle size distribution was known. A correction factor of 1.28 was used for the calculation of the results (losses 22%) when the size distribution was unknown (Ntziachristos et al. 2004). It was also shown that using a constant factor for size distributions without nucleation mode has $<1\%$ error in comparison with the size dependant correction when there is only accumulation mode (peak $>70 \text{ nm}$) (Ntziachristos et al. 2005). However, when there is nucleation mode the losses should be taken into account.

The thermodenuder (without any diluter) in these tests was often used as a volatile removal system. (e.g. to dry diesel exhaust particles before using them to evaluate the performance of various instruments). The volatile removal efficiency of the thermodenuder was investigated during these tests and the results will be shown in the “Results” section.

Evaporation chamber: An evaporation chamber (L [cm] x D [cm] = 7 x 3.5) from Dekati Ltd. was used for some tests. The temperature was set to 330°C . The volume was 67 cm^3 and for a flow rate of 2.6 lpm (the flow rate of modified ejector dilutor downstream of the evaporation chamber) the residence time was $\sim 1 \text{ s}$.

Nanomet: A recently bought rotating disk based system from Matter Eng. was used. This system consists of a primary rotating disk diluter heated at 150°C , a 1 m line, an evaporation tube at 300°C and a secondary simple mixer diluter. Both diluters have adjustable dilution ratios. Total dilution ratio of 250 was used (50 x 5) in these experiments (Potentiometer setting of primary diluter at 50%). The primary dilution ratio was the reduction factor of 80 nm CAST particles from the manufacturer. As the peak of the accumulation mode was close to 80 nm (e.g. see Figure 63) the primary dilution factor of the manufacturer includes partly the losses in the system. The secondary diluter is a simple mixer and is not expected to have losses. Thermophoretic losses were not taken into account. Although preliminary tests showed good

agreement with the rest particle number systems, some issues came up after the exploratory work finished were:

- The 3790 TSI CPC (d_{50} at 23 nm) of the system had problem with the condenser temperature.
- The primary dilution factor was not changing much when the potentiometer setting was changing.
- The peristaltic pump failed during the tests and it was not possible to use the instrument.

For these reasons, the system was used only for a limited number of tests and then it was sent back to the manufacturer for repair. It was not also available for volatile removal efficiency, dilution ratio measurement and penetration measurements.

Old Nanomet: For a limited number of tests the old golden system was also used (previous version of Nanomet). The setting at the potentiometer was 20% (primary dilution ratio 55 with the temperature correction), the dilution temperature was 150°C, 1 m line was used and the evaporation tube temperature was 300°C. The secondary dilution ratio was 5.2 (because no particle counter was used upstream of the evaporation tube. This system was calibrated last time in Feb 2007. Since then it was used in CARB. It arrived back to JRC in Nov 2007. The following problems were found and repaired:

- The axis that connects the rotating disk with the dilution head was broken.
- There was a leakage between the dilution head and the controller unit (the o-rings were missing)

Flow measurements after the repair at JRC showed that the unit should be operating properly. This system was also calibrated in JRC (see Results below).

SPCS: Solid Particle Counting Systems (SPCSs) from Horiba consists of a primary hot diluter (PND1) at 150 to 200 °C, an evaporation tube (300 to 400 °C) and a secondary diluter (PND2) at ambient temperature (Wei et al. 2006). The PND1 can be adjusted between 2:1 to 100:1 or between 8:1 and 1000:1 depending on the orifice being used. PND2 dilution ratio can be adjusted between 10:1 and 50:1. A TSI 3010D is included in the instrument.

For tests at JRC, the temperatures set at the units were:

- Cabinet temperature (before primary dilution): 47°C
- Hot dilution air temperature for PND1: 170°C
- Mixer Temperature for PND1: 170°C (It is set as same as hot dilution air temperature)
- Evaporation tube: 350°C

The manufacturer's dilution ratios are derived from flow rate measurements. The user defines (in the prototype units used) the primary (PND1) dilution ratio, the secondary (PND2) dilution ratio, the primary (PND1) and secondary (PND2) dilution air flow rates and the bypass flow rate. These flows refer at 70 °F (21.1 °C) and 760 mmHg (1 atm) ambient air pressure. The main purpose of the by-pass is to decrease the residence time. As a result the diffusion losses in the transfer line and response time of the instrument are reduced.

Typical values that were used at the exploratory JRC test are (unless otherwise specified):

- PND1: Primary hot dilution ratio: 10, Primary dilution air: 11.5 (lpm)
- PND2: Secondary cold dilution ratio: 8-15, Secondary dilution air: 10.5 (lpm).
- Bypass: 2 (lpm)

The results of SPCS shown in this report are always corrected for the dilution ratios measured from the unit. No correction for particle losses was applied at this report. These issues were separately investigated. More information about the instrument operation can be found in Appendix D.

CPCs comparisons

The set up for the comparison of the CPCs of the SPCS units can be seen in Figure 12. Ambient air was diluted with filtered air to achieve different particle number concentrations and passed through a thermodenuder. The two 3010D CPCs from the SPCS units and a 3790 CPC were downstream of the thermodenuder, so it can be assumed that non-volatile particles were fed to the particle counters. The instruments had similar residence times. The main reason that an extra pump was used in the set up was to ensure that the flow rate through the thermodenuder was ~10 lpm. In addition, the split of the flow was conducted with “T” splitters and not with “Y”. It was observed in the past that when a T splitter is used for two instruments then there are losses and big differences can be found between the instruments. However, when an instrument samples from a T splitter when there is a continuous higher flow, the losses are negligible. Thus the extra pump served also to have a continuous high flow in the tubes. All tests were conducted with a similar way.

The results can be seen in Figure 13. The 3010D CPCs have been corrected for coincidence. The two 3010D CPCs have 1-5% difference with each other across the range of 1 to 10^4 cm^{-3} (Figure 13). The CPC 70507004 (at SPCS-20) measures slightly lower which is in agreement with its lower slope (slope 0.95) compared to the CPC 70524211 (at SPCS-19) (slope 0.99). There is a 11% difference compared with the 3790 CPC (Figure 14).

The 3010D (old golden CPC) and the Nanomet 3790 (3790n) were also compared with the 3790. WHTCs (engine with open filter) were run and the two instruments were connected downstream of the ejector dilutors and the TD. This way it was ensured that the CPCs were measuring only non-volatile particles. The results can be seen in Figure 15 and Figure 16. There is a 5% and 12% difference respectively. The Grimm PMP was compared with the 3790n over transient cycles downstream of a dual ejector system with an evaporation tube in between (Figure 17). Thus non-volatile particles were fed to the two counters. For concentrations $<10^4 \text{ cm}^{-3}$ the slope was 1. At higher concentrations the slope was 0.93.

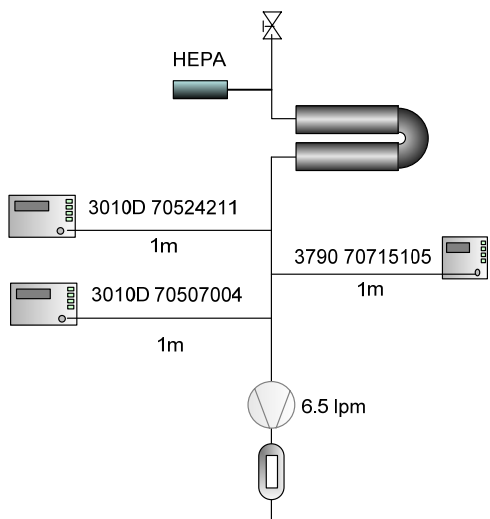


Figure 12: Schematic set up for the comparison of SPCSs' CPCs.

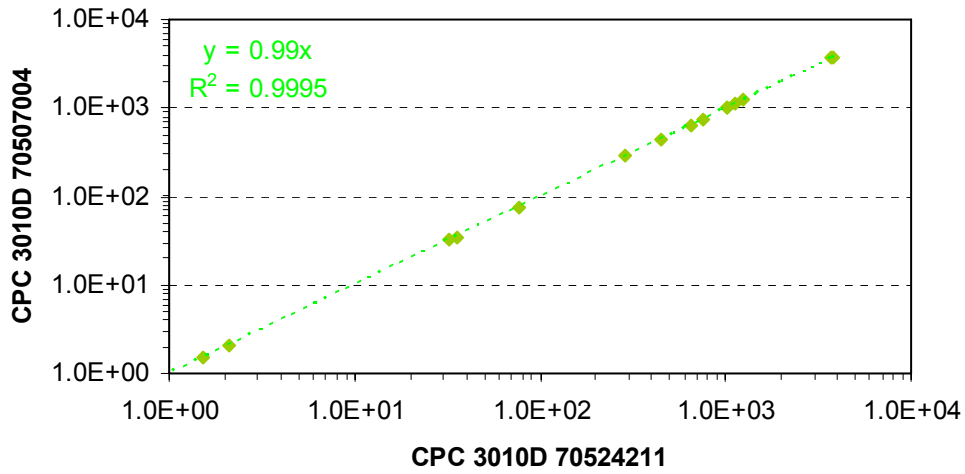


Figure 13: Comparison of the two SPCSs CPCs.

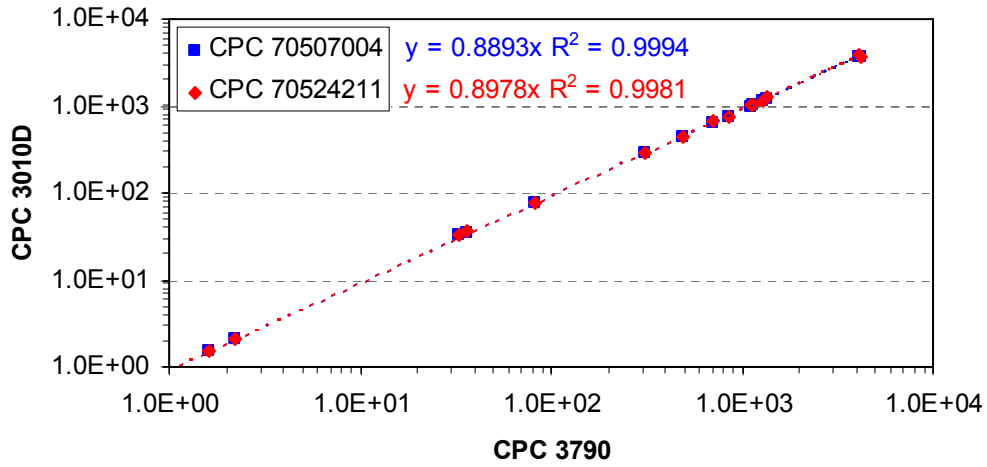


Figure 14: Comparison between SPCSs CPCs and the 3790 CPC.

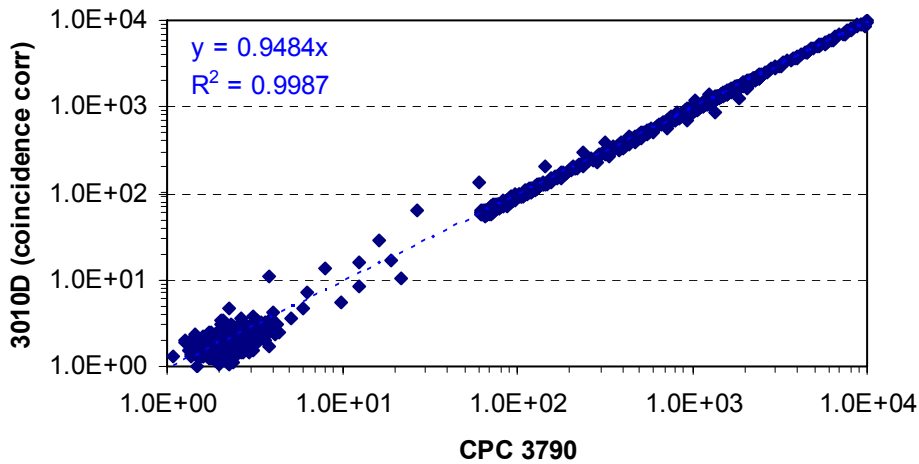


Figure 15: Comparison of the CPC 3010D (old golden) with the CPC 3790.

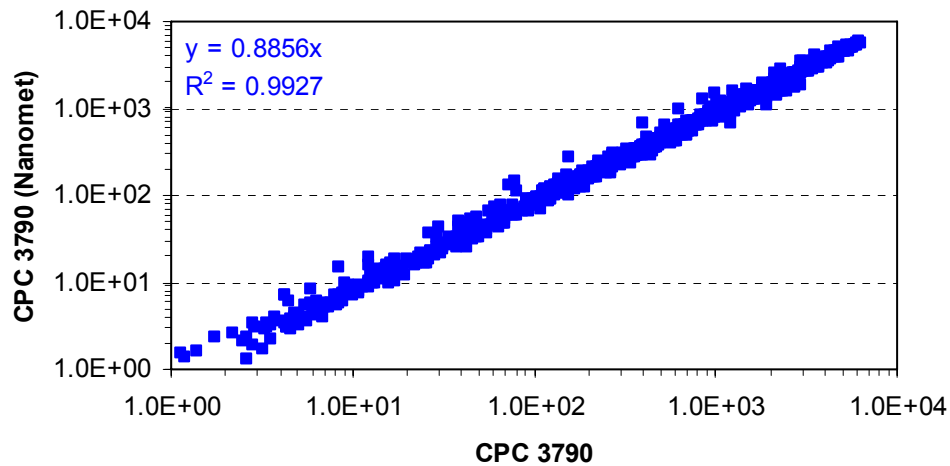


Figure 16: Comparison of the Nanomet 3790n with the 3790.

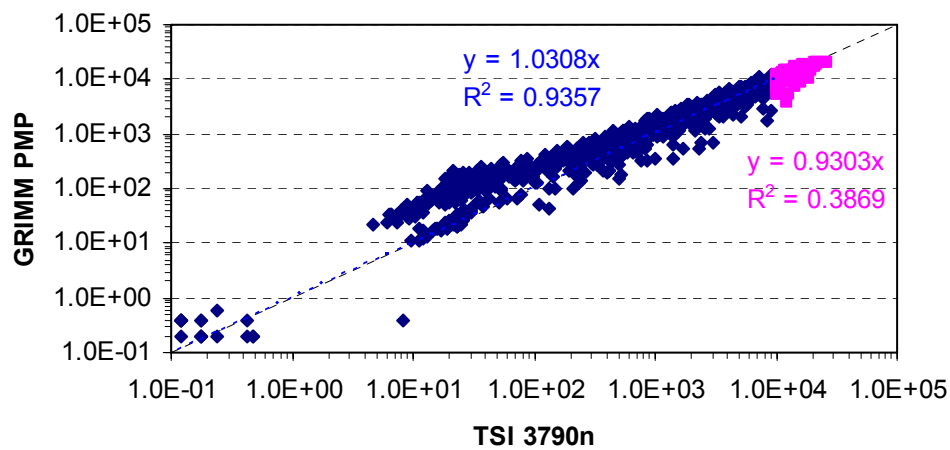


Figure 17: Comparison of the Nanomet 3790n with GRIMM PMP.

Table 4 shows the final corrections that should be applied to the various CPCs based on the previous results. This correction is mentioned in the text every time that is applied (if applied). The important finding is that most counters had minor differences with the exception of one 3790 counter.

Table 4: Slopes and final correction at this report for various CPCs. Numbers in parenthesis are calculated indirectly.

CPC	Manufacturer's slope	Comparison with CPC at SPCS-19	Correction for this report
GRIMM PMP	1.00	(-1%)	+1%
Old golden 3010D	0.97	(+5%)	-5%
3010D (SPCS-19)	0.99	0%	0%
3010D (SPCS-20)	0.95	-1%	+1%
3790	0.99	+11%	-11%
Nanomet 3790n	0.95	(-1%)	+1%

Volatile Removal Efficiency

The set up for the volatile removal tests can be seen in Figure 18. A Horiba C40 particle generator produced particles. For the polydisperse tests a SMPS (TSI 3936 (3080L+3010) or a nano-SMPS (3085N+3025A)) was used upstream and downstream of the systems under investigation (SPCS, old nanomet, TD, EJ+TD, EJ, EJ+ET+EJ). For some tests extra CPCs were also used upstream and downstream of the systems to measure the volatile removal efficiency. For the monodisperse tests a TSI 3080L DMA was used after the generator. Then the 3790 and/or the 3025A were used to estimate the efficiency. For all tests the instruments were connected upstream and downstream at least 2 times and the average value (of the same instrument) is reported.

Table 5 summarizes the results:

- Tests with polydisperse aerosol with peak at 35 nm and concentration $8 \times 10^6 \text{ cm}^{-3}$ (Figure 19) showed that all instruments remove efficiently the C40 particles. However the TD left a small NM with peak at 13 nm.
- Tests with peak at 171 nm an concentration $1.6 \times 10^4 \text{ cm}^{-3}$ (Figure 20) showed again that all systems remove efficiently the C40 particles with the exception of the TD which left a NM with a peak at 16 nm. The low value for the dual ejector system is probably due some small particles around 10 nm. Similar results were drawn with a peak at 207 nm and concentrations in the order of $2 \times 10^4 \text{ cm}^{-3}$.
- A more severe test was repeated with two C40 peaks (around 40 and 200 nm and total concentration $2 \times 10^6 \text{ cm}^{-3}$) (Figure 21). Most systems removed efficiently the C40 particles. However, the hot ejector dilutor and the TD were unable to remove them.
- The monodisperse tests (30 nm concentration 1×10^4) showed that SPCS and TD efficiently remove C40 particles with concentrations $> 10^4 \text{ cm}^{-3}$. The lower efficiency of the old Nanomet was probably due to the high background levels of the instrument (5 cm^{-3}), as it was shown previously with the polydisperse aerosol that it removes C-40 particles.

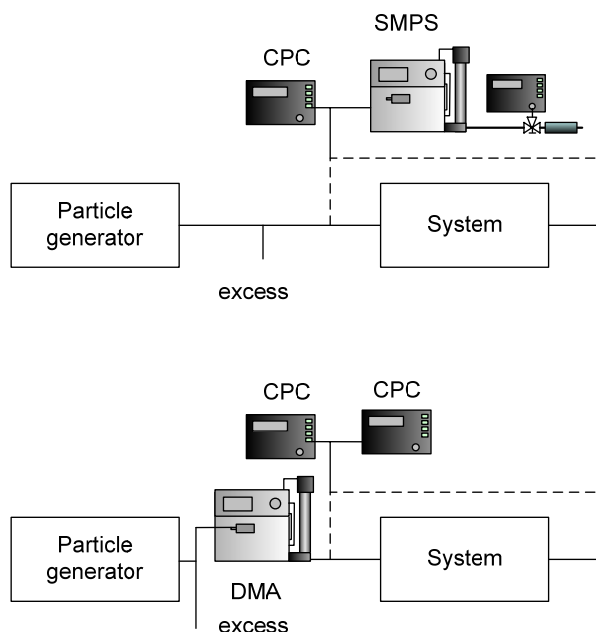


Figure 18: Setup for calibration tests (volatile removal and penetration) a) polydisperse aerosol b) monodisperse aerosol.

Table 5: Summary of volatile removal efficiency results.

Aerosol	Mode 1	Mode 2	Instrument	DR	Mode	nanoSMPS	Eff	3025A	Eff	JRC 3790	Eff
Polydisperse	35	-	Old Nanomet	270	-	8.00E+06	99.99%	-	-	-	-
Polydisperse	35	-	SPCS	150	-	8.00E+06	99.99%	-	-	-	-
Polydisperse	35	-	E+ET+EJ	143	-	8.00E+06	100.00%	-	-	-	-
Polydisperse	35	-	TD	1	13	8.00E+06	99.98%	-	-	-	-
Polydisperse	35	-	EJ+TD	10.5	-	8.00E+06	100.00%	-	-	-	-

Aerosol	Mode 1	Mode 2	Instrument	DR	Mode	SMPS	Eff	3025A	Eff	JRC 3790	Eff
Polydisperse	-	171	EJ+ET+EJ	143	-	1.61E+04	86.45%	2.45E+04	99.94%	2.05E+04	99.97%
Polydisperse	-	171	EJ+TD	10	-	1.61E+04	98.18%	2.45E+04	99.57%	2.05E+04	99.94%
Polydisperse	-	171	TD	1	16	1.61E+04	96.99%	2.45E+04	93.55%	2.05E+04	99.50%
Polydisperse	-	171	SPCS	150	-	1.61E+04	97.80%	2.45E+04	99.97%	2.05E+04	100.00%
Polydisperse	-	207	EJ+ET+EJ	143	-	1.89E+04	81.66%	1.90E+04	99.76%	-	-
Polydisperse	-	207	TD	1	12	1.89E+04	96.78%	1.90E+04	80.26%	-	-
Polydisperse	-	138	Old Nanomet	270	-	1.41E+05	94.37%	-	-	-	-
Polydisperse	35	175	EJ+ET+EJ	143	-	1.74E+06	99.52%	-	-	-	-
Polydisperse	35	175	EJ+TD	10	13	1.74E+06	99.94%	-	-	-	-
Polydisperse	38	204	TD	1	43	3.05E+06	84.01%	-	-	-	-
Polydisperse	40	233	EJ	10	34/210	4.37E+06	26.74%	-	-	-	-
Polydisperse	40	233	SPCS	150	-	4.37E+06	99.99%	-	-	-	-

Aerosol	Mode 1	Mode 2	Instrument	DR	Mode	SMPS	Eff	3025A	Eff	JRC 3790	Eff
Monodisperse	30	-	TD	1	-	-	-	8.02E+04	100.00%	1.00E+04	100.00%
Monodisperse	30	-	Old Nanomet	270	-	-	-	-	-	1.38E+04	89.51%
Monodisperse	30	-	SPCS	150	-	-	-	-	-	1.01E+04	99.45%

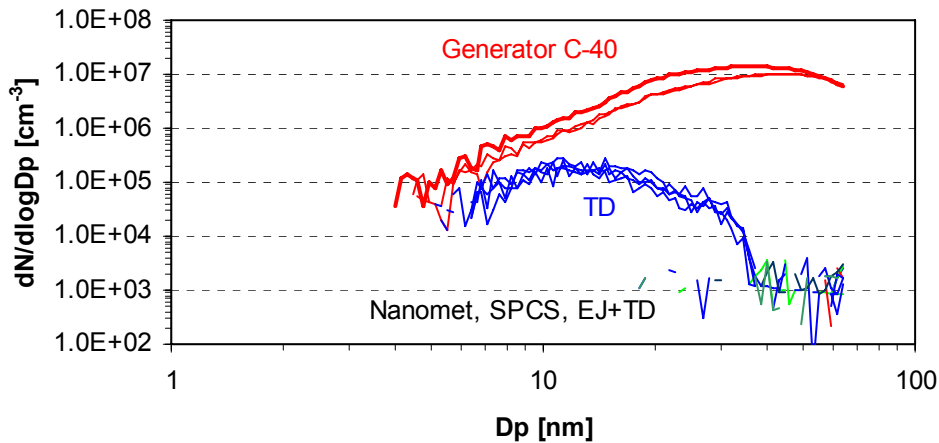


Figure 19: Volatile removal efficiency of various systems sampling polydisperse C40 particles (peak 35 nm).

Volatile Removal Efficiency with diesel engine exhaust gas

The volatile removal efficiency was also checked with diesel engine volatile particles. The set up can be seen in Figure 22. An EEPS was used to measure the particle number size distribution directly from the full dilution tunnel, while SPCS-20 and a 3790 CPC downstream of a thermodenuder were used to measure the non-volatile concentration.

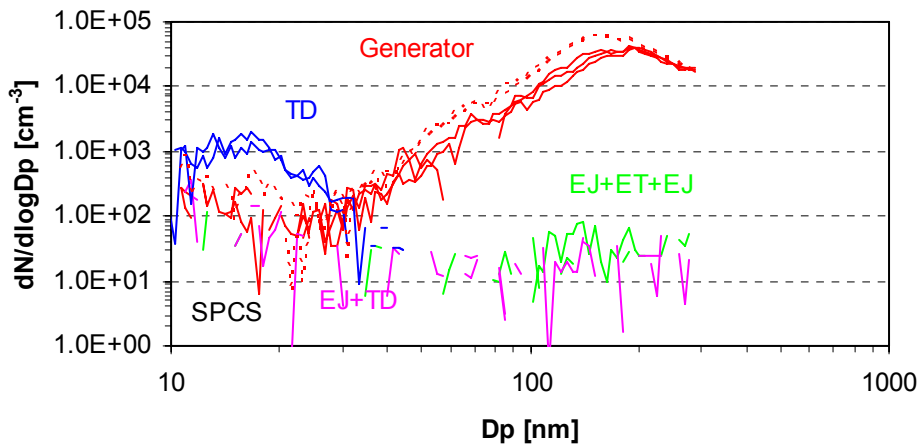


Figure 20: Volatile removal efficiency of various systems sampling polydisperse C40 particles (peak 171 nm).

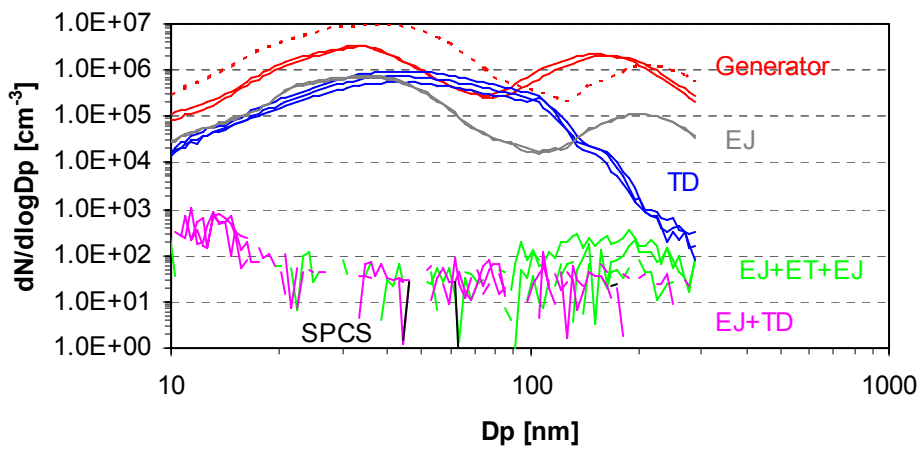


Figure 21: Volatile removal efficiency of various systems sampling polydisperse C40 particles (peaks at 35 and 171 nm).

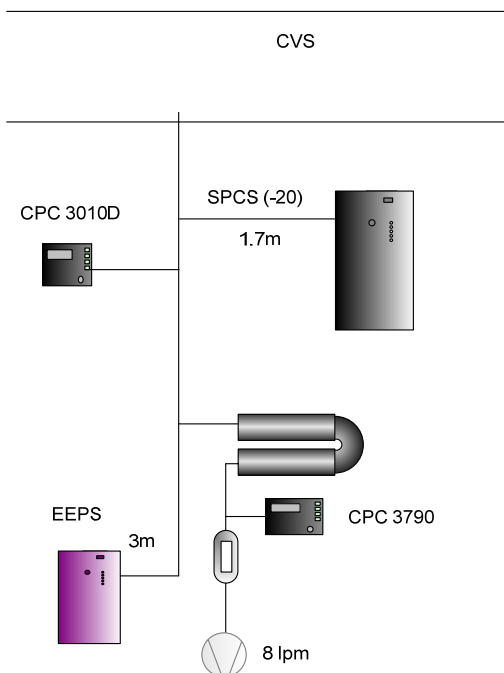


Figure 22: Schematic set up for the removal efficiency evaluation.

To test the ability of the instruments to remove volatiles at higher concentrations a regeneration test was conducted. Figure 23a shows the emissions during mode #10 ESC (regeneration) and mode #7 ESC (loading). Figure 23b shows the (total) particle number size distribution during the tests. Before the beginning of mode #10 the engine was warmed up at a low temperature mode (mode #4) for 10 minutes. The size distribution 1 shows that at the beginning of mode #10 there is only accumulation mode particles as the temperature is still low and no regeneration has started. It should be emphasized however that the concentrations measured are close to the detection limit of the instrument and should be viewed with care. Later a big nucleation mode is formed (size distribution 3). There is a slightly higher accumulation mode indicating that some particles escape from the filter (as the filter cleans). As the time passes and the filter regenerates, the peak of the nucleation mode decreases (size distribution 6). These particles could be formed from the high SO₂ to SO₃ conversion at these high temperatures and the subsequent condensation of hydrocarbons on the formed H₂SO₄ during the cooling in the full dilution tunnel (Giechaskiel et al. 2005, Kittelson et al. 2005, Giechaskiel et al. 2007a, b). As the engine changes from mode #10 to mode #7 a huge nucleation mode is formed (size distribution 7) due to the lack of available surface for condensation. Then as the temperature decreases, also the nucleation mode decreases and finally it disappears (size distribution 8).

A huge increase of particles is observed during the transition from mode #10 to mode #7 due to the decrease of the non-volatile concentration. The volatile concentration is $1.2 \times 10^7 \text{ cm}^{-3}$ and the peak is at 16 nm (Figure 23b). Both SPSC and TD+CPC remove efficiency this high concentration of volatiles (efficiency >99.99%). This is probably the worst condition that the instruments will face during the tests, so it can be safely assumed that they will measure only non-volatiles during the official measurement campaign (no nucleation mode particles will survive). Although the pattern of SPCS and the thermodenuder are identical, there is a 15% difference (taking into account the differences of the CPCs see Table 4). As it will be discussed later this difference can be due to dilution ratio uncertainty, losses in the SPCS, the possible differences in the cut-points of the CPCs and the different heating temperatures at SPCS and the thermodenuder. The thermodenuder in this study was set at 275°C, while the evaporation tube of the SPCS-19 was set to 350°C. This means that some semi-volatiles could be measured downstream of the thermodenuder but not in SPCS. For example, Figure 19 shows that the TD cannot remove completely the volatiles and some of them remain (peak 13 nm). Part of them could be measured by the 3790.

Dilution Ratios

The Dilution Ratios (DR) were measured with 1.52% ($\pm 2\%$) propane gas. An AVL CEB II analyzer was used to measure the diluted gas. The flow had to be throttled to 3 lpm to permit the measurements downstream of the SPCS. The throttled line was used for all tests. Comparison of the “throttled” value to the normal showed that there was no difference (only 2 ppm difference of a measurement at 260 ppm). The background was measured at the beginning of the tests and was found around 20 ppm. This background was taken into account in the calculations of the DRs.

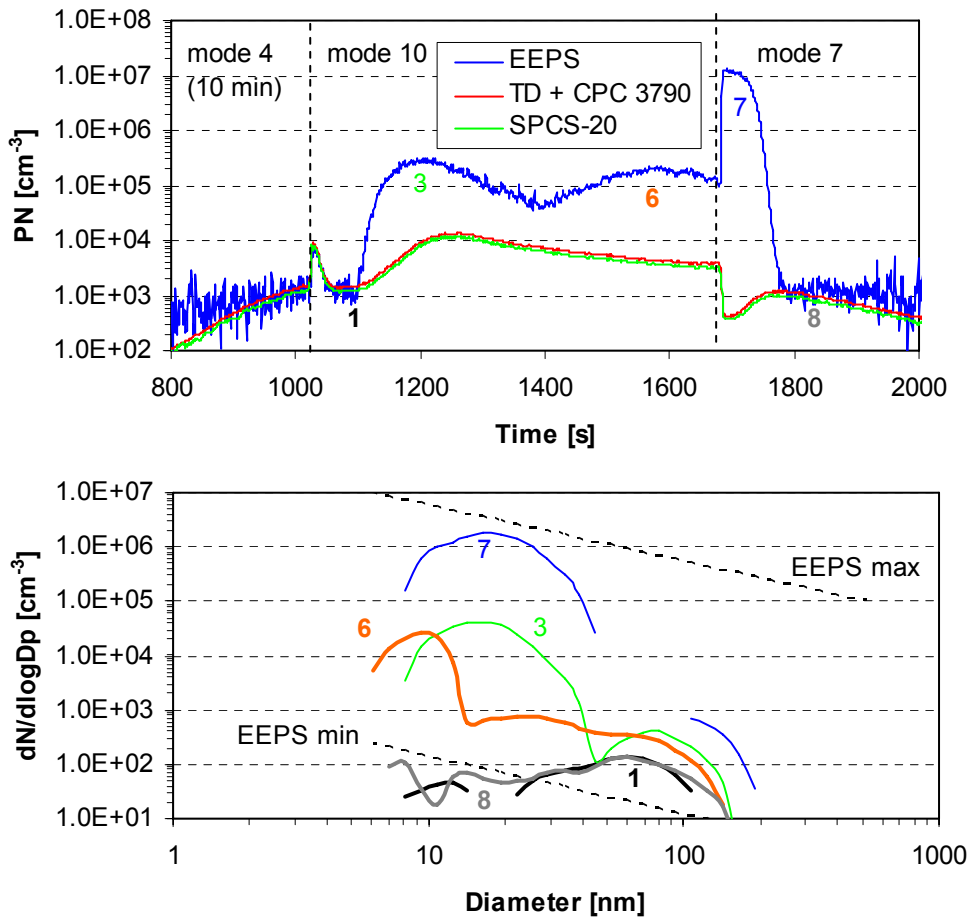


Figure 23: a) Total (EEPS) and non volatile (SPCS, TD+CPC) emissions during the preconditioning phase. Numbers indicate the time moments of the size distribution of the next panel b) Total particle size distribution (from EEPS).

Old Nanomet

The DR was measured at 20% and 60% rotation. Table 6 shows the results. Due to high background level, the uncertainty at 20% and 60% rotation settings was 5% and 2% respectively. The under-pressure (measured with a TSI 4040 flow meter, that measures also pressure, at the inlet of the Nanomet) had as an effect a 25-30% increase of the measured DR.

Table 6: Measured DRs and comparison with manufacturer's value for ambient pressure and underpressure.

DR	Potentiometer 20%	Potentiometer 60%
Manufacturer (PRF)	283	94
Measured at ambient pressure	250 ($\pm 5\%$)	87 ($\pm 2\%$)
Manufacturer's difference (ambient pressure)	-11%	-8%
Measured at under-pressure (-8.5 kPa)	317	113
Effect of under-pressure (-8.5 kPa)	+25%	+29%

Ejectors

The DR was measured with the diluters heated at ambient pressure, under-pressure and overpressure. The primary diluter was heated at 150°C with the blanket, the dilution air was set at 150°C, the evaporation tube at 330°C and the secondary diluter not heated. Table 7 shows the measurements and the results from the model. If the nominal dilution ratios (10.2x11.4) were used the results would be wrong. It is very important for the users of the ejector diluters to apply the correction factors given in Table 3.

The measurements showed that there is an important effect of the pressure upstream of the ejector diluters. The model corrects for this pressure correctly.

Table 7: Measured DRs and comparison with model's value for ambient pressure, overpressure and underpressure.

	<i>Measured DR</i>	<i>Model DR</i>
Ambient pressure	139	139 (=10.2x0.93x11.4x1.3)
Under-pressure (-9 kPa)	194	185
Overpressure (+4 kPa)	128	128
Effect of under-pressure (-9 kPa)	+40%	+32%
Effect of overpressure (+4 kPa)	-8%	-8%

SPCS

Table 8 shows the measured DRs and their difference compared to the software values. The difference is less than ±5%. Table 9 gives the effect of under-pressure on the DR of the instrument. A high under-pressure of 9 kPa has only a minor effect on the DR.

Table 8: Measured DRs and comparison with manufacturer's value for different DR settings.

<i>Setting</i>	<i>Total DR</i>	<i>Measured DR</i>	<i>Measured DR</i>
10x15	150	144.7	3.7%
25x15	375	399.7	-6.2%
40x15	600	584.2	2.7%
10x15	150	144.2	4.0%
10x25	250	253.2	-1.3%
10x40	400	425.9	-6.1%
10x15	150	144.7	3.7%
40x15	600	549.0	9.3%

Table 9: Measured DRs and comparison with manufacturer’s value for ambient pressure and under-pressure .

<i>DR</i>	<i>Measured</i>	<i>Software</i>
Ambient pressure	148	150
Under-pressure (-9 kPa)	140	-
Effect of under-pressure (-9 kPa)	-6%	-

To further investigate the under-pressure effect, a TSI 4040 flowmeter (which measures also pressure and temperature) was connected upstream of the SPCS-19. A pump was also connected in parallel to affect the pressure (Figure 24). SPCS-19 and the pump were sampling ambient air through a tube that its inner diameter was changed with a throttling valve. Figure 25 shows the difference between the flow rate and the measured from SPCS value. At ambient pressure there was no difference and at -10 kPa under-pressure the SPCS flow rate was -1.5% less. This difference means a real DR 1.5% less than the SPCS indicated. However, it is within the uncertainty of the 4040 flowmeter at these low flowrates (3.5 lpm while the specific flowmeter goes up to 300 lpm). It is interesting to note that a -10 kPa under-pressure decreased the sample flow rate 4%, but this decrease was taken into account in the dilution ratio calculation, as this flow rate was measured correctly (1.5% uncertainty). The flow rate measurement was also checked at different SPCS-parameters at ambient pressure and the difference with the 4040 flow meter was always $\pm 1.5\%$.

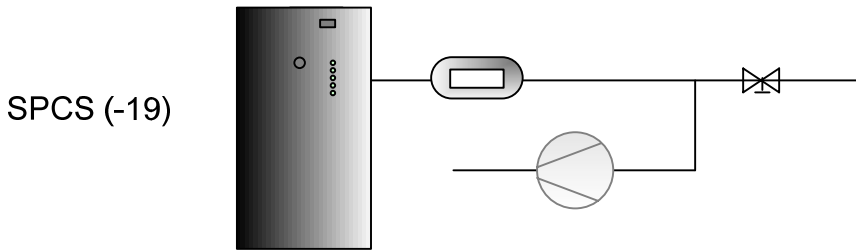


Figure 24: Set up for the measurement of the sample flow rate for different pressures

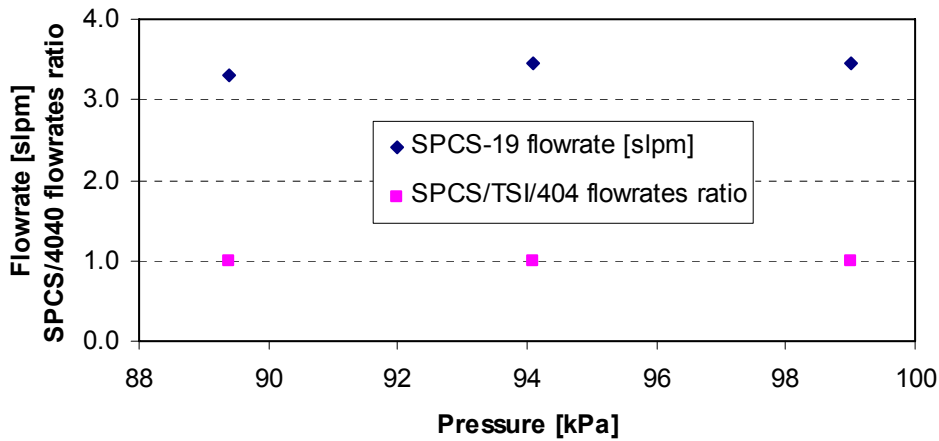


Figure 25: Effect of under-pressure on SPCS’s sample flow rate.

Penetrations

The penetrations were measured with monodisperse aerosol at diameters 30, 50, 70 and 100 nm. The set up can be seen in Figure 18b. The JRC salt generator (evaporation-condensation technique) gave peaks in the range of 15-30 nm. In addition, the 3025A was used which has a 50% cut-point at 3 nm. For the 100 nm particles the HORIBA salt generator was used (nebulizer). However, for lower diameters it gave very strange results, probably because the peak was around 70 nm and for lower diameters (30 and 50 nm) the multi-charge effect was very high. In addition, the 3790 PNC was used for these experiments and the low efficiency (for salt particles) at 30 nm had as a result high uncertainty to the measurements (small change of the diameter a few nm changes sharply the counting efficiency).

Old Nanomet

The penetrations were measured with 20% rotation. A DR value of 250 was used for the calculation of penetrations (see Table 6). The results are in close agreement with the results of AEA during the 2 years duration of the light duty programme (Figure 26) (Andersson et al. 2007, Giechaskiel et al. 2008b). Table 10 gives the measured penetration values for various diameters.

It should be emphasized at this point that downstream of the DMA the pressure is 1-3 kPa less than the ambient pressure where the DR measurements were conducted. As the rotating disk diluter is a volumetric diluter, this under-pressure affects its DR. This effect was estimated from Table 6. This ratio was around 1.05 and this correction was applied to the penetrations presented.

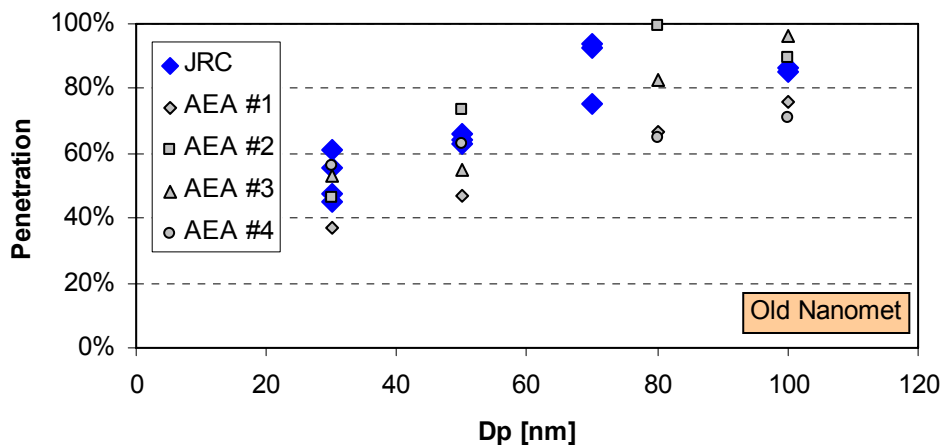


Figure 26: Old Nanomet's penetrations at JRC. AEA's results during the light duty PMP programme are also shown.

Table 10: Average penetrations and standard deviation of the penetrations.

Diameter	30 nm	50 nm	70 nm	100 nm
Penetration	52%±7%	65%±1%	91%±10%	90%±1%
PMP Light duty	49%±8%	60%±11%		83%±124%

SPCS

The penetrations were measured at 10x15 setting. A DR of 148 was used for the calculations (Table 9). Figure 27 shows the results and Table 11 gives the average results. These results are higher than the published data (Wei et al. 2008). According to the manufacturer solid particle losses should be less than 15% for monodisperse aerosol (Wei et al. 2006) and 5% for polydisperse aerosol (Wei et al. 2008). However 30% losses for 30 nm particles were measured here. It is possible that the particles generated by the evaporation-condensation technique are affected in the evaporation tube (e.g. they shrink). This would shift the penetration values to the left (lower diameters). This has to be further investigated (e.g. see humidity effect on NaCl particles, e.g. Biskos et al. 2006).

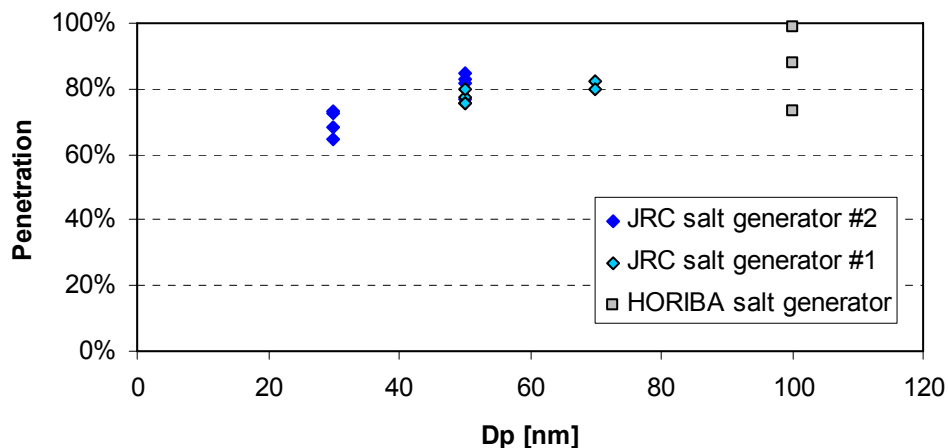


Figure 27: SPCS's penetrations at JRC.

Table 11: Average penetrations and standard deviation of the penetrations

Diameter	30 nm	50 nm	70 nm	100 nm
Penetration	70%±4%	82%±3%	81%±2%	86%±12%

Particle Reduction Factors (PRF)

The particle reduction factors are the ratio of upstream to downstream concentration of a monodisperse aerosol.

Old-Nanomet

The results are shown in Table 12. The losses of 30 nm particles are very high and:

$PRF(30nm)/PRF(100nm)=1.74$ (much higher than the 1.3 allowed)

$PRF(50nm)/PRF(100nm)=1.31$ (much higher than the 1.2 allowed)

$PRF(average)=1/3*[PRF(30)+PRF(50)+PRF(100)]=394$

The $PRF(average)$ (which would be required by the legislation to be used) is very different than the $PRF(70nm)=293$ where is the peak of accumulation mode. Using the $PRF(average)$ for this systems will lead to wrong conclusions. The $PRF(70)$ should be used for the PMP HD tests. This value is around 8% higher than the manufacturer's dilution value for the specific settings (272).

Table 12: Average PRF and standard deviation of the PRF

<i>Diameter</i>	<i>30 nm</i>	<i>50 nm</i>	<i>70 nm</i>	<i>100 nm</i>
PRF	508±71	383±49	293±39	291±3
Ratio to 100 nm	1.74	1.31	1.01	1.00

SPCS

The PRF ratios (Table 13) are within the specification.

The average $PRF = 1/3 * [PRF(30) + PRF(50) + PRF(100)] = 190$ close to $PRF(70nm) = 184$ where is the peak of accumulation mode. The average PRF is 26% higher than the DR 150 that would be used. The PRF(70) is 23% higher.

Table 13: Average PRF and standard deviation of the PRF

<i>Diameter</i>	<i>30</i>	<i>50</i>	<i>70</i>	<i>100</i>
PRF	214±12	183±6	184±4	172±25
Ratio to 100 nm	1.24	1.06	1.07	1.00

Further SPCS investigation

DR of SPCS: SPCS units might be used with different dilution settings than the 10x15 depending on the emission levels of the engines. For this reason, it was investigated whether there is an effect of the dilution settings to the final emissions measured. SPCS-20 was connected to PSS-20 and was used with constant dilution ratio to measure the emissions of the engine (with an open filter). SPCS-19 was connected to CVS with a 4 m heated at 47°C line. The dilution ratios of SPCS-19 were varied during the steady state test (mode #7) at these days. Figure 28 shows an example of the comparison of the two instruments.

For the evaluation of the effect of the dilution settings on the final emissions the two SPCS were synchronized and their emission levels were matched such as the ratio of the two SPCSs was 1 at dilution settings of SPCS-19 10x15. Figure 29a shows the effect of the primary dilution ratio (PDR) on the ratio of the two SPCS by keeping the secondary dilution ratio (SDR) constant. Increasing the PDR from 10 to 25 the ratio of the two SPCS decreases ~5%. Further increasing the PDR to 40 the ratio returns to the original values. Figure 29b shows the effect of the SDR on the ratio of the two SPCS by keeping the PDR constant. It is also observed that increasing the SDR from 15 to 25 the ratio decreases 3-5% and then by further increasing the SDR to 50, the ratio returns to the original values.

These results also indicate that the change of the dilution settings shouldn't affect the results. The differences were within experimental uncertainties (±5%), especially taken into account that the two instruments were sampling from different positions (CVS and partial flow system) and the CPC temperatures were 35-40°C (as it was the last test of the day). These results are in close agreement with the ratios of the gas measurement results (shown previously in Table 8, and also shown in Figure 29).

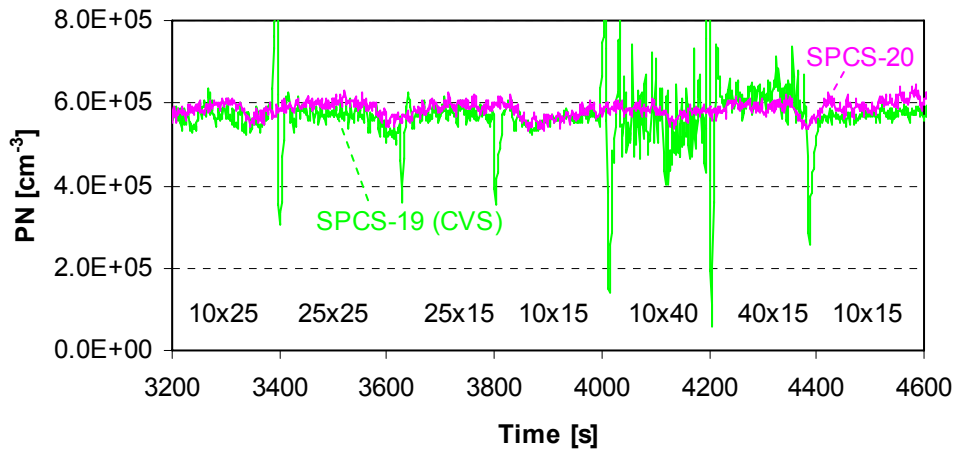


Figure 28: Comparison of SPCS-20 (at a partial flow system with constant DR) and SPCS-19 (at CVS with different DRs)

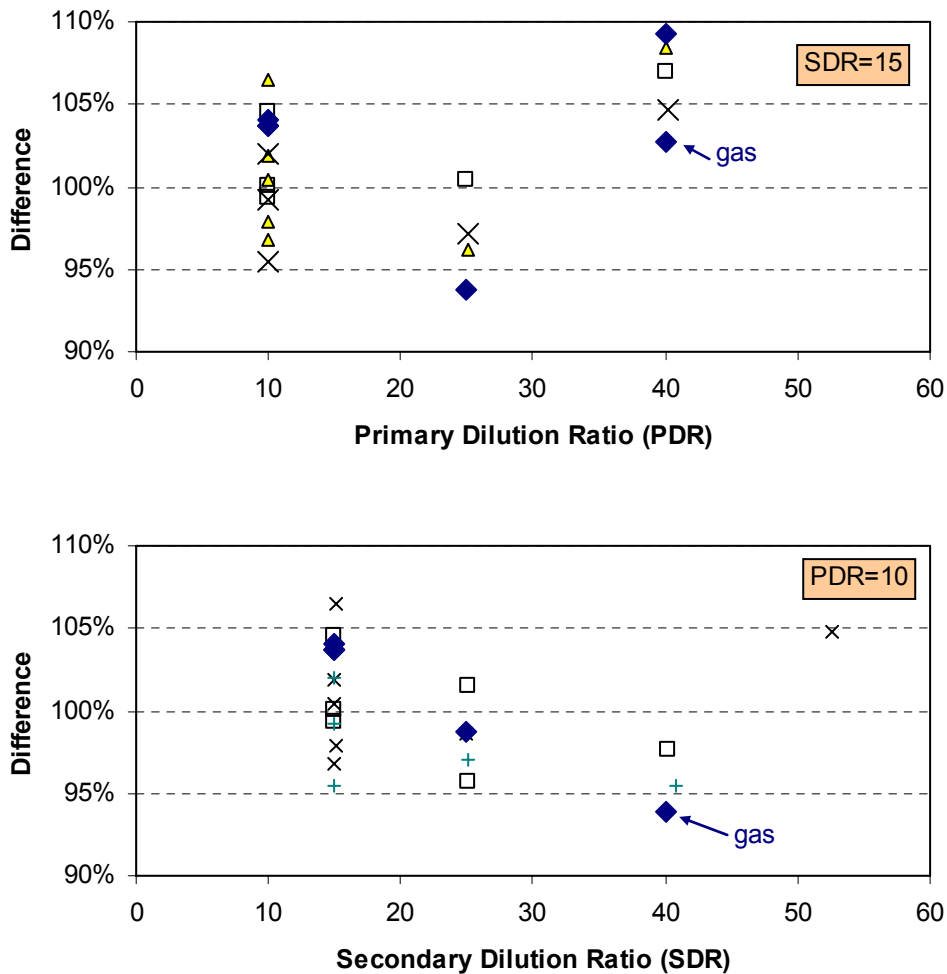


Figure 29: SPCSs ratio (DR 10x15 reference value) by changing a) the primary dilution ratio (PDR) and b) the secondary dilution ratio (SDR). The gas measurements from Table 8 are also shown.

Effect of high DRs on emission pattern: The settings that will be chosen for SPCS units (DR 10x15) ensure that a high sample flow rate is sampled from the units (1.3 lpm). However, at high dilution ratios this flow rate decreases (e.g. at DR 40x25 is 0.3 lpm). Pressure fluctuations change this flow rate. The lower the flow rate, the higher the effect. The different flow rate (compared to the anticipated), also affects the split ratio and the exhaust flow rate that enters the partial flow system. The effect of high dilution ratios was investigated during ETC cycles with the engine and an open filter. This was the worst case, as for the other cycles the effect was almost negligible.

Figure 30 shows a detail of the ETC cycle for SPCS-19 which was connected at CVS for three days with three different dilution ratio settings. The emission patterns are similar. Figure 31 shows the same detail of the same cycles for SPCS-20 which was connected at PSS-20. The SPCS-20 pattern of the 10x15 dilution ratio settings is similar with the SPCS-19 with DR 10x15. However, as the dilution ratio increases the instability also increases. This has to do with the lower sample flow rate instability as explained previously. Increasing the bypass flow rate (1 lpm) doesn't improve the situation (Figure 32). This means that the most important parameter for SPCS connected at a partial flow system is the sample flow rate for the first diluter (Figure 33). High secondary dilution ratios and low primary dilution ratios should be preferred rather than high primary dilution ratios and low secondary dilution ratios.

The effect of this instability is shown in Figure 34. For each dilution ratio setting four cases are shown: Emissions by multiplying the average total DR with the average CPC concentration for the cycle, emissions by multiplying the second by second total DR and second by second CPC concentration for SPCS-19 and SPCS-20. For DR 10x15 there is no difference between second by second or average by average emissions for both SPCS-19 and SPCS-20. The difference between the two SPCSs is 5%, a difference which will be discussed later (section comparison of systems). With DR 40x25 the situation is more sensitive. In this case, the emissions estimated by the second by second or by the average by average multiplications are completely different. The second by second emissions for the SPCS-20 are 4 times lower than the average by average. This has to do with the negative values of the DR. If these values are removed the second by second emissions are 80% higher than the average by average. Repeating the tests with dilution ratio 40x25 and higher bypass flow rate (so the sampling total flow rate was equal with the 10x15 case) didn't improve the results. The second by second results led to 100% overestimation of the emissions. The situation is better when the DR is increased by increasing the secondary dilution ratio. In this case (10x50) the average and the second by second results for SPCS-20 are close to the SPCS-19 results.

These results indicate that the total dilution ratio should increase by increasing the secondary dilution ratio for the SPCS connected at a partial flow system. For CVS any dilution ratio can be used. Moreover if the average by average value is different than the second by second value (more than 5%) the user should investigate more the results.

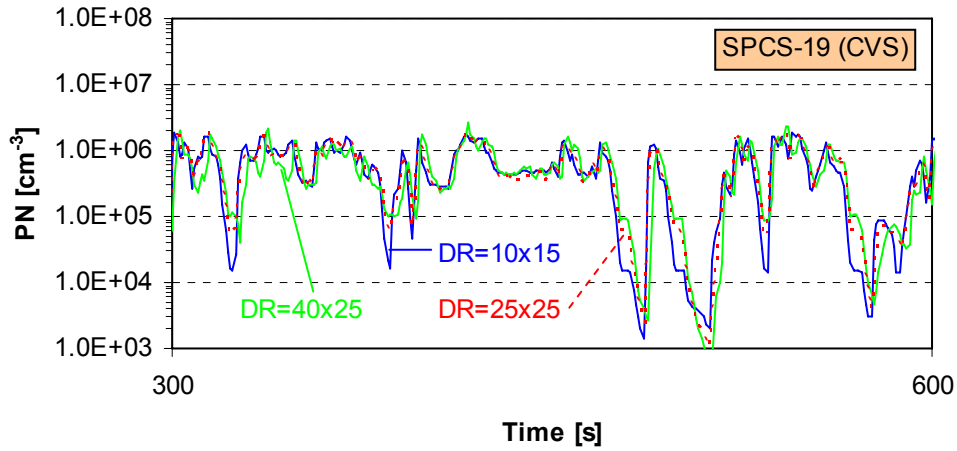


Figure 30: Particle number flux during a part of the ETC cycle 3 different days with different dilution ratio settings (SPCS-19 at the CVS).

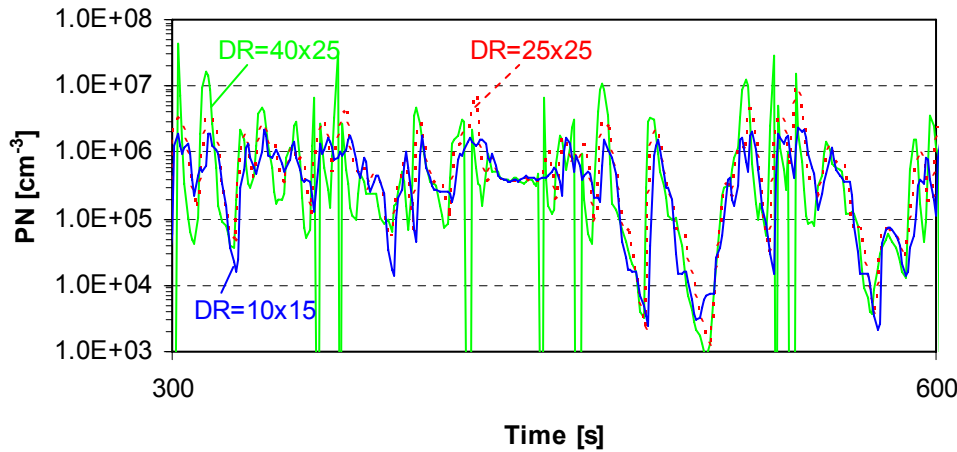


Figure 31: Particle number flux during a part of the ETC cycle 3 different days with different dilution ratio settings (SPCS-20 at the PSS-20).

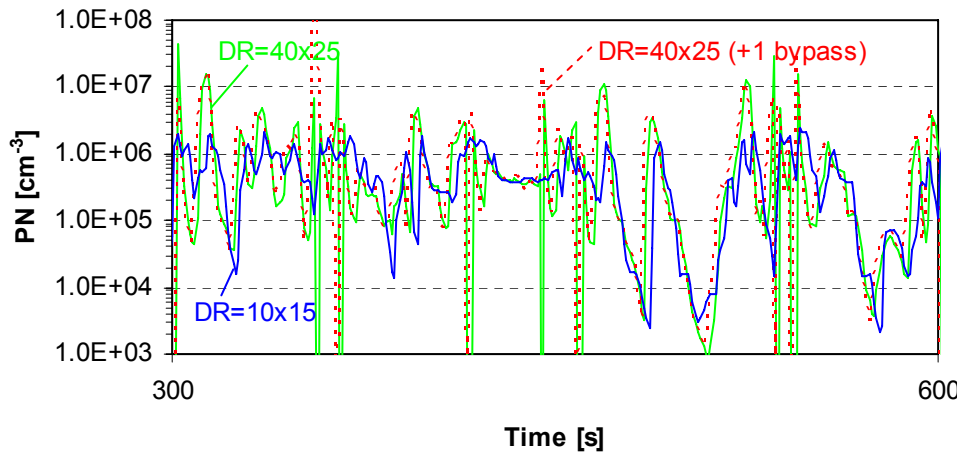


Figure 32: Effect of bypass on the instability

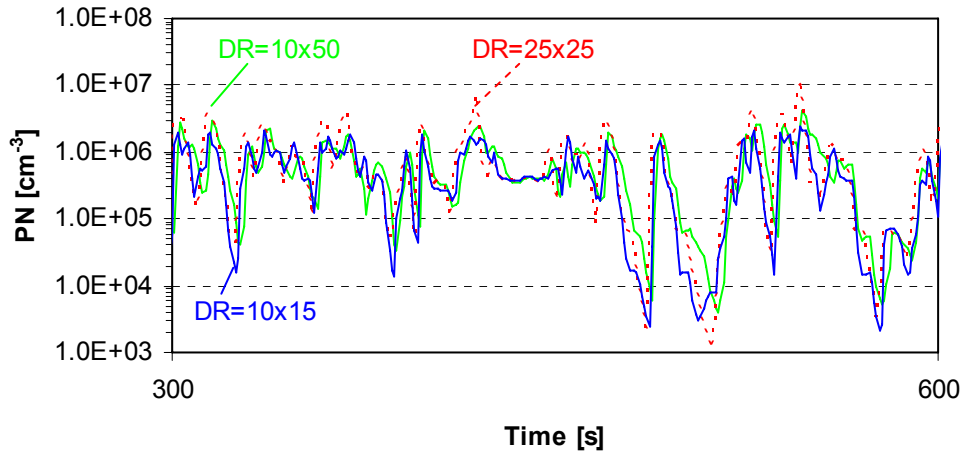


Figure 33: Particle flux for different dilution settings.

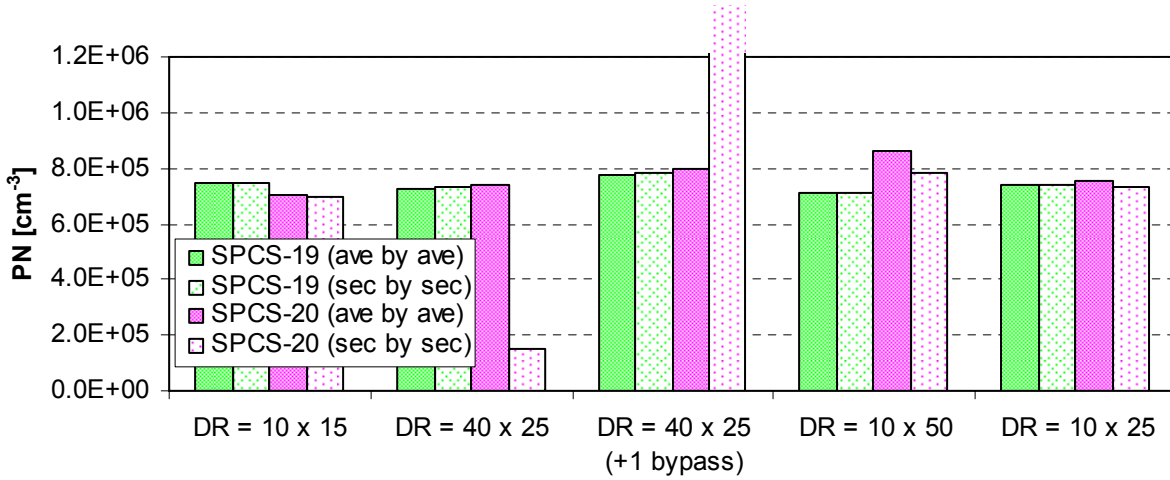


Figure 34: Summary of the emissions with the SPCS (SPCS-19 at CVS, SPCS-20 at PSS-20).

COMPARISON OF PARTICLE NUMBER SYSTEMS

Comparison of SPCSs

The two SPCS were compared with each other using the set up of Figure 35. Only non-volatile particles were fed to the instruments (through the thermodenuder) in order to ensure that any differences wouldn't be due to volatile particles but due to dilution ratio uncertainties. A 3790 CPC was also connected in order to measure the "absolute" particle levels. The 3010D were corrected for coincidence, but it was <1%. The CPC correction was also applied (1 for SPCS-19, 1.01 for SPCS-20 and 0.89 for the golden 3790).

The results of a cold WHTC can be seen in Figure 36. Generally, all instruments followed the pattern of the cycle and the emissions were at similar levels. CPC 3790 was measuring more than 10^4 cm^{-3} the first 200 s of the cycle. Although it is not suggested by the manufacturer, measurements in our lab have found that the linearity for the 3790 holds true up to $4 \times 10^4 \text{ cm}^{-3}$. Nevertheless, this part of the cycle was not taken into account for the comparison of the instruments. These high emissions at the beginning of the cycle also confirm that the use of at least one dilutor is necessary.

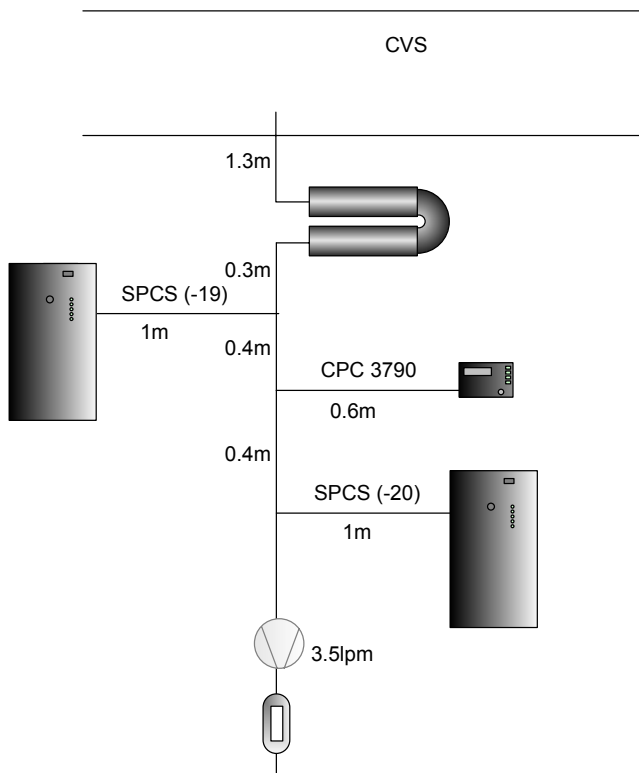


Figure 35: Schematic set up for the comparison of SPCSs at the primary dilution tunnel.

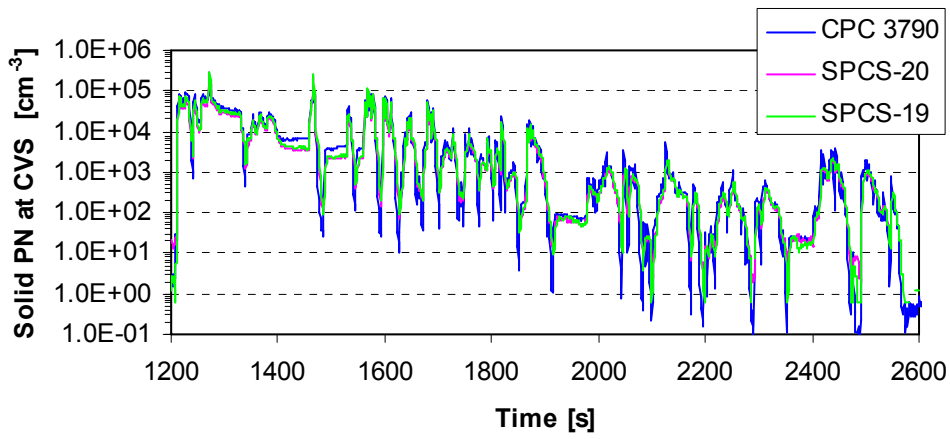


Figure 36: Comparison of SPCSs sampling from the primary dilution tunnel over a cold WHTC.

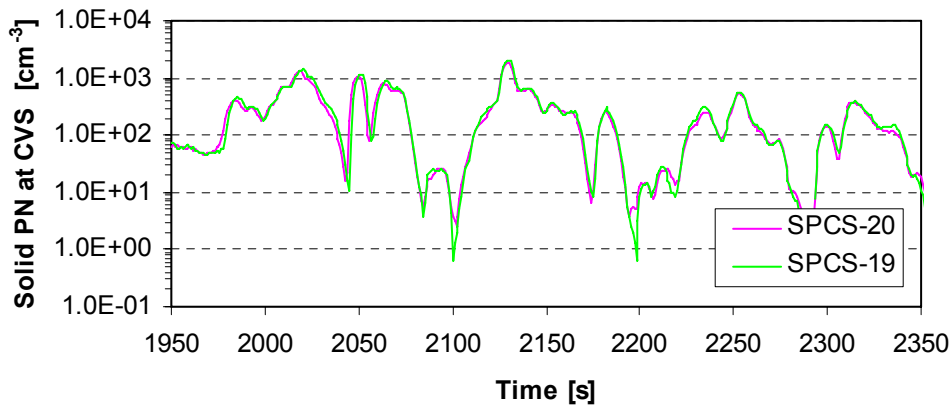


Figure 37: Comparison of the two SPCSs.

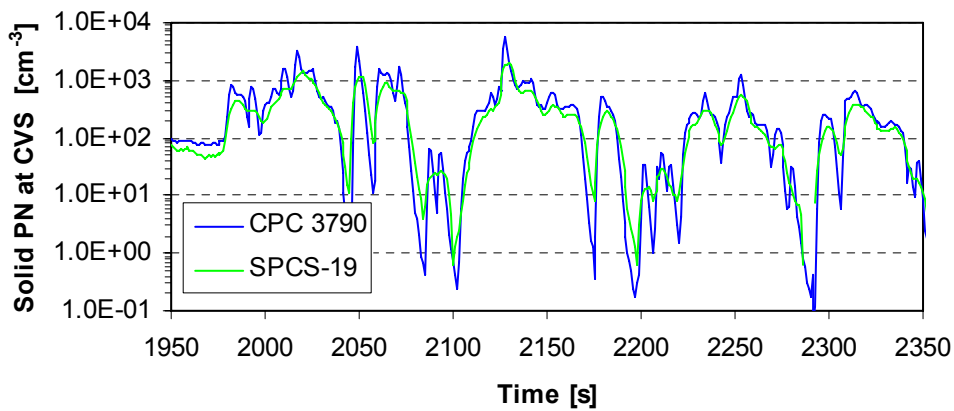


Figure 38: Comparison of SPCS with a 3790 CPC.

Figure 37 compares the two SPCS units (a detail from Figure 36). The pattern is identical and the emission levels have ~5% difference (SPCS-19 measures higher). This difference could be partly attributed to the “T” connections used. Although for SPCS-19 was sampling 3.5 lpm from a total flow of 11.5 lpm, SPCS-20 was sampling 3.5 from 7 lpm, thus having losses due to the different split ratio (see discussion of paragraph “CPC comparison”). This small difference is within experimental uncertainties and was not further investigated. The extra diffusion losses in SPCS-20 due to the longer residence time to the instrument (0.15 s) should be negligible.

Figure 38 compares SPCS-19 with the 3790 CPC. The difference in this case is 10% (3790 measures higher). This 10% can be attributed to dilution ratio uncertainties or thermophoretic losses in the SPCS. Moreover semi-volatile particles due to the different temperatures between the thermodenuder and the evaporation unit of SPCS could contribute to this difference (see paragraph “Volatile removal efficiency”). The SPCS was used with a secondary dilution ratio of 8 which is unfavorable for thermophoretic losses (Wei et al. 2006). Similar results were found from other tests at lower concentrations.

Hot-cold dilution

In order to investigate if the 10% difference (previous paragraph) was due to losses or dilution ratio uncertainties the two SPCS were run in parallel but one with hot dilution (SPCS-19) and the other with cold (SPCS-20, all heaters were set to ambient temperatures) (see Figure 35). As the dilution ratio is calculated from measured flow rates (with low temperatures at the orifices, see Annex D), the different temperatures of the heater shouldn’t affect the dilution ratio estimation. So any difference observed between cold and hot units should be due to thermophoretic losses. The difference of the two SPCS from -5% (SPCS-20 lower, Figure 37) changed to +10% (SPCS-20 higher) indicating that probably the 15% difference is due to thermophoretic losses in the unit. These were more or less the losses were also found during the characterization of the SPCS (see section Characterization of systems).

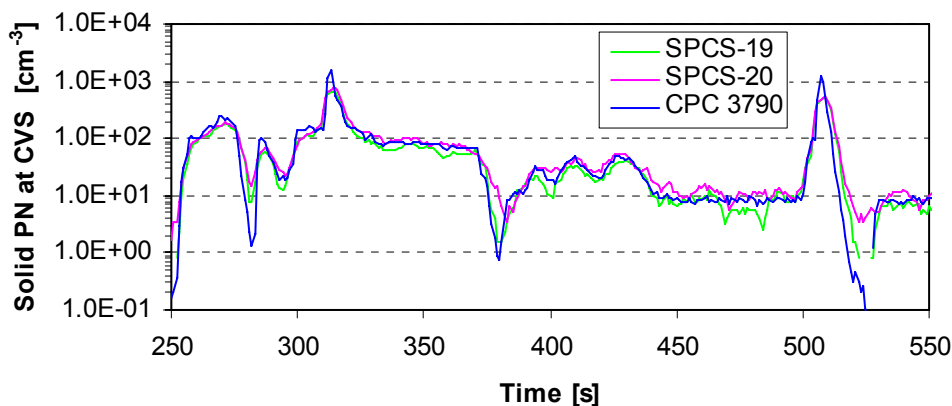


Figure 39: Comparison of SPCSs from the same sampling point using different dilution temperatures (SPCS-20 cold).

Comparison of SPCSs at the same partial flow system

The target was to compare the results from the two SPCS unit when measuring in parallel from the same partial flow system. When sampling from the primary dilution tunnel the two units

had 5% difference and the emissions patterns were the same. It was desirable to confirm the operation of the SPCS units at partial flow systems where the conditions are less ideal compared to the full dilution tunnel.

Figure 40 shows the schematic set up. Both SPCS units were connected to PSS-20 with tubes of length 1.5 and 6 m. The results can be seen in Figure 41 for steady state tests and Figure 42 for transient tests. SPCS-19 measured 10% higher than SPCS-20 for both steady states and transient tests. The extra 5% difference (10% here, compared to 5% seen at the full dilution tunnel in Figure 37) probably has to do with the “T” split of the flow to the two SPCS units. One SPCS was used with bypass flow of 3 lpm and the other with 1 lpm resulting in residence times of 0.94 s and 0.42 s respectively. However, the different flow rates might have affected the particle split to the two units. In this case there was not an extra pump to decrease the losses at the “T” splitter (see discussion at section “CPCs comparison”). This means that the extra 5% difference should be attributed to the experimental set up and not to the SPCS units. It should be also noted that the pattern at steady state is wavier than it was in the full dilution tunnel. This has to do with the pulsations from the partial flow system.

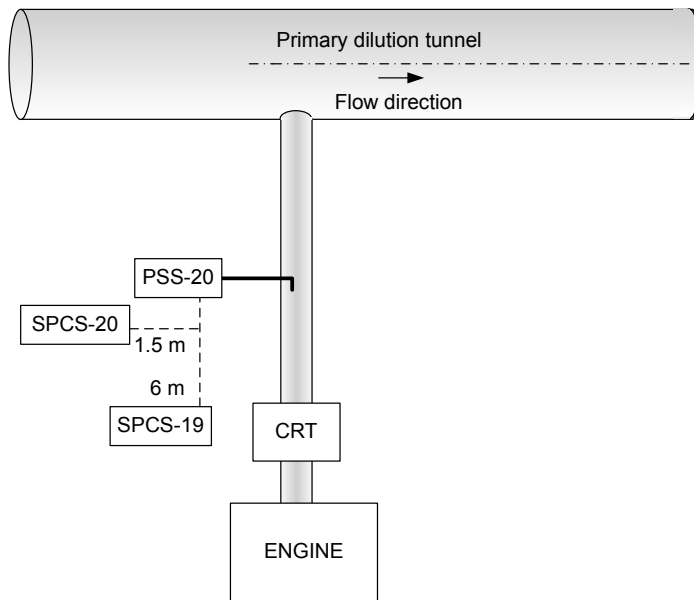


Figure 40: Schematic set up for the comparison of SPCSs at partial flow systems.

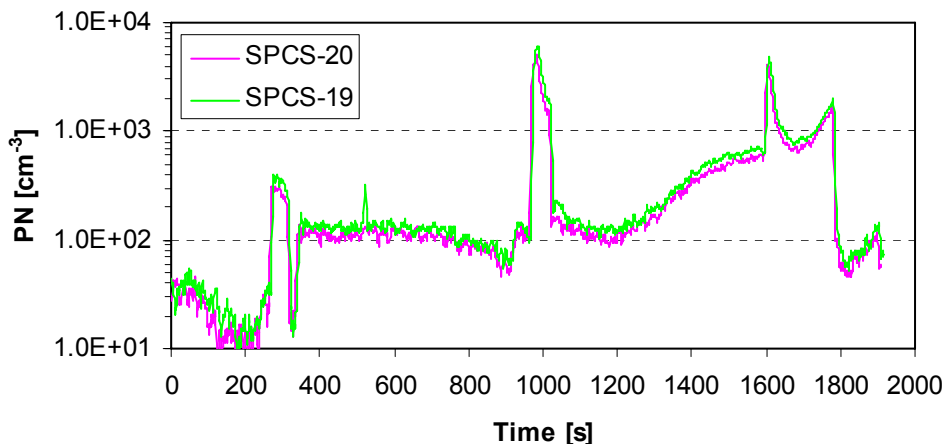


Figure 41: Steady state tests with both SPCS sampling from PSS-20.

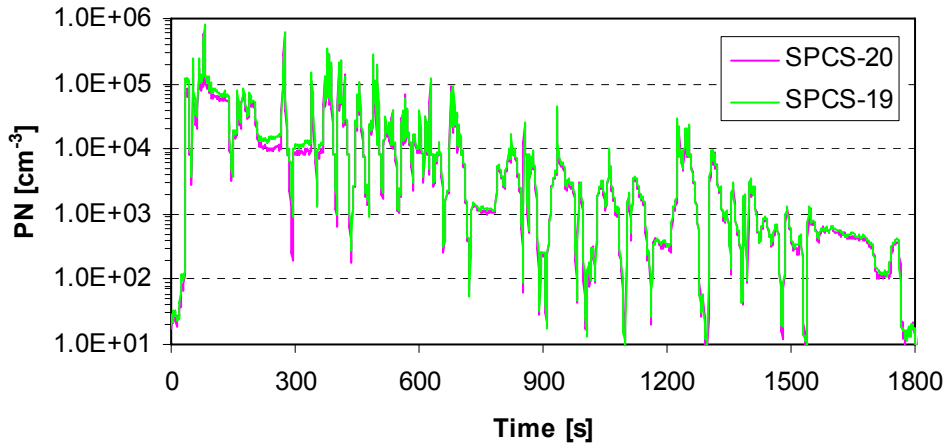


Figure 42: Cold WHTC with both SPCS sampling from PSS-20

Comparison of SPCSs at different partial flow systems

The two SPCS units were connected to the two partial flow systems to check if similar emission levels were measured. SPCS-20 was connected to SPC-472 with a 1.5 m line and SPCS-19 to PSS-20 with a 6 m line (Figure 43).

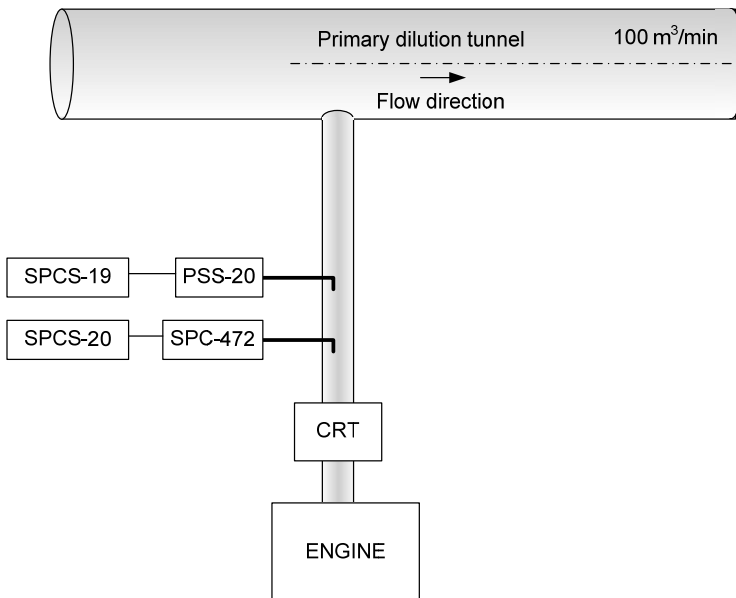


Figure 43: Schematic set up for the comparison of SPCSs at different partial flow systems.

The same settings were used at the two SPCS, thus the residence time in the tubes were 0.42 and 0.94 respectively.

The same settings were used at the two partial flow systems are:

- CVS: 100 m³/min
- PSS-20: G_{tot} =2500 nl/h, G_{edf} =7200 kg/h, G_{PN} =extracted flow=150 nl/h
- SPC-472: G_{tot} =0.83 g/s, r =0.041%, feedback=3.5 lpm

The results can be summarized in Table 14. There is a 30% and 53% difference of the SPC-472 and PSS-20 with the full dilution tunnel at the cold WHTC and -10 and 29% in the hot WHTC.

Table 14: Particle number results during a cold (left) and hot WHTC (right).

System	SPC-472	PSS-20	CVS 3790	System	SPC-472	PSS-20	CVS 3790
Average CPC [cm^{-3}]	3.71E+03	4.42E+03	2.68E+03	Average CPC [cm^{-3}]	1.81E+01	2.64E+01	1.90E+01
Average CPC [m^{-3}]	3.71E+09	4.42E+09	2.68E+09	Average CPC [m^{-3}]	1.81E+07	2.64E+07	19009670
equiv. CVS [m^3]	2818	2784	3000	equiv. CVS [m^3]	2818	2784	3000
kWh	24	24	24	kWh	24	24	24
Number emissions [kWh^{-1}]	4.35E+11	5.13E+11	3.35E+11	Number emissions [kWh^{-1}]	2.13E+09	3.06E+09	2.38E+09

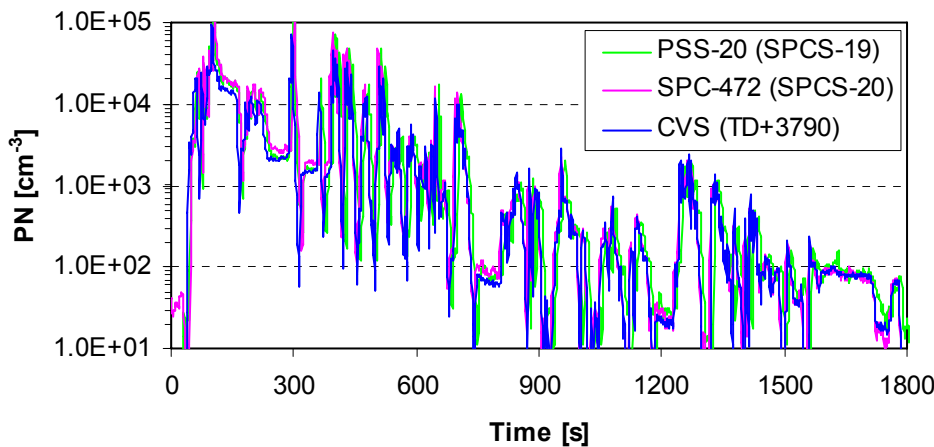


Figure 44: Comparison of full flow and partial flow systems (high emissions cold WHTC).

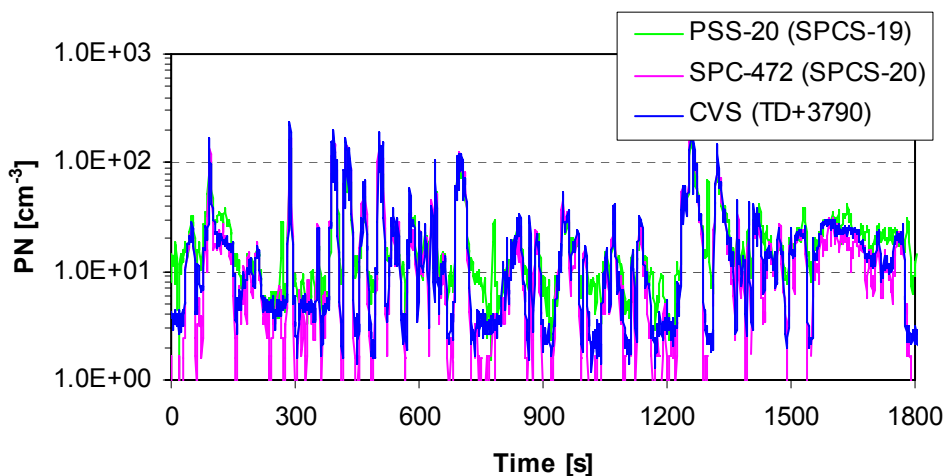


Figure 45: Comparison of full flow and partial flow systems (low emissions hot WHTC).

A close look at the values show that the 150 nl/h that was set at PSS-20 is not the correct one, as the extracted flow from the SPCS-19 was 3.45 slpm (=191 nl/h). This error was taken into account by correcting the real time emissions with Eq. 9 and 10. With this correction the difference of PSS-20 to CVS from 53% dropped to 20% and from 29% to 3%. These differences

Figure 47 compares ejector based systems with SPCS-19 over a cold WHTC. Figure 48 compares the same systems during an ESC cycle. The preconditioning of the engine at rated speed is also included in the figure. The dual ejector system (EJ+ET+EJ+3010D) has a 10% difference with the ejector with thermodenuder system. However, it is important to note that at the beginning of the cold WHTC the emissions of the EJ+TD+3790 are higher from the EJ+ET+EJ+3010D system and then at the end of the cycle they are equal. This indicates that there might be semi-volatile particles at the beginning of the cycle that are not efficiently removed from the thermodenuder due to the lower temperature used (275°C) compared to the evaporation chamber (330°C). SPCS measures 15% lower than the ejector plus thermodenuder system with the 3790 CPC (EJ+TD+3790). If the SPCS 70 nm PRF is used the SPCS measures 5-10% higher. Compared to the dual ejector system SPCS with the 70 nm PRF measures 10% higher. It should be noted that the dual ejector system has a background of around 40 cm⁻³ even though a HEPA filter was used at the dilution air line. It seems that separate HEPA filters should be used at each ejector dilutor dilution air line.

Figure 49 compares the SPCS-19 with Nanomet and the thermodenuder system (TD+3790). The Nanomet showed +13% higher emissions than the thermodenuder system and the SPCS-19 measured 17% lower emissions, in agreement with the previous results. Using the 70 nm PRF the SPCS and TD system have similar results. The Nanomet results have to be seen with caution as the system had to be sent back to the manufacturer for repair. It should be mentioned that the background of the Nanomet is around 70 cm⁻³, much higher than the SPCS's background (almost 0 cm⁻³).

Comparison of the SPCS with the old Nanomet also led to similar conclusions (Figure 50). Using the dilution ratio of the instruments there was a 15% difference (old Nanomet higher), but using the 70 nm PRFs for both instruments, the SPCS measures 2% higher.

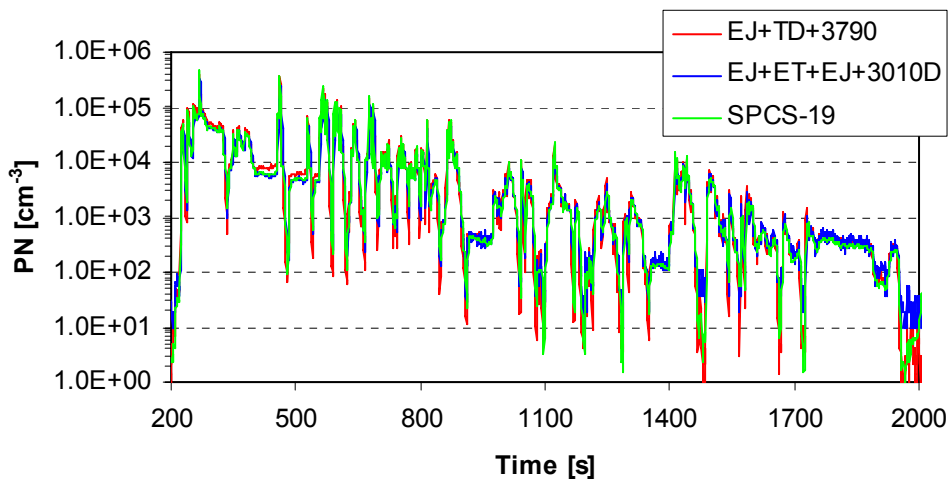


Figure 47: Comparison of different particle number systems over a cold WHTC.

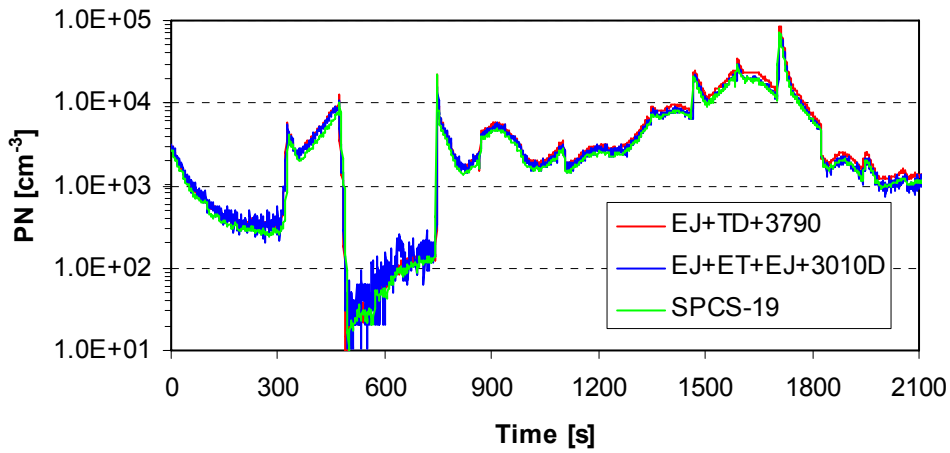


Figure 48: Comparison of different particle number systems over steady states.

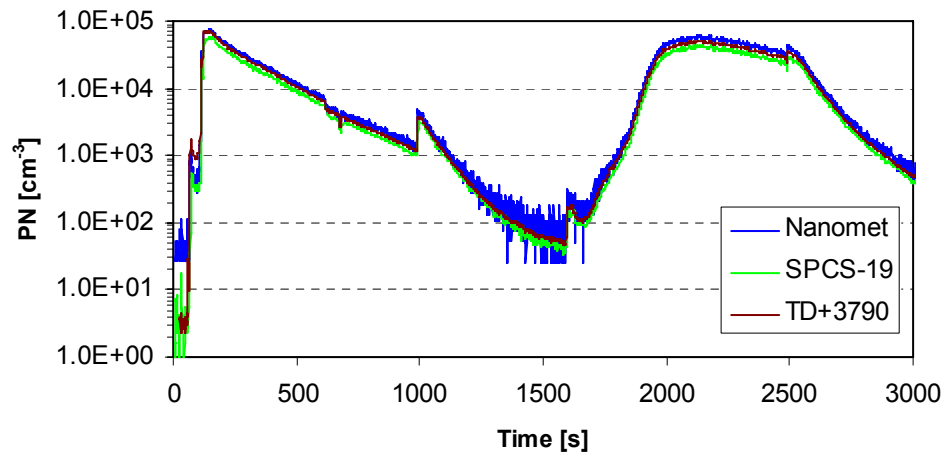


Figure 49: Comparison of different particle number systems over steady states.

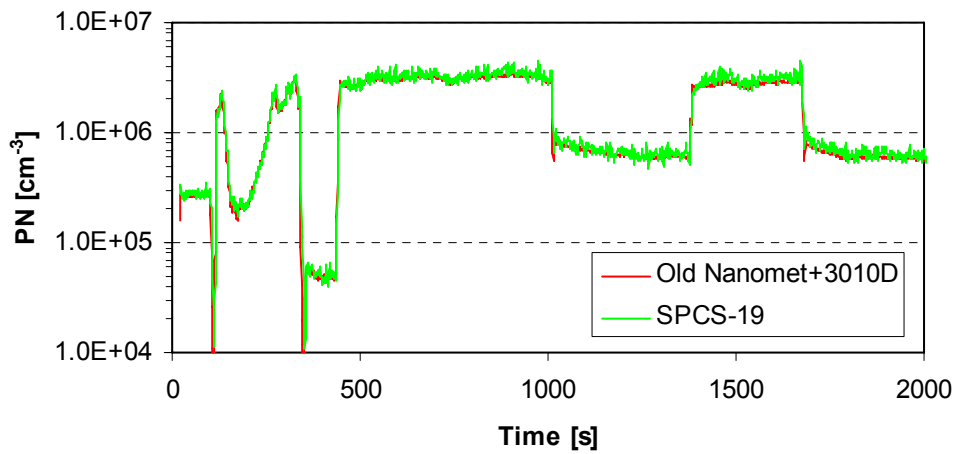


Figure 50: Comparison of different particle number systems over steady states.

SAMPLING PARAMETERS

Cyclone effect

It was desirable to check if the cyclone (and the under pressure caused by the 90 lpm pump) would affect the particle number emission. For this reason one SPCS was connected to the primary dilution tunnel through a cyclone (with a 90 lpm pump also operating) and the other without cyclone (Figure 51). The results can be seen in Figure 52 for a cold WHTC and in Figure 53 for steady states. The difference between the SPCSs was ~5% indicating that the cyclone had negligible effect on the SPCS. The same differences were observed when the SPCS were measuring in parallel (see Figure 37). The absolute levels of the instruments remained at the same levels as the 10% difference with the 3790 (downstream of a thermodenuder) was the same with the 10% difference found in Figure 38.

Heated line

At a next step the effect of the 4 m heated line was tested as one SPCS would be connect to the primary dilution tunnel with the 4 m heated line and the other at the partial flow systems with short insulated line. Figure 54 shows the set up for the investigation of the effect of the heated line. Downstream of a thermodenuder, SPCS-19 was measuring with the heated line and SPC-20 without. A 3790 CPC was also connected to measure the absolute levels.

The results can be seen in Figure 55. SPCS-19 measures 5% higher than SPCS-20 which is in perfect agreement with the difference of the two units when sampling in parallel (Figure 37). This means that the heated line has negligible effect on particle emissions (within experimental uncertainties). Theoretical calculations of the diffusion losses in the 4 m heated line confirm that the losses should be <5% for 23 nm particles and <2% for 100 nm particles (laminar flow). The residence time in the heated line is 1.3 s (SPCS flow rate 3.5 lpm and internal diameter 6 mm) and is within the requirements of Reg. 83 for light duty vehicles. In Reg. 83 it is stated that the residence time from the dilution tunnel to the first diluter should be <3 s and probably this requirement will be included in the Reg. 49 if particle number measurement is added to the regulation. Moreover, no smoothening of the emissions pattern is observed.

No tests with the heated line at 190°C were conducted as the maximum temperature observed at the particle number sampling point at CVS is around 100°C (ESC cycle). Usually the temperature at the sampling point is around 60°C. It must be emphasized that the thermophoretic losses at the tests conducted should be negligible as the full dilution tunnel was used with high flowrates (>80 m³/min) and thus the diluted exhaust gas temperature was <100°C. With higher diluted exhaust gas temperatures the effect of the cyclone and the heated line (and generally the sampling lines) could be greater.

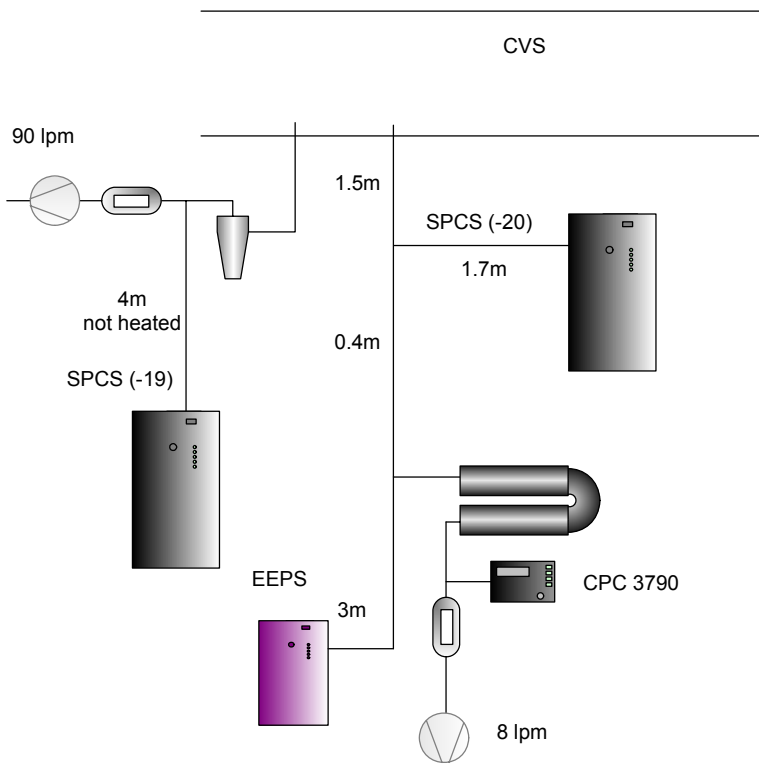


Figure 51: Schematic set up for the effect of cyclone.

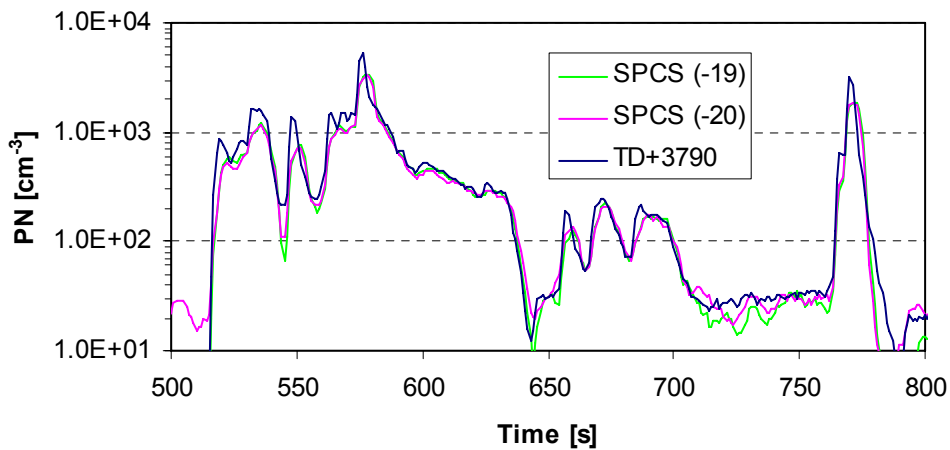


Figure 52: Effect of cyclone on SPCS results during a transient test (SPCS-19 was used downstream of a cyclone).

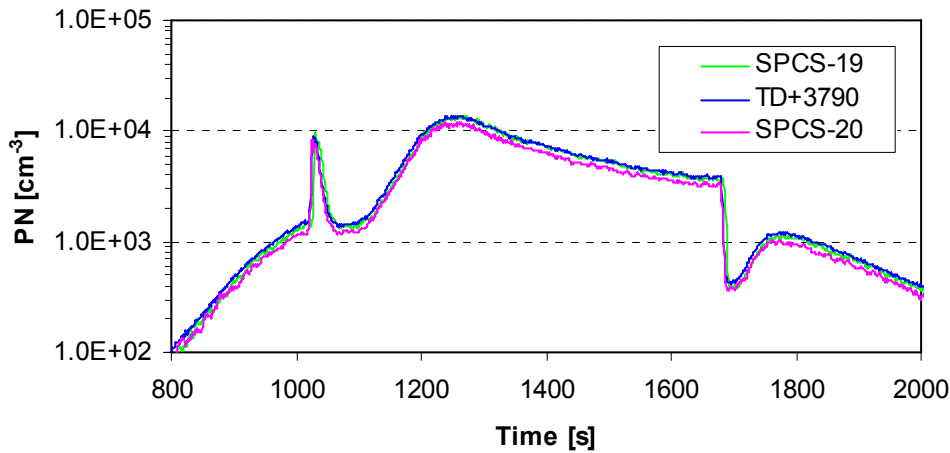


Figure 53: Effect of cyclone on SPCS results during steady states (SPCS-19 was used downstream of a cyclone).

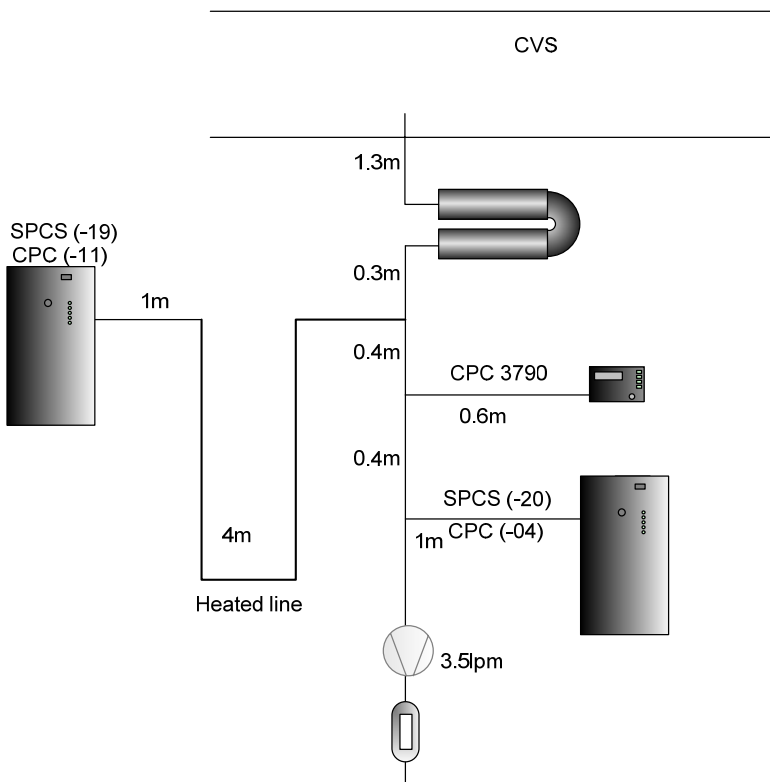


Figure 54: Schematic set up for the effect of the heated line.

Figure 56 summarizes the effect of different parameters on the results of SPCS-19. As reference instrument a 3790 CPC was used downstream of a thermodenuder (correction 1.28, CPC differences also taken into account and PRF was used for the SPCS-19). Each point indicates a measurement (cycle or steady state). It can be observed that SPCS and 3790 have no difference over the whole range. The cyclone and the heated line have negligible effect on the emissions of the SPCS.

In summary, any difference between the SPCSs at the partial flow system (no 4 m heated line) and the full flow system (with 4 m heated line) should be attributed to differences of the sampling systems and not to the SPCSs or the 4 m sampling line or the cyclone. A max 5% difference should be expected between the to SPCS systems (Figure 37).

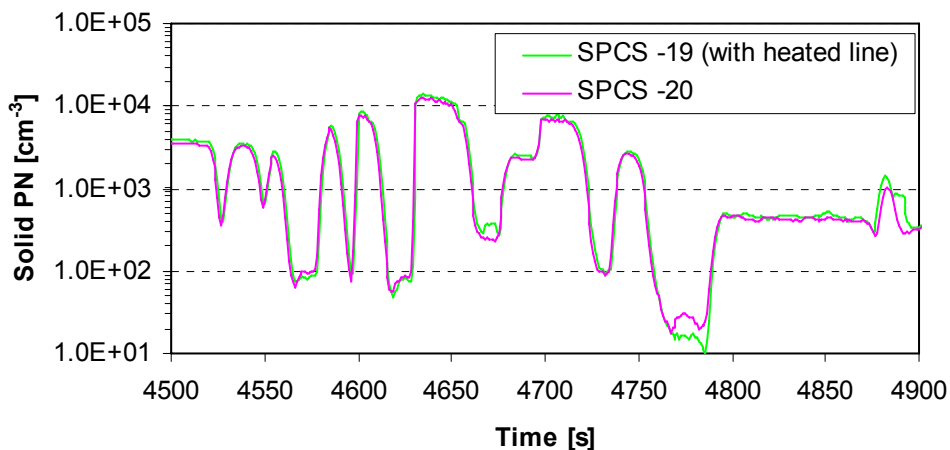


Figure 55: Effect of a 4 m heated line (at 47°C) on SPCS results.

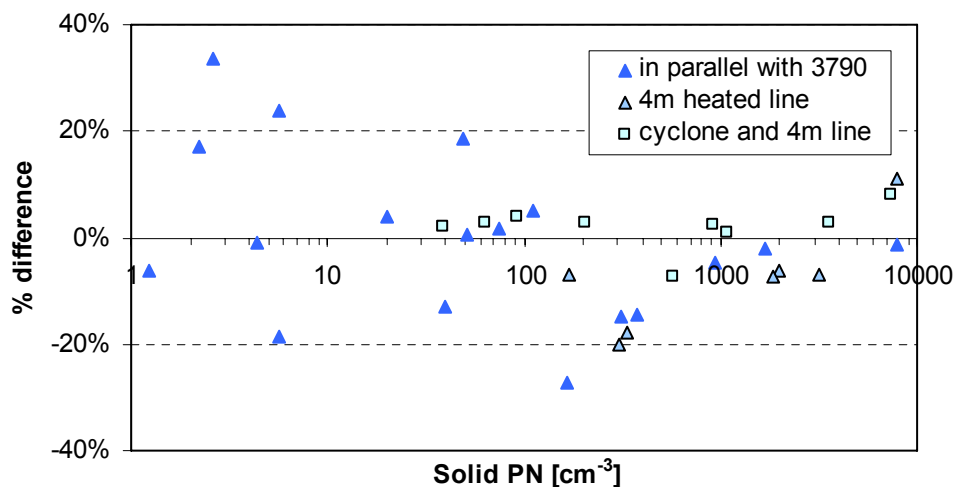


Figure 56: Effect of sampling parameters on SPCS-19 emissions (difference compared to a 3790 CPC downstream of a thermodenuder).

PRE-CONDITIONING TESTS

The target of the pre-conditioning tests was to specify the appropriate pre-conditioning at the end of each measurement day to condition the CRT and to ensure identical conditions for the next day's measurements, improving this way the repeatability of the experiments. The longer the after-treatment devices are conditioned, the more repeatable the measurements are (Giechaskiel et al. 2007). However, it was desirable to find the minimum time required as the daily protocol will be very long (Andersson et al. 2008).

For the pre-conditioning tests the set up of Figure 57 was used (as at that time the Golden instruments weren't available yet). PN emission were measured directly from the CVS with a 3025A CPC (total particles, d_{50} 3 nm) and a 3010 downstream of a thermodenuder and an ejector dilutor (non-volatile particles, d_{50} 10 nm). To investigate the effect of preconditioning a "mini cycle" was defined which consisted of modes #2, #8, #3, and #1 of the ESC cycle. The results of this "mini cycle" should be representative of the variability that would be observed with any other cycle as it included both low and high temperature modes.

Initially the CRT was conditioned only with 30 min of modes #7, #9, #11 which are low temperature modes. The exhaust gas temperature at these modes is $<300^{\circ}\text{C}$ and it can be assumed that the CRT loads (no regeneration). In this case, the emissions measured at the mini cycle were very low (Figure 58). When the same mini cycle was repeated after preconditioning at mode #10, where the exhaust gas temperature is very high and the CRT regenerates, the non-volatile emissions were very high (Figure 58). This can be explained by the lower efficiency of the CRT when it's not loaded with soot.

It was decided that the preconditioning should include both a regeneration and a loading phase thus avoiding high emissions during the official cycles where the CRT regenerates for the first time. Combining a 10 min regeneration phase at mode #10 and a 20 min loading phase at mode #7 resulted in emission levels of the mini cycle somewhere in between (Figure 58).

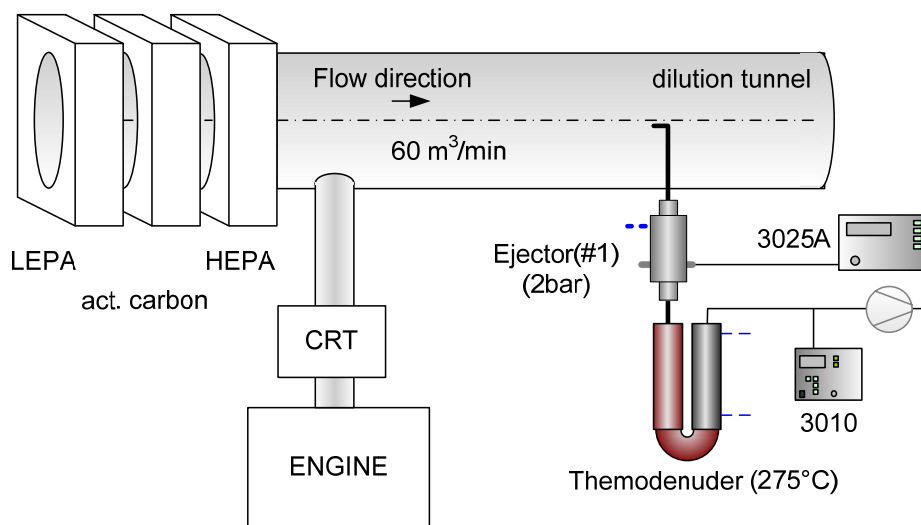


Figure 57: Schematic set up for the pre-conditioning tests.

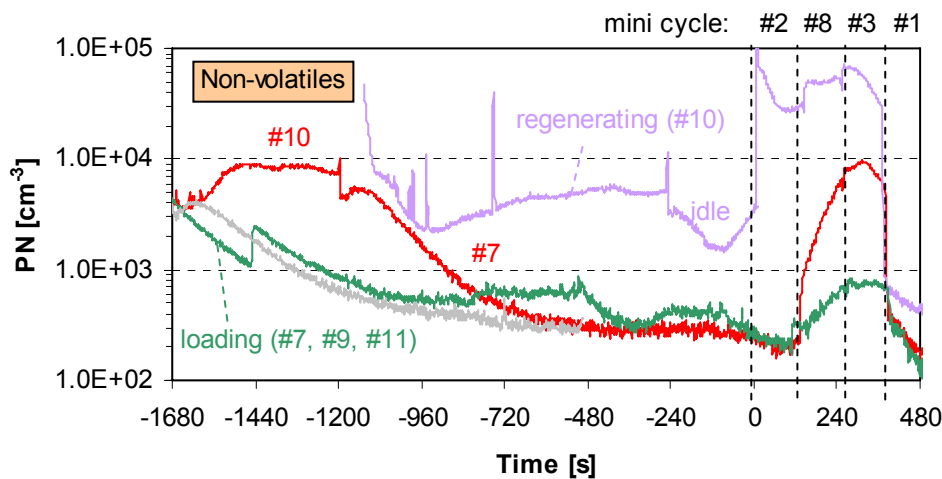


Figure 58: Pre-conditioning effect on particle emissions of a “mini cycle” consisting of modes #2, #8, #3 and #1 of ESC. Modes #7, #9, #11 are low temperature modes (the CRT loads), while mode #10 is high temperature mode (the CRT regenerates).

With the 10 min at mode #10 plus 20 min at mode #7 pre-conditioning, the emissions of the mini-cycle were checked on two consecutive days (with the preconditioning conducted the previous day or immediately before the mini cycle) and the results are shown in Figure 59. The repeatability was not very good (CoV 70%) and this probably had to do with the insufficient duration of the regeneration phase (10 min at mode #10). As it can be seen in the figure at the end of the 10 min of mode #10 the (non-volatile) emissions tend to stabilize, but still they haven't reached the same level.

Repeating the tests with a regeneration phase of 15 min and a loading phase of 30 min the repeatability improved (and the average emissions increased) (Figure 60) (CoV 40%). At the end of 15 min of the regeneration mode the emission levels are more similar. It can be also noticed that the 10 min at mode #10 is definitely not enough as in the specific cases the emission levels would be very different (see vertical line at 10 min of mode #10 in Figure 60). So it was decided to use the 15 min at mode #10 and 30 min at mode #7 preconditioning for the official PMP tests. The expected variability is in the order of 40%.

Figure 61 shows total and non-volatile emissions during the pre-conditioning tests. As it can be seen there are a lot of volatile particles during the regeneration phase even with low sulfur fuel and lubricant (Vaaraslahti et al. 2005). There are also differences during the loading phase which have to do with the different cut-points of the instruments and the thermodeuder losses. It is also interesting to note that the emissions during the “mini cycle” are mainly non-volatile particles as the concentrations of the two instruments (3025A and 3010) are similar. The emissions during the pre-conditioning was discussed previously (Figure 23).

The adequacy of the 15 min at mode #10 was also proven during the official tests at AVL_MTC, where it was shown that after the 15 min at mode #10 for the next 100 min the emissions are almost stable (slightly increasing over time). Figure 62 shows the emissions during the preconditioning at JRC for some tests (mode #10 and #7) from the partial flow system and from AVL_MTC during the 2 h lubricant aging from a partial flow system with the same parameters. Obviously 15 min is the minimum required time.

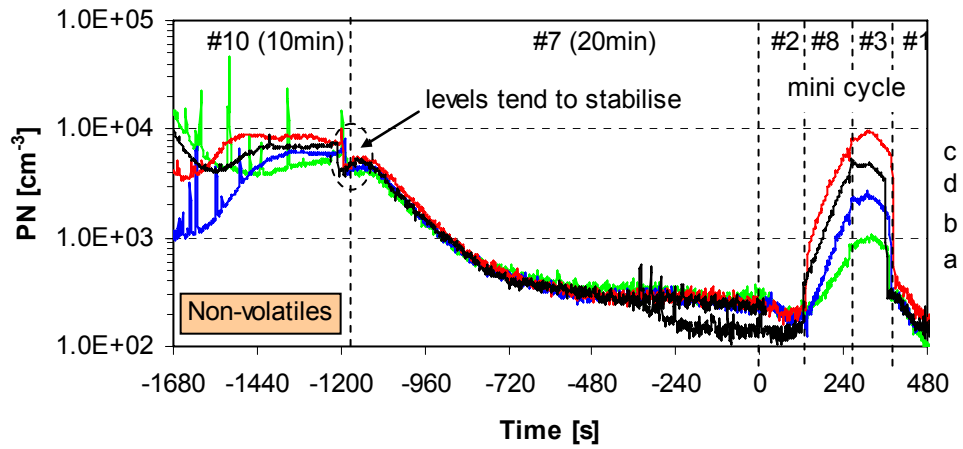


Figure 59: Pre-conditioning of 10 min (mode #10 ESC) and 20 min (mode #7 ESC).

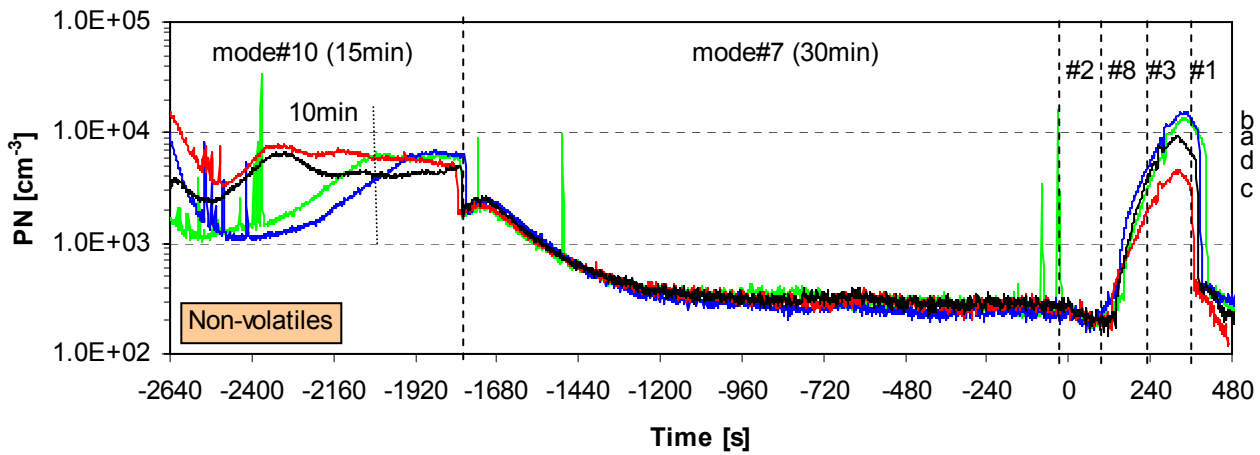


Figure 60: Pre-conditioning of 15 min (mode #10 ESC) and 30 min (mode #7 ESC).

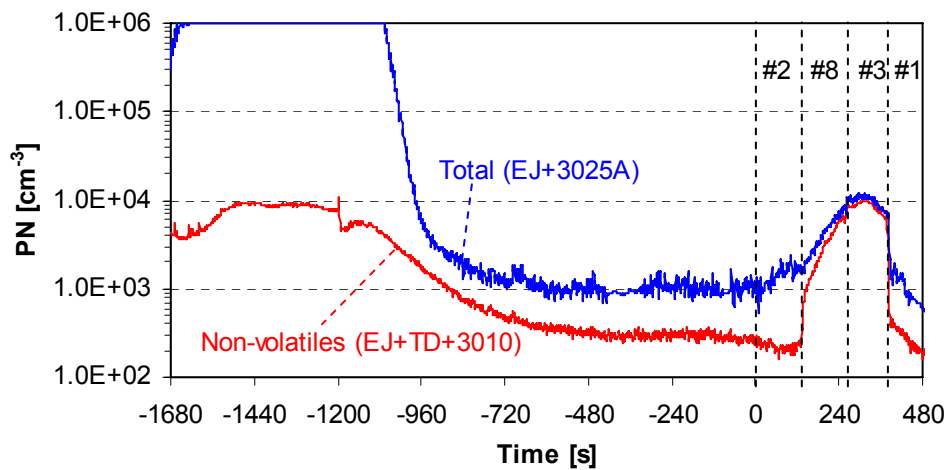


Figure 61: Total and non-volatile particles during the pre-conditioning.

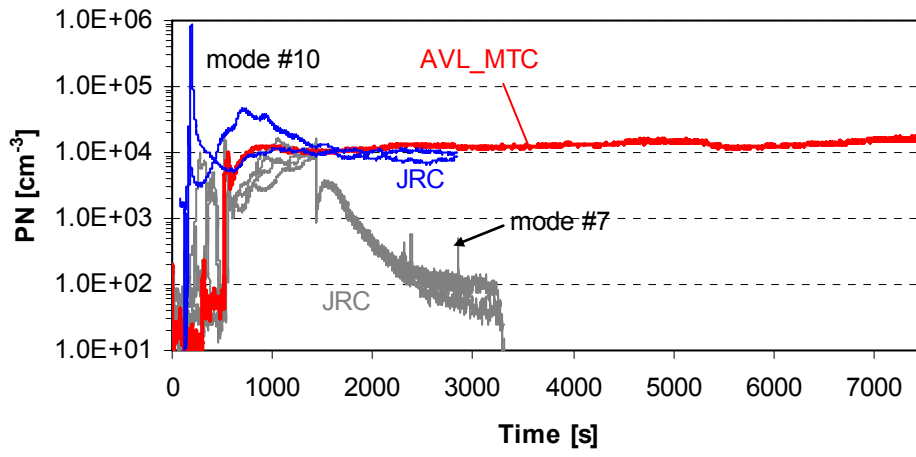


Figure 62: Emissions during mode #10 (ESC).

CONTINUITY PROTOCOL

The daily protocol includes many tests, but doesn't specify the times between the tests. So, in theory, one lab could run the tests one after the other and another lab with pauses of a few hours. In order to avoid emission differences between labs due to different engine temperatures the "continuity protocol" (CP) is introduced, where the engine is run for a few min before the beginning of the test/cycle. The CP is applied only to ETC and ESC cycles because for the WHSC a warm up phase at mode #9 (WHSC) is required by the future legislation. For cold WHTC the engine must be cold and for hot WHTC the engine is warm from the previous cold WHTC.

The CP was decided to be 5 min at mode #7 (ESC) with 3 min at idle. The justification for this decision was that the temperature should be low enough not to cause regeneration. Even the low temperature mode #4 could affect the emissions during cycle as it can be seen in Figure 63 where the emissions during the CP increase over time. Indeed, the emissions of 3 ETCs were dependent on the duration of the CP at mode #4. With mode #7 the emission stay low indicating that the filter is loading and thus the emissions during the beginning of the next test will be low, thus the effect of the CP will also be lower.

The 3 min of idle after 5 min at mode #7 were necessary for the automated systems to run the following cycle.

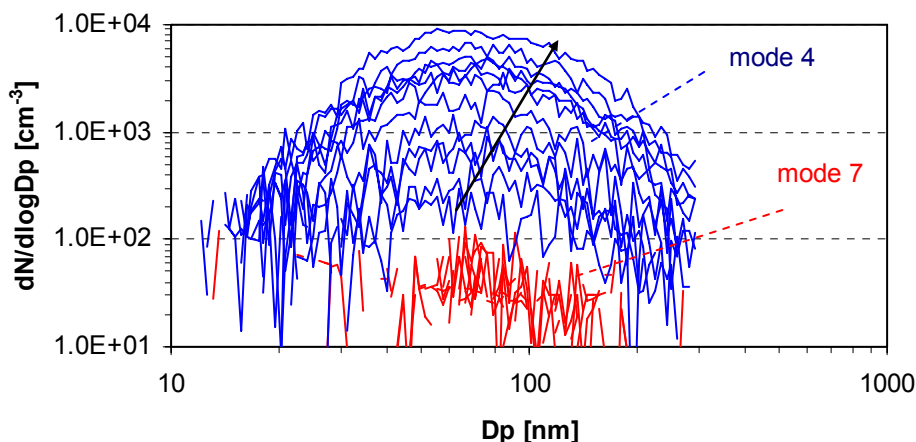


Figure 63: Continuity protocol at mode 4 and 7. Mode 4 emissions increase over time.

Note that the 10 min preconditioning at mode #9 (WHSC) before the beginning of the WHSC will affect the status of the CRT as it is a high temperature mode (>300°). Thus the number emissions at this cycle might be more variable.

REAL TIME EMISSIONS

Cold WHTC

Figure 64 shows the emissions of a cold WHTC as measured with an EEPS (blue line) and SPCS-19 (green line). It can be assumed that EEPS measures total particles (volatiles and non-volatiles) and SPCS-19 non-volatiles. As the two instruments have different cut-points, EEPS signal was corrected with the CPC 3010D counting efficiency (red line). The difference of the “corrected” EEPS and the SPCS-19 should be volatile particles (>23 nm) at CVS. However, as the two instruments were not calibrated with each other, only the trends will be discussed and not the absolute values. For the discussion here, SPCS-19 was multiplied by a factor (0.7) in order to have always lower or equal emissions with the EEPS (corrected with the CPC 3010D efficiency).

As it can be seen, high emission of particles are observed only at the beginning of the cycle. It is believed that blow-out of loose solid particle depositions, as the filter is exposed to highly transient operation with respect to the thermal and flow conditions, results to the increased particle number. In addition, they can be particles formed by the nucleation-condensation of semi-volatile material earlier stored within the substrate and/or the particulate layer and released during the cold-start cycle as the CRT heats up.

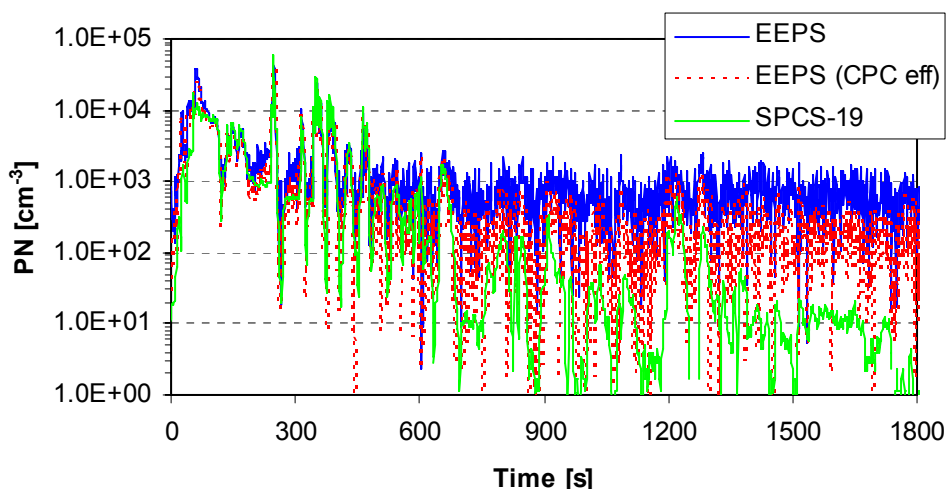


Figure 64: Emissions during a cold WHTC.

Figure 65a shows the first seconds of the cycle. At the beginning of the cycle SPCS-19 emissions are lower than EEPS “corrected” emissions indicating that there are volatile particles. This can be seen in Figure 65b (size distribution A with nucleation mode). Later (75+ s) the emissions of the two instruments are similar, meaning that the volatiles >23 nm are negligible after this point. Figure 65b shows that the size distributions at this part are without nucleation mode (size distribution E) or the nucleation mode is below 23 nm (size distributions D).

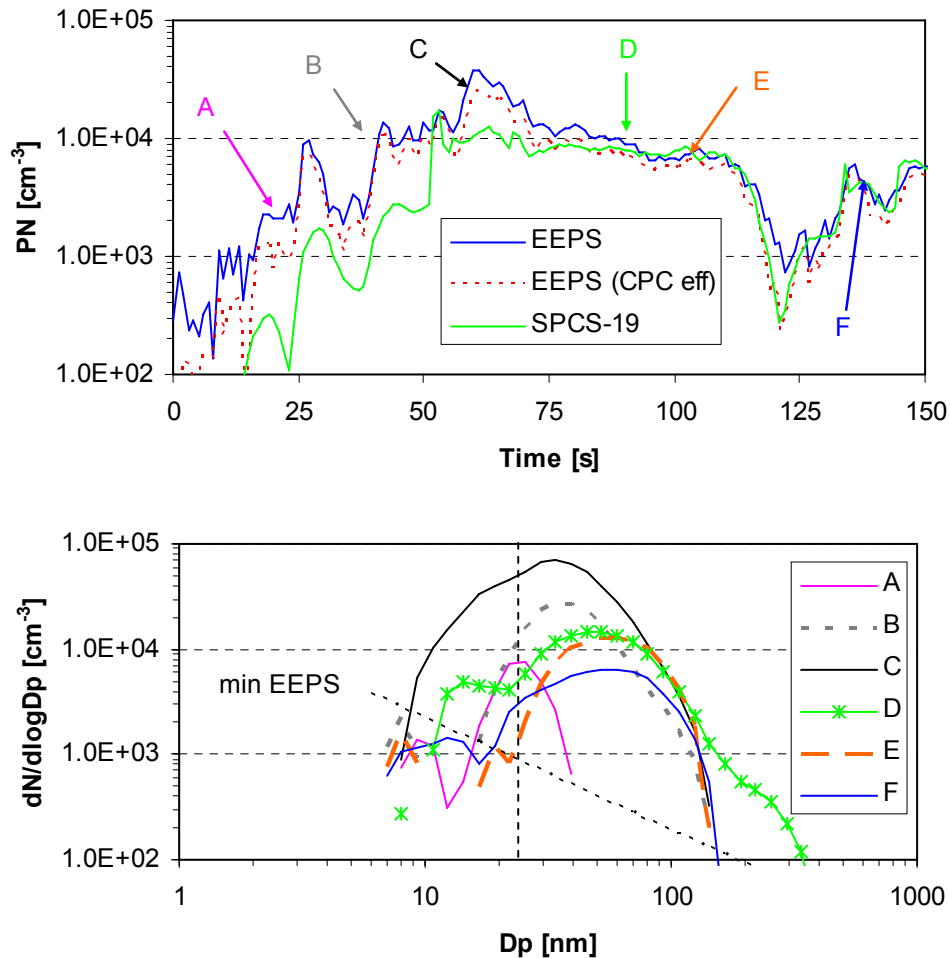


Figure 65: a) Beginning of a cold WHTC. Arrows indicate the times that the size distributions of the second figure correspond. b) Size distributions during a cold WHTC. The times for each distribution are indicated with an arrow at the first figure.

As the EEPS does not have high sensitivity (see Figure 1 – min of 1000 cm^{-3}), a 3025A was connected to the CVS downstream of two ejector dilutors. The results of the cold WHTC can be seen in Figure 66. It is confirmed that at the beginning of the cycle there are a few particles below 23 nm (which could be volatiles or non-volatiles). It should be noted that at the strange behavior of the 3025A at the end of the cycle (smoothed emissions) has to do with the averaging that the instrument uses at low concentrations.

In order to investigate whether the particles at the beginning of the cycle are volatiles or non-volatiles, the 3025A was connected downstream of the SPCS, in parallel with the 3010D of SPCS-19. The results can be seen in Figure 67. It is confirmed that there are some non-volatile particles <23 nm at the beginning of the cycle.

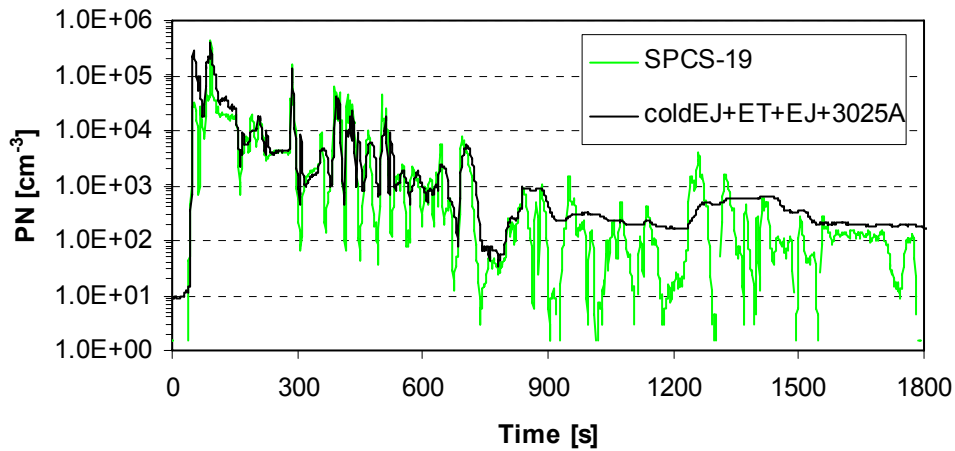


Figure 66: Cold WHTC emissions.

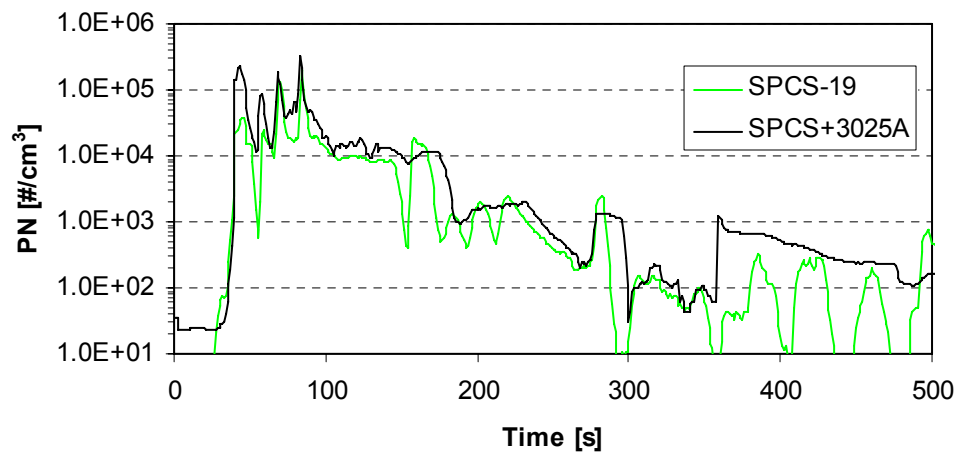


Figure 67: Comparison of a 3010D and a 3025A downstream of SPCS.

Hot WHTC

The emissions of a hot WHTC are shown in Figure 68 as measured with a 3010D directly connected at the CVS and a CPC 3790 downstream of a TD. The emissions are very low (peaks below of 100 #/cc). It can also be observed that the volatiles >23 nm are very low. The emissions were much lower than the sensitivity of the EEPS (connected at CVS or connected downstream of the TD – Figure 69), so no size distributions are shown.

A 3025A connected downstream of the SPCS also didn't show any (non-volatile) particles (Figure 70). The 3025A at low concentrations gives the average emissions; for this reason its signal is smoothed.

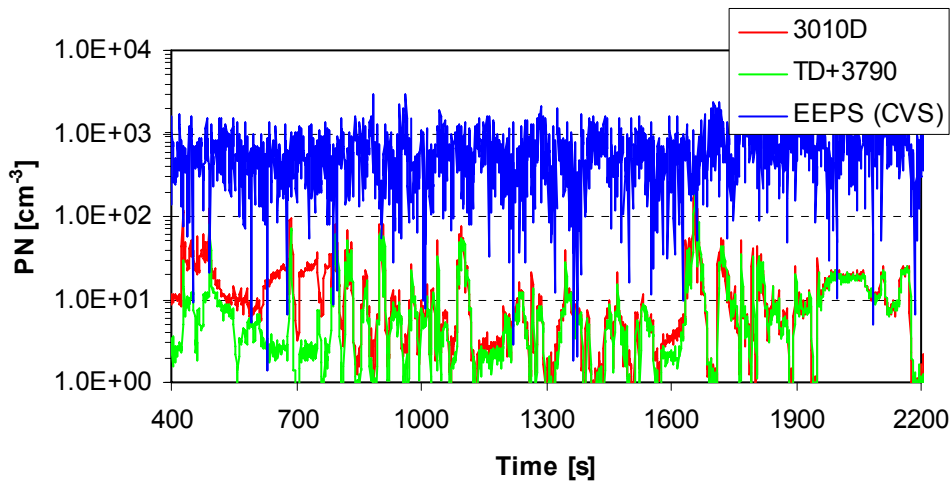


Figure 68: Emissions (>23 nm) during a hot WHTC.

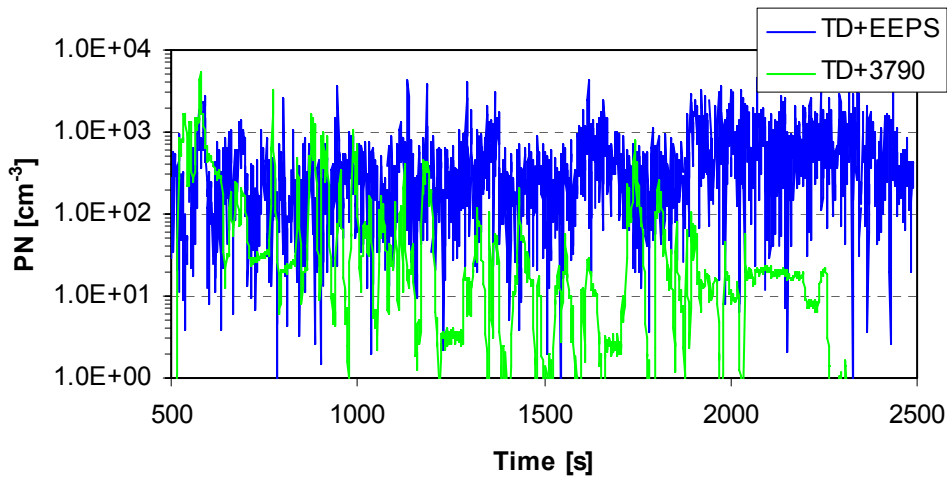


Figure 69: Emissions downstream of a TD.

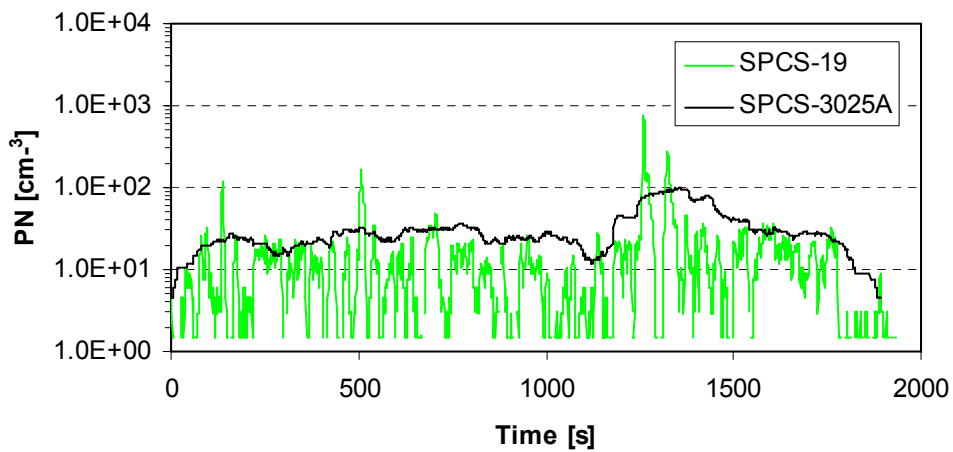


Figure 70: Comparison of a 3010D and a 3025A downstream of SPCS.

WHSC

The emissions during a WHSC (with the preconditioning at mode #9) can be seen in Figure 71. As it can be seen the emissions increase at high speed/torque modes where the temperature increases. This increase in the temperature has two effects: 1) the CRT regenerates, thus cleans and more non-volatile particles are emitted 2) the SO_2 to SO_3 conversion increases thus leading to higher volatile emissions. No EEPS was available for this measurements to measure the size distributions. A 3025A connected downstream of the SPCS showed negligible non-volatile particle emissions below 23 nm (Figure 72).

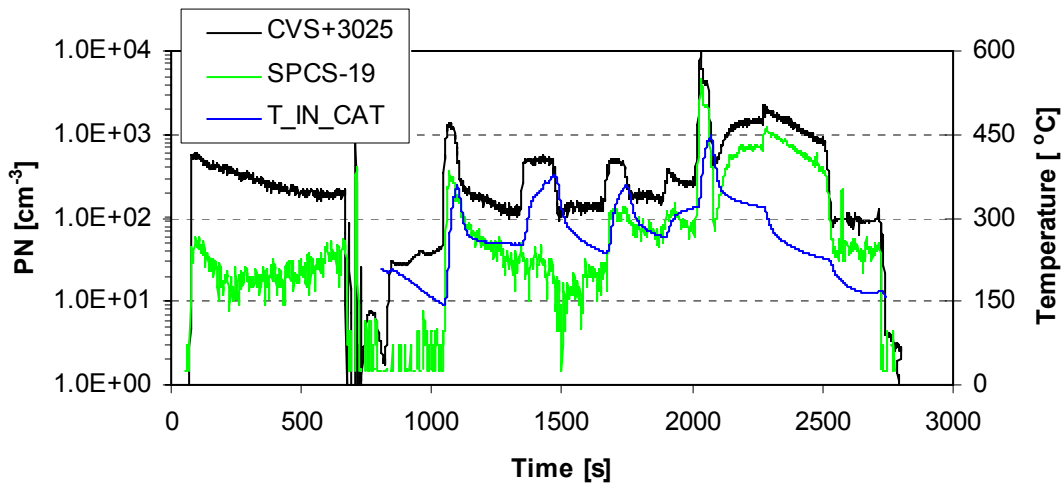


Figure 71: WHSC emissions.

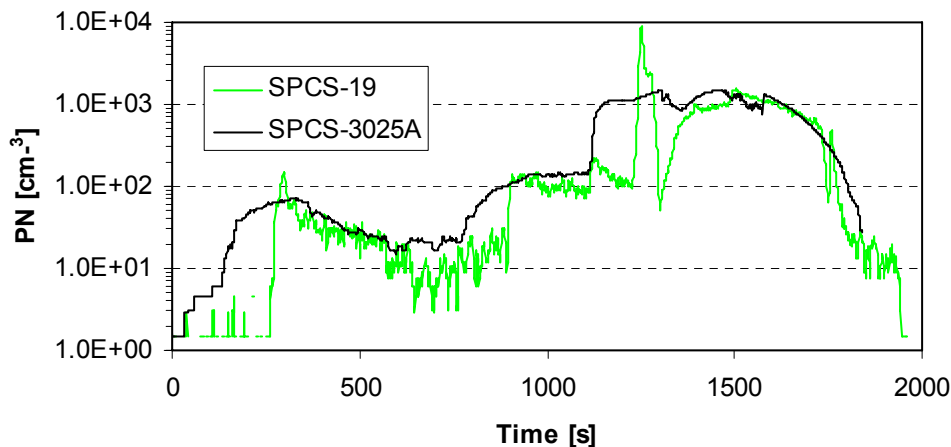


Figure 72: Comparison of a 3010D and a 3025A downstream of SPCS.

ETC

The emissions during an ETC (with the pre-conditioning phase) can be seen in Figure 73. The emissions are very low as at the hot WHTC. The EEPS, connected at CVS was not possible to measure anything as the emissions were below its sensitivity limit. For this reason a 3025A was connected directly at CVS (Figure 74). It can be observed that there are some volatile particles at CVS. The difference between the 3025A and the 3010D is approximately +50%. However, when the 3025A was connected at the SPCS the emissions of the 3025A were very low (Figure 75). The difference between the two counters was 15%.

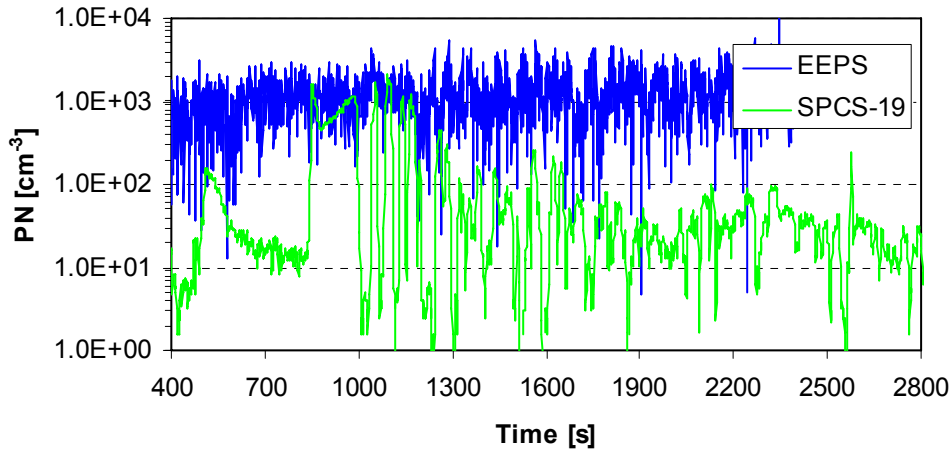


Figure 73: ETC emissions with EEPS and SPCS.

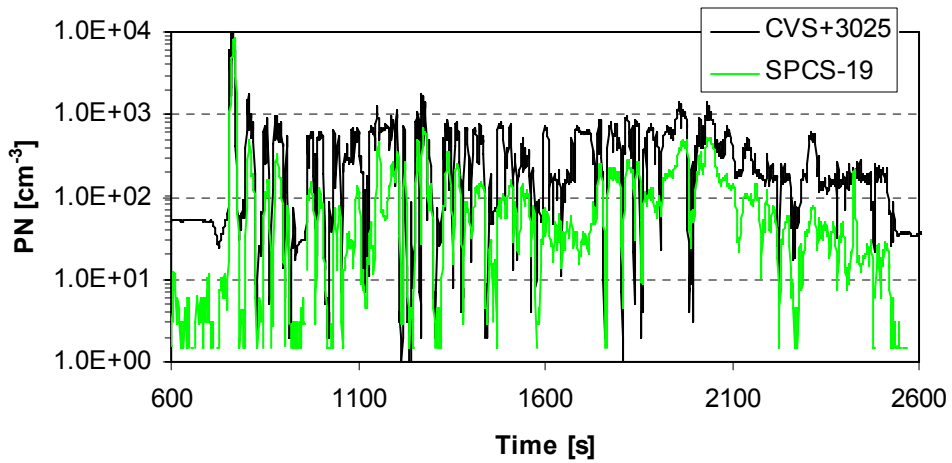


Figure 74: Total (>3 nm) and nob-volatile (>23 nm) particles over an ETC.

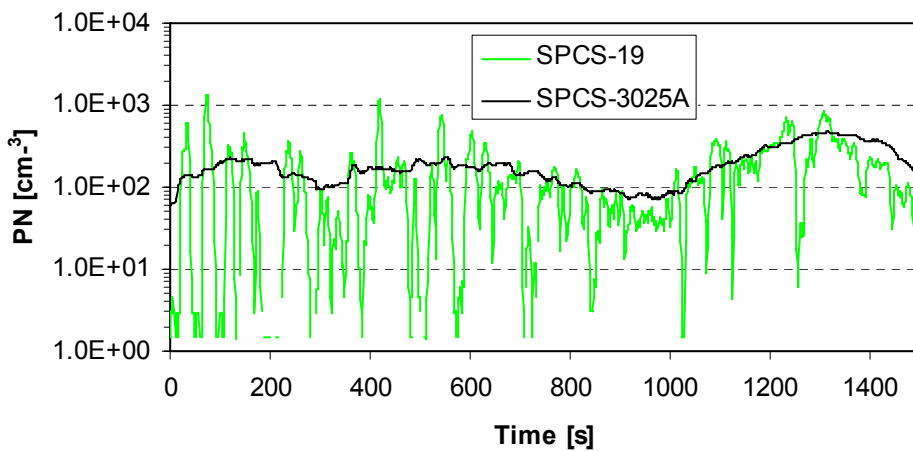


Figure 75: Non-volatile particles >3 and >23 nm over an ETC.

ESC

Figure 76 shows the total (EEPS) and non-volatile (SPCS-19) emissions over an ESC. The SPCS-19 was multiplied by a factor to match the EEPS emissions (0.7). This difference of the two instruments was not investigated. In the same figure the speed and torque of the cycle are given. It is confirmed that high particle emissions are observed at high speed/load modes where the CRT regenerates and more non-volatile particles are emitted.

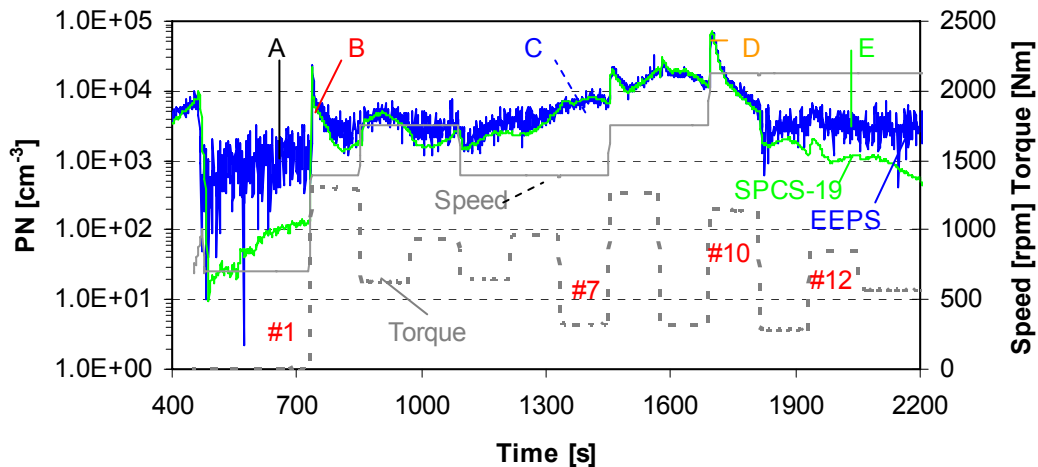


Figure 76: Emissions over an ESC.

Figure 77 shows the size distributions measured from EEPS at different points of the cycle. At idle (point A) there is a small peak at 80 nm but its close to the noise level of the instrument. The first measurable peak (point B, at mode #2) has a its peak at 70 nm. The emissions during the next modes are accumulation mode particles with peaks around 60-70 nm (e.g. point C). There might be also a NM but it's close to the detection limit of the instrument. The peak at mode 10 has also only accumulation mode at 60 nm (D). At all these points SPCS-19 and EEPS had similar emission levels, so all these particles are non volatiles and probably there are no other volatiles or solids at lower diameter (or their concentration is small). At modes #11-13, EEPS measures higher indicating that there must be also volatile particles or non-volatiles below 23 nm. Size distribution E shows a small accumulation mode and indication of nucleation mode (close to the noise levels of the instrument).

Another ESC was repeated using a 3025A directly at CVS (corrected for CPC differences and losses in SPCS). As it can be seen (Figure 78) there is an increase of volatile particles (or non-volatiles below 23 nm) at mode #2 (and #4) as the temperature increases and the CRT regenerates. This increase of particles was not observed with EEPS because it was below its sensitivity limit. At the rest high temperature modes (e.g. mode #10) there is no big difference between the two instruments because most volatiles condense on the non-volatile particles which are quite high due to the cleaned state of the CRT. These particles are non-volatiles. This was confirmed when the 3025A was connected at SPCS (Figure 79). The difference between the 3010D and 3025A was small.

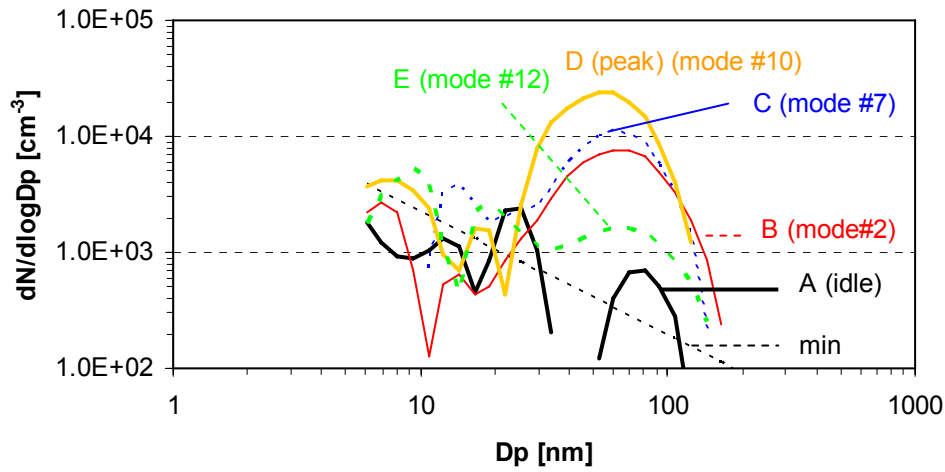


Figure 77: Size distributions.

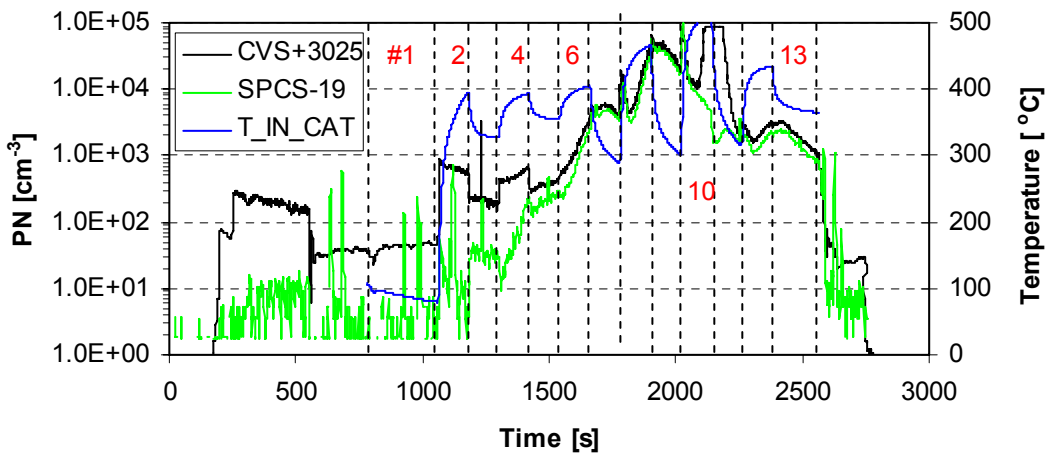


Figure 78: Particle emissions over an ESC and exhaust gas temperature.

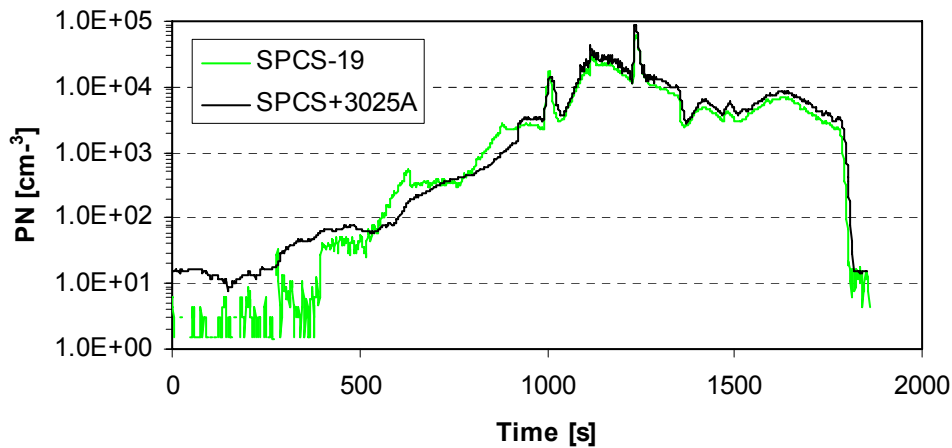


Figure 79: Non-volatile (>3 and >23) nm emissions over an ESC.

Steady states

Figure 80 shows the particle emissions during regeneration (mode #10) and loading (mode #7) of the CRT. The pattern is as follows:

- Blow out of particles due to the acceleration.
- Increase of volatiles due to the increase of the temperature (see also discussion of Figure 23).
- Decrease of solids at mode #7. For a short period high amount of volatiles due to the increased temperature and decrease available surface.
- Decrease of volatiles. Only solids are emitted.
- Repeat of the cycle.

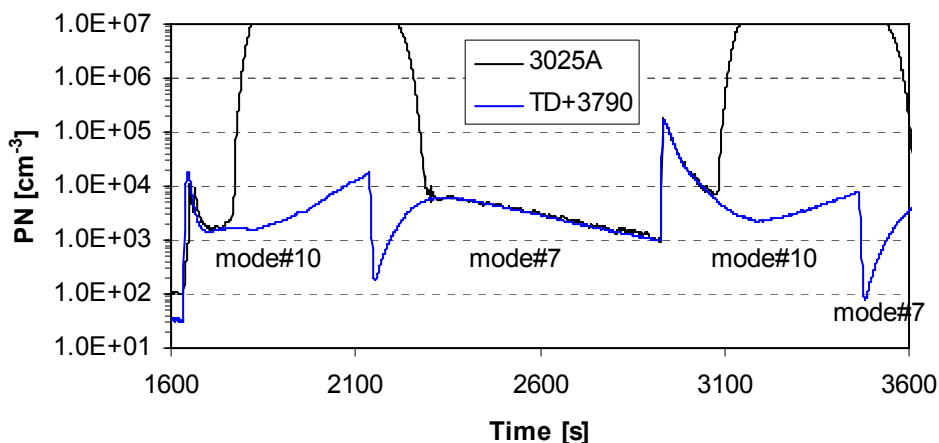


Figure 80: Particle emissions during steady states.

A 3936 SMPS was connected at CVS and Figure 81 and Figure 82 show the above mentioned trends for modes #10 and #7 respectively. There is an increase of volatiles (but also AM) at mode #10 gradually till an equilibrium is reached. These particles with peak of 20 nm are mainly volatiles because they were not measured downstream of the TD or the dual EJ system. The AM is non-volatile particles as the concentrations measured with SMPS were at similar levels with the concentration measured from SPCS.

In order to investigate the non-volatile emissions <23 nm a nano-SMPS was used during mode #10 and #7 downstream of a TD. The results are shown in Figure 83. There is a small indication of small particles at mode #10. In order to confirm that they are non-volatiles and not particles due to inefficient removal of volatile particles from the TD, a 3025A was connected at the SPCS during the mode mode #10. The results are shown in Figure 84a. Indeed, during the regeneration of the CRT some non-volatile particles <23 nm exist. The concentration is very low (10^6 cm^{-3} taking into account the dilution in CVS). Moreover, they are not always observed (Figure 84b).

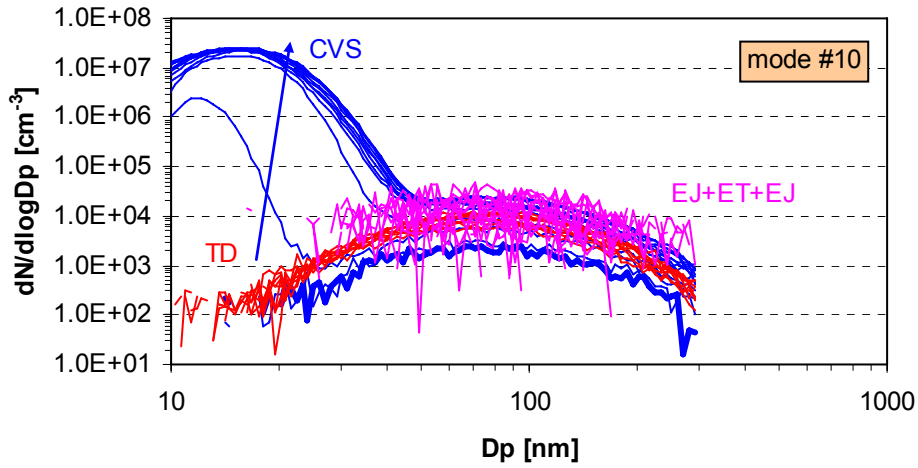


Figure 81: Size distributions at mode #10 (ESC).

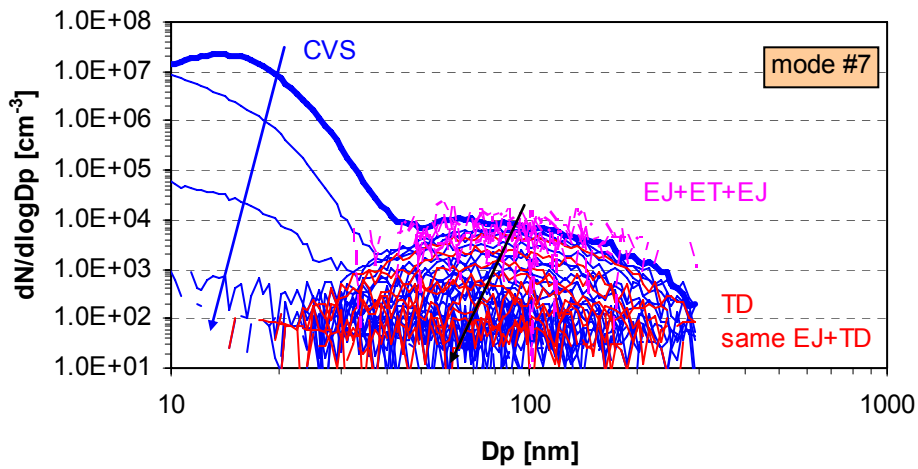


Figure 82: Size distributions at mode #7 (ESC).

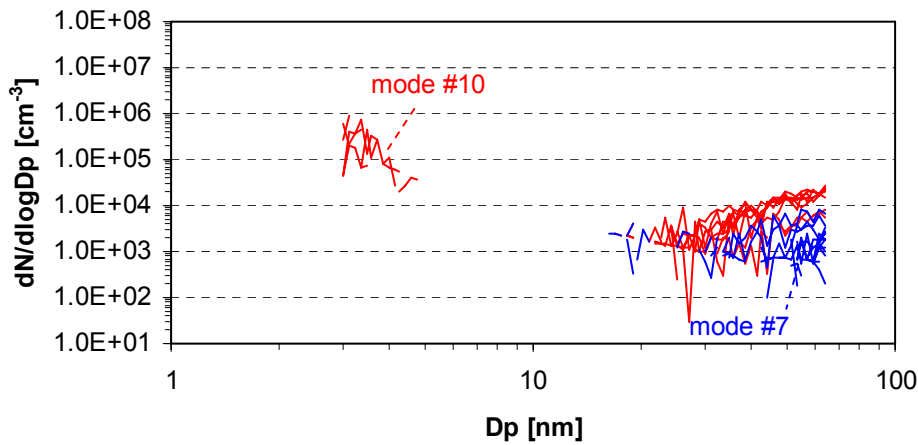


Figure 83: Size distributions with nano-SMPS downstream of a TD.

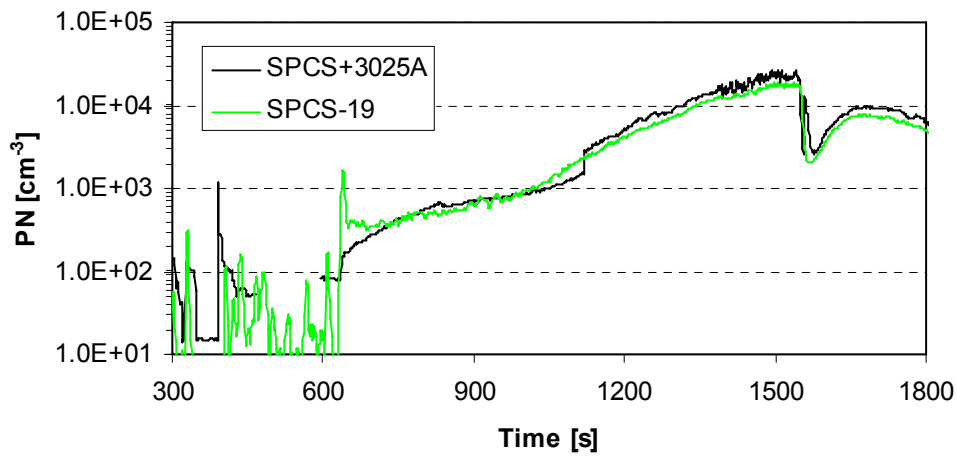
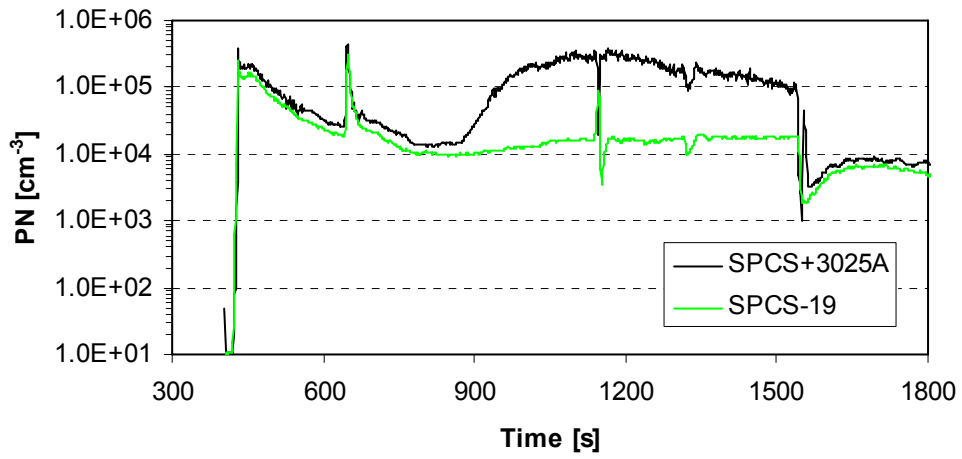


Figure 84: Non-volatile (>3 and >23 nm) during mode #10 (ESC).

DMM

DMM was available during the validation tests (official PMP tests in June 2008). In this section the comparison with PM and SPCS is shown. DMM was usually used downstream of a thermodenuder. A 1.28 correction was applied to the DMM results. No background correction was applied. Figure 85 shows the difference between DMM and CVS PM. Figure 86 shows the difference between DMM number and SPCS.

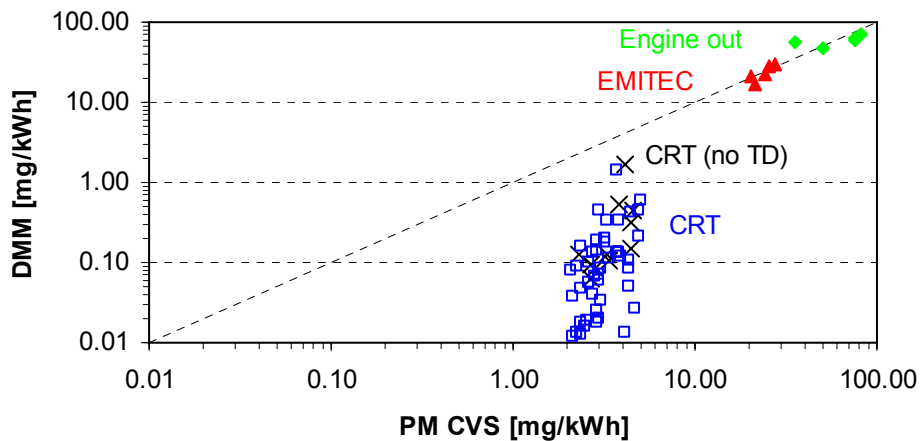


Figure 85: Difference of mass emissions between DMM and filter PM at CVS.

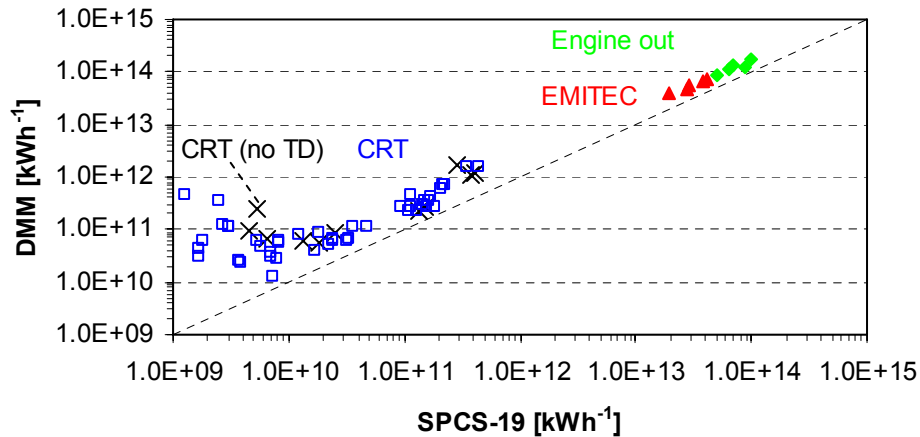


Figure 86: Difference of number emissions between DMM and SPCS at CVS

Table 15: Difference between DMM (downstream of a TD) and PM from CVS.

	WHTC cold	WHTC hot	WHSC	ETC	ESC
PM CRT	-89% ($\pm 11\%$)	-97% ($\pm 2\%$)	-98% ($\pm 1\%$)	-99% ($\pm 1\%$)	-97% ($\pm 2\%$)
PM EMITEC	-22%	-8%	2%	10%	8%
PM Engine	60%	-8%	-13%	-13%	-20%
PN CRT	200% ($\pm 54\%$)	7097%	341%	691%	96% ($\pm 2\%$)
PN EMITEC	96%	72%	91%	75%	83%
PN Engine	72	79%	46%	71%	100%

Table 15 shows the difference between DMM and PM (CVS) or PN (SPCS-19 at CVS) for all the cycles and different after-treatment devices CRT, open filter EMITEC, engine out). PM difference for high emissions (engine out and EMITEC) is $\pm 20\%$. However for the CRT case DMM measures less than 10% of the filter results. This confirms that a high amount of volatiles is collected on the filter.

The differences in number are quite high. In the engine out and EMITEC cases the DMM measured 75% higher number emissions. In the CRT case the differences are more than 100%.

These differences can be understood by looking at the real time patterns. The engine out comparisons (e.g. Figure 87 for a cold WHTC and Figure 88 for an ESC) shows that the DMM is between SPCS (>23 nm) and Nanomet with a 3010 (>10 nm), indicating that probably it's cut-point is somewhere between.

When looking at the CRT emissions, which in general are low it seems that the DMM overestimates the number emissions (Figure 89) as it measures even higher than the 3025A. Similar conclusion can be drawn by the ESC (Figure 90). It has to be emphasized also that the DMM background is relatively high for CRT engines (Figure 91), as during an ETC cycle only a few peaks could be observed.

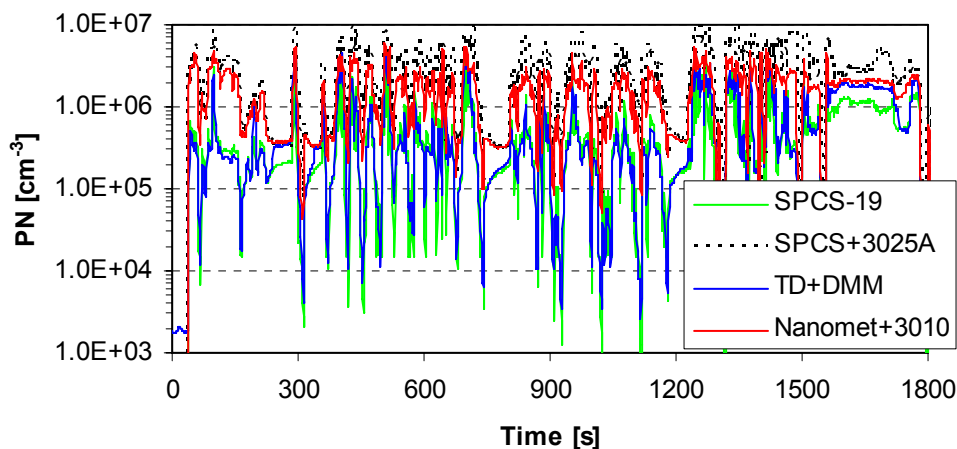


Figure 87: Comparison of DMM with SPCS and 3025A over a cold WHTC (Engine out).

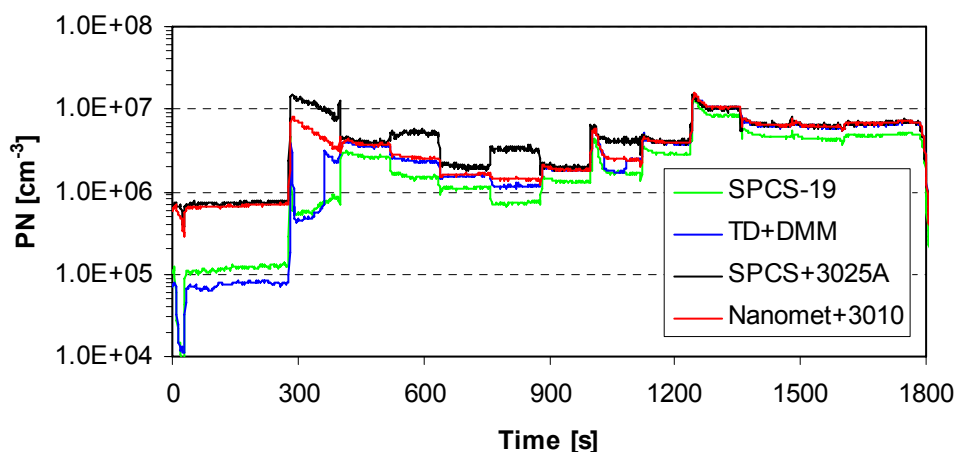


Figure 88: Comparison of DMM with SPCS and 3025A over an ESC (Engine out).

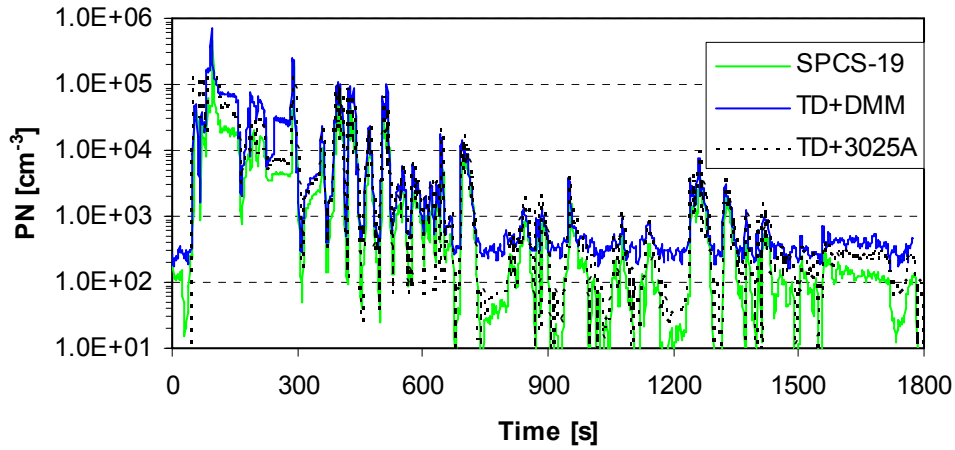


Figure 89: Comparison of DMM with SPCS and 3025A over a cold WHTC (Engine with CRT).

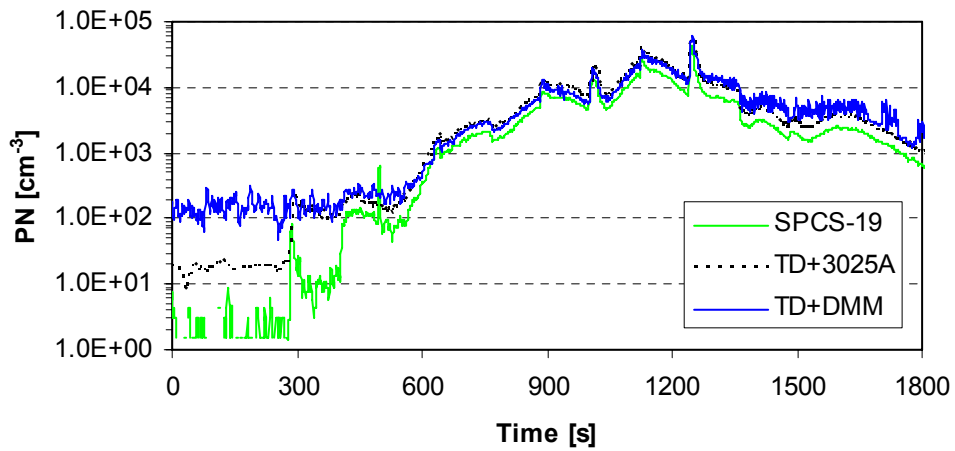


Figure 90: Comparison of DMM with SPCS and 3025A over an ESC (Engine with CRT).

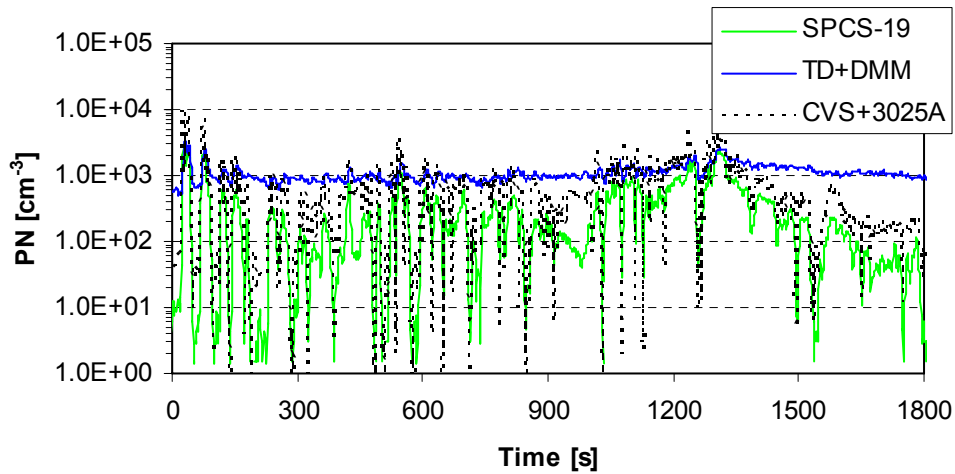


Figure 91: Comparison of DMM with SPCS and 3025A over an ETC (Engine with CRT).

4. CONCLUSIONS

After the light-duty inter-laboratory exercise the heavy-duty phase will begin. Although the protocol between the two exercises will be similar there are some open issues due to the different nature of light-duty and heavy-duty testing:

- Different cycles and longer testing.
- Different after-treatment devices and pre-conditioning.
- Possibility to use partial flow systems

Target of the exploratory work at JRC was to define and finalize the measurement protocol. The conclusions of the exploratory work in JRC VELA-5 with the Golden Engine (with a continuous regenerating filter) using low sulfur fuel and lubricant are:

Facilities

In order to meet the PMP HD protocol requirements the following actions were taken:

- The secondary tunnel was heated externally in order to have filter temperature of $47\pm 5^{\circ}\text{C}$ for at least 0.2 s. Filter holders for 47 mm filters were bought. HEPA and Carbon filters were also installed at the dilution air line of the secondary tunnel.
- The partial flow sampling system PSS-20 (Control Sistem) complied with the PMP requirements, so only the cyclone was insulated.
- The partial flow sampling system SPC-472 (AVL) was upgraded by the manufacturer (cyclone, heating of the filters, 47 mm filter holders). As the extracted flow for the number system (downstream the cyclone) couldn't be taken into account in the software, a feed back flow (same flow rate with the one extracted) was added downstream the electromagnetic valve after the filter. The PM results have to be corrected for this flow rate (see report for official PMP tests). The feed back flow was filtered pressurized air through a mass flow controller. Finally, HEPA and Carbon filters were also installed at the dilution air line of SPC-472.
- One HEPA filter was also installed at the filtration system of the ejector dilutors.

Mass and number background

The mass and number background was measured with the engine off (for the full flow system) or by sampling through a HEPA filter for 30 min (for the partial flow systems). The results (after the facilities were upgraded with HEPA and carbon filters at the dilution air lines) were:

- The mass background level of the secondary tunnel of the full dilution method was in the order of 20 μg after 30 min sampling.
- The mass background level of the partial flow systems (SPC-472 and PSS-20) was higher (35 μg after 30 min sampling).
- The number background of the primary and secondary tunnel was $<5\text{ cm}^{-3}$.
- The particle number background of the SPCS-472 level was $<15\text{ cm}^{-3}$ when HEPA filters were installed. The number background of PSS-20 was $<50\text{ cm}^{-3}$ (with its own filter, no extra HEPA filter installed).

Filter (PM) tests

Target of these tests was to find a proper flow range for the PM measurements. PM measurements at the secondary tunnel of the full flow dilution tunnel with different filter face velocities (over a WHSC) showed that:

- For the same flow rate the PM emissions were lower with the 47 mm filters compared to the 70 mm (TX40), probably due to the higher filter face velocity.
- For the 47 mm filters (TX40) similar emissions were found between 40 and 60 lpm.

For these reasons a 50 lpm flow rate was decided for the official PMP tests (for full flow and partial flow systems with 47 mm filters).

- Generally, the mass emissions were close to the background levels (but higher).
- Comparison with a DMM showed that most of the mass on the filter is volatiles (volatile artifact).

Characterization of particle counting and sampling systems

Target of these systems was to check if the existing particle number systems comply with the PMP and future legislation requirements (particle number concentration reduction factor PRF, volatile removal efficiency of C40 particles, calibration constants of number counters).

Checks of some condensation particle counters (CPCs) showed that:

- The particle number counters of the two Golden instruments correlated very closely (1-4% lower the CPC at SPCS-20).
- Most PMP counters correlated very well with differences of the slopes of less than $\pm 5\%$ with one exception (a 3790). This system was sent back to TSI.

Volatility checks showed that:

- The volatile removal efficiency (checked with C40 monodisperse or polydisperse particles) for SPCS, Nanomet, dual ejector system and the ejector plus thermodenuder was $>99\%$. One hot ejector dilutor alone couldn't remove the C40 particles. The thermodenuder alone could decrease the C40 particles but a small peak at 13 nm was usually remaining.
- The volatile removal efficiency of the Golden instruments (and the thermodenuder) was found adequate as diesel engine nucleation mode with mode peak at 16 nm and concentration of $1.2 \times 10^7 \text{ cm}^{-3}$ could be evaporated.

The measured dilution ratios with propane gas showed that:

- The SPCS dilution ratios were usually within $\pm 5\%$ of the software values. Even a 10 kPa under-pressure had a very small effect on the dilution ratio (6%).
- Further investigation of SPCS dilution ratios showed that when this system is connected to a partial flow system and a high primary dilution ratio (>25) is used, uncertainty in the final result is possible due to the high pressure fluctuations. In this case, the average dilution ratio of the cycle should be used to have small difference from the "true" cycle emissions.
- The old Nanomet's dilution ratios were 10% lower than the measured from the manufacturer. This had to do probably with the different measurement approaches. The manufacturer measures the particle reduction factor at 80 nm.
- A 10 kPa under-pressure at the inlet of the old Nanomet affected the dilution ratio 25-30%.

- The dual ejector system is sensitive in temperature and pressure changes. For this reason the factors given in Table 3 should be applied for the correct estimation of the dilution ratio. For example, 10 kPa under-pressure affects the dilution ratio 30-40%.

The penetration tests showed that:

- The old Nanomet has high losses of 30 nm particles (50%). At 70-100 nm the losses were found 14%.
- The SPCS losses at 30 nm were found 30% and at 100 nm 14%.
- Ejector dilutor losses were found negligible.

The Particle Reduction Factors:

- For old Nanomet the average PRF leads to a high value due to the high PRF at 30 nm (due to the high losses in this size). The PRF at 70 nm should be used (293). This value is 8% higher than the manufacturer's dilution value.
- For SPCS the average PRF (at dilution ratio setting 10x15) is 190, 26% higher than the software value. The 70 nm PRF is 22% higher.
- PRF measurements are conducted in slight under-pressure (downstream of a DMA) and apply for this under-pressure. If the system is going to be used at different pressure (e.g. at overpressure), this has to be taken into account. For CVS (which is at slight under-pressure) the correction is negligible.
- For the official tests the manufacturer's dilution values will be used as the penetration experiments were conducted only for a few systems. Moreover, it hasn't been investigated if there is any effect of the high temperatures of the evaporation tube at the NaCl generated particles.

Comparison of particle number systems

Target of these tests was to estimate the anticipated differences between different particle number systems.

- The two Golden units (SPCS) have <5% difference with each other.
- Preliminary tests showed satisfactory agreement of the Golden instruments at the same partial flow system, at different partial flow systems and between full and partial flow systems. These issues will be investigated in more detail during the validation exercise tests.
- Very good agreement between different measurement systems (Nanomet, ejector dilutors with thermodenuder or evaporation tube) was found. The differences taking into account only the dilution ratios was $\pm 15\%$. Using the PRFs the difference was $\pm 5\%$.
- The number emissions were much higher than the background levels for most cycles. However, some systems (Nanomet, ejectors) had a background similar to the hot WHTC and ETC cycle emissions.

Conclusions about the set up

Target of these tests was to investigate how much would be the effect on particle number emissions of the differences in the set ups.

- The cyclone (laminar or turbulent flow) had negligible effect on the number emissions. This means that for number measurements it is not necessary. However, it's highly recommended in order to protect the instruments from larger particles. In addition,

insulation of the cyclone and the tubes is highly recommended to decrease thermophoretic losses during high temperature modes.

- The 4 m (at 47°C) heated line had minor effect on the emissions (<5%). This means that one SPCS can be connected to the CVS through 4 m line (heated at 47°C), while the other SPCS can be connected to the partial flow system with a short insulated line.

Pre-conditioning

Target of these tests was to define a pre-conditioning at the end of the measurement day (for the after-treatment devices) to have repeatable cold start emissions.

- The preconditioning of the measurements was found to be important for the particle measurements. Different pre-conditionings led to different emission levels.
- It was suggested a minimum preconditioning of 15 min at mode #10 (ESC) for regeneration of the CRT and 30 min at mode #7 (ESC) for loading at the end of the day to have relatively repeatable cold start emissions the next day.

Continuity protocol

Target of these tests was to define a conditioning of the engine (and the after-treatment devices) before the cycles ETC and ESC (for hot WHTC there is no preconditioning, only 10 min soak, and before WHSC there is a 10 min conditioning at mode #9 according to the legislation).

- Before ESC and ETC cycles it was shown that the engine should be warmed up at mode #7 for 5 min. Then idle 3 min follows for the preparation of the automated systems.
- Higher engine modes would lead to regeneration of the after-treatment device and variable emissions during the next cycle. Probably the WHSC, which is preceded by a high engine mode, will have more variability than the rest cycles.

Real time emissions (engine with CRT)

Target of these tests was to investigate the emission levels during that should be expected during the official tests.

- High emissions of non-volatile particles were measured at the beginning of a cold cycle. These particles can be blow-out of loose solid particle depositions, as the filter is exposed to highly transient operation with respect to the thermal and flow conditions. The volatile emissions are low at this part of the cycle. However, nucleation mode particles can be observed. They can be particles formed by the nucleation-condensation of semi-volatile material earlier stored within the substrate and/or the particulate layer and released during the cold-start cycle as the CRT heats up. The emissions can be as high as 10^{-6} cm^{-3} . Thus, a dilution of 100:1 should be enough for a CPC that measures up to 10^{-4} cm^{-3} .
- During hot cycles the non-volatile emissions are low. Low volatile emissions are also measured.
- During cycles (e.g. steady cycles) where the temperature increases above the regenerating point, high volatile emissions are measured even though low sulfur fuel and lubricant are used. These particles were removed from the number systems.
- During cycles (e.g. steady cycles) where the temperature increases above the regenerating point, high non-volatile emissions are also measured.
- During the regeneration of the CRT non-volatile particles <23 nm can also be observed, but their concentration is low.

Parameters

- For the full dilution tunnel flow rate of 80 m³/min was selected. This flow rate is the maximum that can be used from all participating labs.
- For the secondary dilution tunnel a total flow rate of 50 lpm was selected (0°C, 1 bar). The dilution air flow rate was set to 25 lpm (dilution ratio 2:1). Thus, it will be possible for labs to reach the 47±5°C by heating the secondary tunnel and/or the secondary dilution air.
- For the partial flow systems the total flow rate was chosen 3000 nl/h (or 1.08 g/s) and the split ratio 0.00626% (or G_{edf} 6200 kg/h). This way the dilution ratio of the full dilution tunnel and the partial flow systems will be the same. This favors the number measurements but leads to different total dilution ratio for PM between the partial flow systems and the secondary tunnel at the full dilution tunnel.
- Labs with different CVS flowrates or PM flowrates can estimate the required r (to have the same dilution ratios in CVS and the partial flow system) from equation 5b. However, for the validation exercise all labs will use the same parameters for the partial flow systems (irrespective of the CVS settings) for better comparability.
- For the golden systems (SPCS) the settings are: PND1 10:1, primary dilution air flow rate 11.5 lpm, bypass 2 lpm, PND2 15:1, secondary dilution air flow rate 10.5 lpm. SPCS-19 will be used at the CVS and SPCS-20 at the partial flow system.

REFERENCES

Andersson J., Clarke D., Watson J. (2004). UK Particulate Measurement Programme (PMP): A Near US 2007 Approach to Heavy Duty Diesel Particulate Measurements – Comparison with the Standard European Method. SAE 2004-01-1990

Andersson J., Giechaskiel B., Munoz-Bueno R., Dilara P. (2007). Particle Measurement Programme (PMP): Light-duty Inter-laboratory Correlation Exercise (ILCE_LD)-Final report (EUR 22775 EN) GRPE-54-08-Rev.1, <http://www.unece.org/trans/main/wp29/wp29wgs/wp29grpe/grpeinf54.html>

Andersson J, Clarke D. (2008). UN-GRPE PMP Phase 3: Inter-laboratory Correlation Exercise: Updated Framework and Laboratory Guide for Heavy Duty (HD) Engine Testing. A Document For The UK Department for Transport

Biskos G., Malinowski A., Russell L., Buseck P. R., Martin S. T. (2006). Nanosize Effect on the Deliquescence and the Efflorescence of Sodium Chloride Particles. *Aerosol Sci. Technol.*, 40, 97-106

CFR (2001). Code of Federal Regulations Title 40 Part 86 Subpart N – Emission Regulations for New Otto-Cycle and Diesel Heavy-Duty Engines; Gaseous and Particulate Exhaust Test Procedures (Revised July 1 2001). “US2007”

EMIR1 2007. Kannel A., Rydström A., De Serves C. Industry Report on Exhaust Particle Measurements: A work within the EMIR1 project

Giechaskiel B., Ntziachristos L., Samaras Z. (2004). Calibration and Modeling of Ejector Dilutors for Automotive Exhaust Sampling, *Measurement Science & Technology* 15:1-8

Giechaskiel B., Ntziachristos L., Samaras Z., Casati R., Scheer V., Vogt R. (2005). Formation Potential of Vehicle Exhaust Nucleation Mode Particles On-Road and in the Laboratory, *Atmospheric Environment*, 39, 3191-3198

Giechaskiel B., Ntziachristos L., Samaras Z., Casati R., Volker S., Rainer V. (2007a). Effect of speed and speed transition on the formation of nucleation mode particles from a light duty diesel vehicle. SAE Technology Paper 2007-01-1110.

Giechaskiel B., Munoz-Bueno R., Rubino L., Manfredi U., Dilara P., De Santi G., Andersson J. (2007b). Particle Measurement Programme (PMP): Particle Size and Number Emissions Before, During and After Regeneration Events of a Euro 4 DPF Equipped Light-duty Diesel Vehicle, SAE 2007-01-1944

Giechaskiel B., Dilara P., Andersson J. (2008a). Particle Measurement Programme (PMP) Light-Duty Inter-laboratory Exercise: Repeatability and Reproducibility of the Particle Number Method. Accepted in *Aerosol Sci. Technology*

Giechaskiel B., Dilara P., Sandbach E., Andersson J. (2008b). Particle Measurement Programme (PMP) Light-Duty Inter-laboratory Exercise: Comparison of Different Particle Number Measurement Systems. Accepted in *Measurement Sci. Technology*

ISO16183 Heavy-Duty Engines – Measurement of gaseous emissions from raw exhaust gas and of particulate emissions using partial flow dilution systems under transient test conditions.

Khalek I. 2005. 2007 Diesel Particulate Measurement Research. CRC Project E-66 Phase 1.

Khalek I. 2006. 2007 Diesel Particulate Measurement Research. CRC Project E-66 Phase 2.

Khalek I. 2007. 2007 Diesel Particulate Measurement Research. CRC Project E-66 Phase 3.

Kittelson, D.B.; Watts, W.F.; Johnson, J.P.; Rowntree, C.; Payne, M.; Goodier, S.; Warrens, C.; Preston, H.; Zink, U.; Ortiz, M.; Goersmann, C.; Twigg, M.V.; Walker, A.P.; Caldow R. (2006). On-road evaluation of two Diesel exhaust after treatment devices. *J. Aerosol Sci.*, 37, 1140 – 1151

Liu, W., Osmondson, B.L., Bischof, O.F., Sem, G.J. (2005). Calibration of Condensation Particle Counters. SAE 2005-01-0189

Ntziachristos, L., Giechaskiel, B., Pistikopoulos P., Samaras Z., Mathis U., Mohr M., Ristimäki J., Keskinen J., Mikkanen P., Casati R., Scheer V. and Vogt R. (2004). Performance and Evaluation of a Novel Sampling System for Exhaust Particle Characterization, SAE 2004-01-1439

Ntziachristos, L., Giechaskiel, B., Pistikopoulos, P., Samaras, Z. (2005). Comparative Assessment of Two Different Sampling Systems for Particle Emission Type-Approval Measurements, SAE 2005-01-0198

PMP (2003). Report of the GRPE Particle Measurement Programme (PMP): Government Sponsored Work Programmes, <http://www.unece.org/trans/doc/2003/wp29grpe/TRANS-WP29-GRPE-specinf01e.pdf>

Reg. 49 – Rev. 4 – Uniform Provisions Concerning the Approval of Compression Ignition (CI) and Natural Gas (NG) as well as Positive Ignition (PI) Engines Fuelled with Liquefied Petroleum Gas (LPG) and Vehicles Equipped with CI and NG Engines and PI Engines fuelled with LPG with regard to the Emissions of Pollutants by the Engine. <http://www.unece.org/trans/main/wp29/wp29regs/r049r3e.pdf>

Reg. 83 - Rev.3 - Emission of Pollutants According to Engine Fuel Requirements, <http://www.unece.org/trans/main/wp29/wp29regs81-100.html>

Vaaraslati K., Keskinen J., Giechaskiel B., Solla A., Murtonen T., Vesala H. (2005). Effect of Lubricant on the Formation of Heavy-Duty Diesel Exhaust Nanoparticles. *Environ. Sci. Technol.* 39, 8497-8504

Wei, Q., Akard, M., I. Asano, M. Rahman (2008). Penetration Calibration and Verification for the Solid Particle Counting System with Polydisperse and Monodisperse Particles. SAE 2008-01-1178

Wei, Q., Oestergaard, K., Porter, I. Asano, A., A. Masayuki, M. Rahman, K. Takeshi, Y. Goto (2006). Real-time Measuring System for Engine Exhaust Solid Particle Number Emission – Performance and Vehicle testing. SAE 2006-01-0865

Wei, Q., Oestergaard, K., Porter, S., Ichiro, A., Adachi, M., Montajir, M. (2006). Real-time Measuring System for Engine Exhaust Solid Particle Number Emission – Design and Performance. SAE 2006-01-0864

DEFINITIONS, ACRONYMS, ABBREVIATIONS

BG	Background
CoV:	Coefficient of Variance
CPC:	Condensation particle Counter
CRT	Continuous Regenerating Trap
CVS	Constant Volume Sampling
DPF:	Diesel Particulate Filter
DR:	Primary Dilution Ratio
EEPS	Exhaust Engine Particle Sizer
EGR:	Engine Gas Recirculation
EJ	Ejector dilutor
ESC	European Steady Cycle
ET:	Evaporation Tube
ETC	European Transient Cycle
EU	Evaporation Unit
HEPA	High Efficiency Particle Filter
JRC:	Joint Research Centre
LEPA	Low Efficiency Particle Filter
MFC	Mass Flow Controller
PFS	Partial Flow System
PM:	Particulate Matter
PMP:	Particle Measurement Programme
PN:	Particle Number
PND	Particle Number Diluter
PSS	Control Sistem Partial Flow System
PTS	Secondary Dilution Tunnel
RT	Residence Time
SMPS	Scanning Mobility Particle Sizer
SPC-472	AVL Smart Sampler
SPCS	Solid Particle Counting System
TD	Thermodenuder
TX40	TX40H120-WW
VELA:	Vehicles Emissions Laboratory
WHSC	World Harmonized Steady Cycle
WHTC	World Harmonized Transient Cycle

Note: The term *non-volatile* and *solid* particles are used interchangeably and indicate particles that survive downstream of a thermodenuder (275°C) or a hot dilution (150°C) plus an evaporation tube (>300°C).

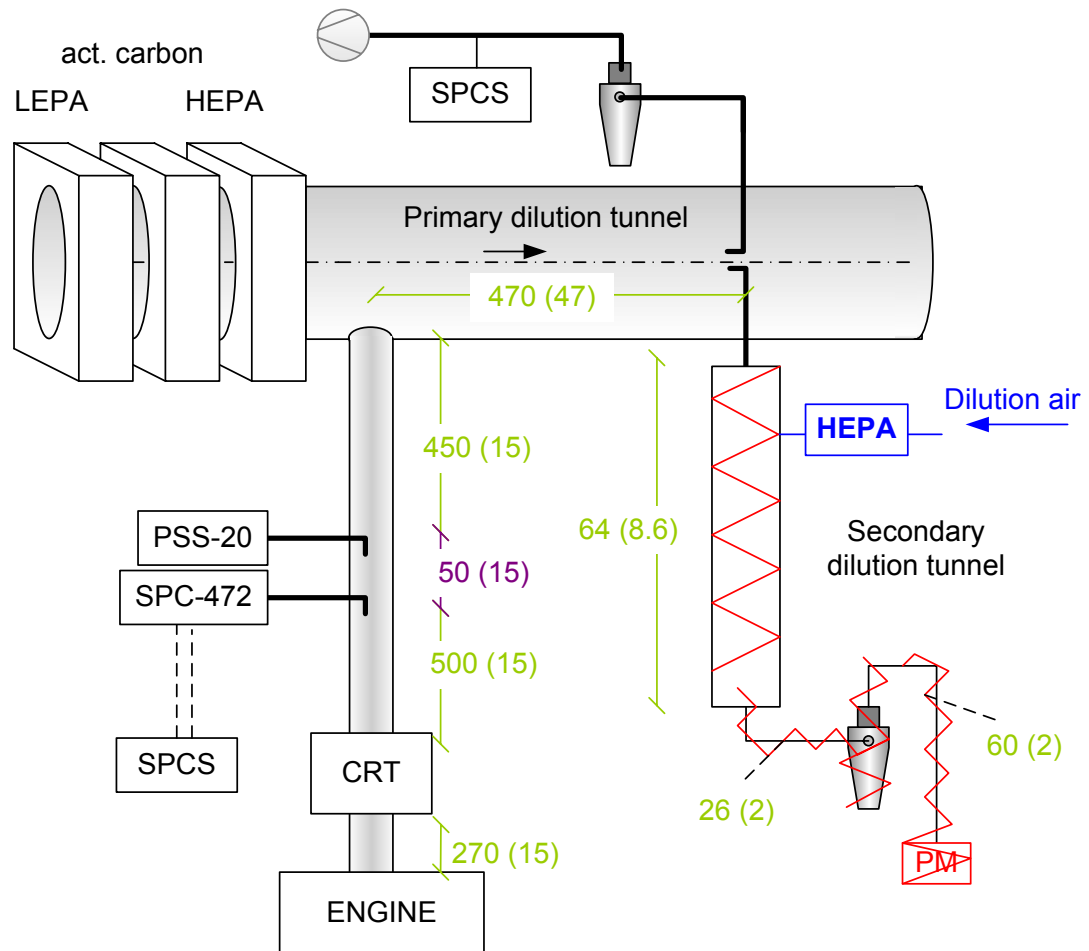
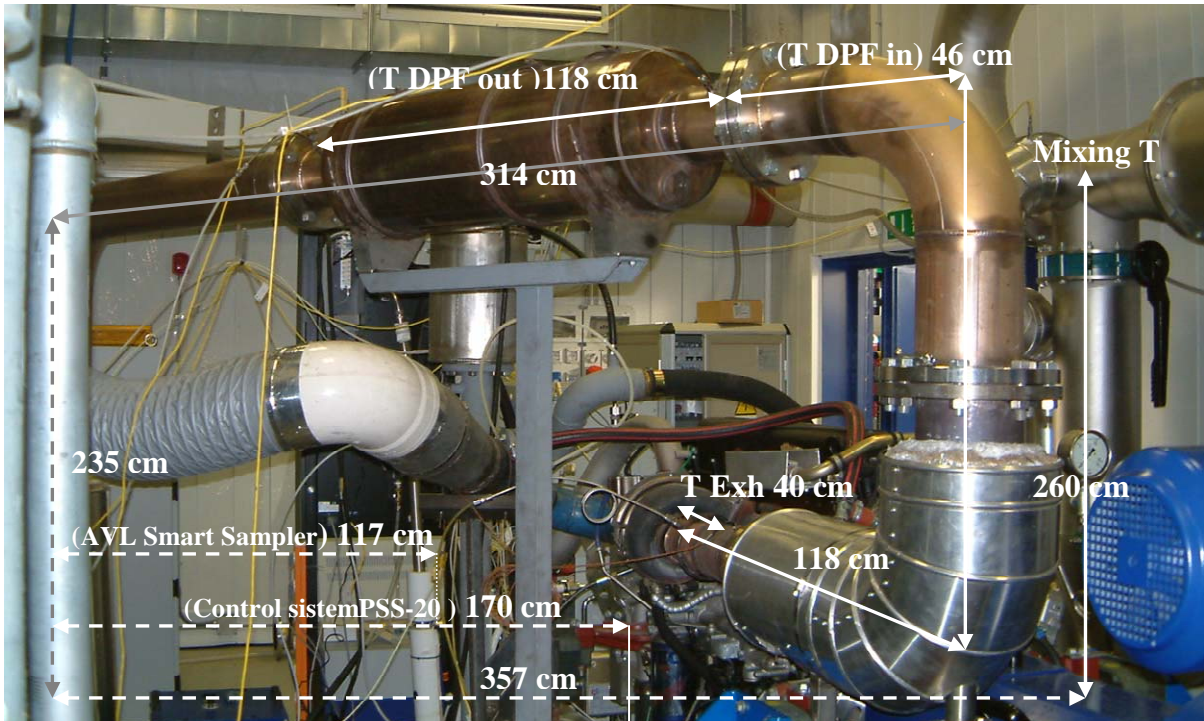
Note: the term *dilution ratio* and *dilution factor* are used interchangeably and indicate the ratio of total flow to the sample flow.

ANNEXES

Annex A. Test fuel specifications for the exploratory work and the validation exercise.

APPELATION : gazole type CEC RF 06-03 PMP		Reference of analysis : 9460	
N° of samples : 0	N° of batch : B7277051	Date: 05/06/2007	
COMPLIANCE CERTIFICATE	<input type="checkbox"/>	BULLETIN OF ANALYSIS	<input checked="" type="checkbox"/>
DIESEL FUEL		RESULTS	UNITS
PHYSICAL DATA			METHODS
Density 15 °C	834.9	kg/m3	EN ISO 3675-98
Viscosity 40°C	2.654	cSt	ASTM D 445
DISTILLATION			
IBP	171	°C	ASTM D 86
5 % Vol	196	°C	ASTM D 86
10 % Vol	204	°C	ASTM D 86
20 % Vol	224	°C	ASTM D 86
30 % Vol	242	°C	ASTM D 86
40 % Vol	262	°C	ASTM D 86
50 % Vol	277	°C	ASTM D 86
60 % Vol	291	°C	ASTM D 86
70 % Vol	304	°C	ASTM D 86
80 % Vol	318	°C	ASTM D 86
90 % Vol	334	°C	ASTM D 86
95 % Vol	346	°C	ASTM D 86
FBP	357	°C	ASTM D 86
FBP	357	°C	ASTM D 86
E 250 °C	33.8	%Vol	ASTM D 86
E 350 °C	96.1	%Vol	ASTM D 86
CETANE NUMBER			
Cetane number	53.1	index	ISO 5165-98
Flashpoint	67	°C	EN 22719
COMPOSITION			
Poly-aromatics	5.1	%Mass	IP 391
COLD BEHAVIOUR			
Cold Filter Plugging Point (CFPP)	-17	°C	EN 116, NF M 07042
COMBUSTION			
Lower Calorific Value	46.4	MJ/kg	ASTM D 4868
%C, %H, %O	86.7/13.2:<0.2	%Mass	GC / Calculated
COMPLEMENTARY DATA			
Oxidation stability	2	g/m3	ISO 12205
Copper Strip Corrosion at 50 °C	1	merit	ISO 2160
Sulfur content	7	mg/kg	ISO 4260 / ISO 8754
Conradson Carbon Residue on 10% Dist.Residue	<0.2	%Pds/%mass	ISO 10370
Ash content	<0.001	%Pds/%mass	ISO 6245
Neutralisation Number	<0.02	mg KOH/g	ASTM D 974
Sediment content	6	mg/kg	ASTM D 2276
Fatty Acid Methyl Ester	<0.2	%Mass	
Water content	30	mg/kg	EN ISO 12937
HFRR 60°C	310	µm	ISO/DIS 12156

Annex B: Experimental set up details



Numbers indicate distances in cm and numbers in parenthesis indicate the inner diameter of the tubes in cm

Annex C: Cyclone cut-points (URG-2000-30EP, 91 lpm 2.5 µm)

<i>Flow Rate [lpm]</i>	<i>Cut-Point [µm]</i>
1.0	99.76
3.5	35.84
6.0	23.07
8.5	17.36
11.0	14.06
13.5	11.89
16.0	10.35
18.5	9.19
21.0	8.29
23.5	7.56
26.0	6.96
28.5	6.46
31.0	6.03
33.5	5.66
36.0	5.34
38.5	5.05
41.0	4.80
43.5	4.57
46.0	4.37
48.5	4.18
51.0	4.01

<i>Flow Rate [lpm]</i>	<i>Cut-Point [µm]</i>
51.0	4.01
53.5	3.86
56.0	3.72
58.5	3.59
61.0	3.47
63.5	3.36
66.0	3.25
68.5	3.15
71.0	3.06
73.5	2.98
76.0	2.90
78.5	2.82
81.0	2.75
83.5	2.68
86.0	2.62
88.5	2.56
91.0	2.50
93.5	2.45
96.0	2.39
98.5	2.34
101.0	2.30

*No information was given by the manufacturer regarding the steepness of the curve at specific flowrates.

Annex D: Operation of SPCS

The SPCS units that will be used in the validation exercise are two prototypes (SN 4034719 and 4034720) (Figure D1). These units are different from the prototype that was used in the Light-Duty inter-laboratory exercise (SN 4309947). The particle number counters in the SPCS units are CPCs 3010D (SN 70507004 with flow 1.02 lpm and slope 0.95, SN 70524211 with flow 1.01 lpm and slope 0.99). The CPC 70507004 was initially at the SPCS 4034719. After some modifications the CPC was placed at the SPCS 4034719. All the results presented here and the tests that will be conducted in the future have been and will be conducted with this combination. So:

- SPCS-19: SPCS 4034719 with CPC 3010D 70524211
- SPCS-20: SPCS 4034720 with CPC 3010D 70507004



Figure D1: SPCS units in VELA-5.

The flow schematic of SPCS can be seen in Figure D2. The sample enters a cabinet which is held in constant temperature (set by the user usually at 47°C). Only a small part of the flow is diluted in the primary hot mixer (HD), as the rest is bypass flow. The user sets the temperature of the primary dilution air (usually at 150-200°C). The dilution ratio is calculated from the flow rates. The primary dilution air flow rate is defined by MFC 1 and the sample flow rate is measured upstream of the mixer. A small part of the diluted sample enters the evaporation unit (EU) usually set to a temperature between 300 and 400°C. Then it is diluted in the cold diluter mixer (CD). The dilution ratio is calculated from the flow rates (sample measured upstream of the evaporation unit and dilution air defined from MFC 3).

The aerosol flow rate Q_{s1} is measured by the orifice flow meter. Two flow orifices, CFO-1 and CFO-2, are enclosed in the orifice flow meter. Each orifice in the orifice flow meter covers a range of aerosol sample flow. For example, based on the desired dilution ratio, the sample flow can be calculated from the above equation while the dilution air flow is set at the desired value. If the sample flow rate is falling into the flow range covered by CFO-1, the calibration curve for CFO-1 is used. If the sample flow rate is falling into the flow range covered by CFO-2, the calibration curve for CFO-2 is used. The function for choosing a right orifice has been automated in the control software. Since multiple orifices are enclosed in the orifice flow meter, PND1 provides a wide dilution ratio range.

The measured Q_{s1} with the orifice flow meter is compared to the calculated Q_{s1} from Eq. D1 in real-time. If the difference is outside the pre-set tolerance, the PID loop will change the Q_{s1} by adjusting the make up air at MFC2 to decrease the difference within the pre-set tolerance. For example, increasing the flow rate on MFC2, the flow rate of the sample flow decreases. This way the dilution ratio can be kept constant even when the sample inlet conditions change greatly (for example, pressure, and temperature change during a transient test).

A small fraction of the aerosol from the PND1 moves into the evaporation unit (EU). A temperature controller controls the wall temperature of the EU in the range of 300 to 400°C. While aerosol moves through the EU, volatile particles are vaporized to gas phase. Solid particles in the aerosol flow through the EU without particle losses.

Then, the high temperature aerosol from the EU is diluted by the cold diluter PND2 which is located downstream of the EU. The cold diluter PND2 consists of an orifice flow meter, mass flow controllers MFC3 and MFC4, a mixer (CD), and a critical orifice, etc.

The orifice flow meter is insulated and installed upstream of the evaporation unit. It measures aerosol flow into the PND2 and the evaporation unit. The dilution air temperature on the cold diluter is as same as that in the ambient air. The flow rate of the dilution air is controlled by a mass flow controller, MFC3. As at PND1, the dilution ratio on the PND2 is controlled by adjusting either the dilution air flow from MFC3 or the make up air flow from MFC4. The user sets the dilution air flow at MFC3 to determine the sample flow rate. The SPCS keeps then the dilution ratio constant by adjusting the make up air from MFC4 through the integrated PID loop. For example, for a constant dilution ratio and dilution air flow, if the aerosol flow through the orifice flow meter is increased outside the tolerance limits, the make up air flow from MFC4 will decrease to bring it back within the tolerance limits. As a result, dilution ratios at the PND2 are kept constant. The dilution ratio on the cold diluter (PND2) DR_{PND2} is:

$$DR_{PND2} = \frac{Q_{air2}}{Q_{s2}} + 1 \quad \text{Eq. D2}$$

Where:

Q_{air2} is the dilution air flow rate on the PND2 at 70 °F (21.1 °C) and 760 mmHg

Q_{s2} is the aerosol flow through the orifice flow meter

The total dilution ratio DR on the SPCS is:

$$DR = DR_{PND1} DR_{PND2} \quad \text{Eq. D3}$$

Finally, the aerosol with solid particles moves into the condensation particle counter, TSI CPC 3010D. It measures solid particle number concentration in real-time. The counting efficiencies at different diameters for this counter meet the PMP recommendation.

Software operation

Figure D3 shows the main screen of the unit’s software and the analog input display. Figure D4 explains the flow rate measurement positions. The user sets the Bypass flow, the hot and cold dilution ratios (HD DR, CD DR) and the hot and cold dilution flow rates (HD Dil and CD Dil at MFC 1 and 3 respectively). The main purpose of the Bypass flow is to decrease the residence time; as a result, the diffusion losses in the transfer line and response time of the instrument are reduced. The HD Dil and CD Dil flowrates determine the sample flow rates for the hot and cold diluter respectively. The values of the dilution air (HD Dil and CD Dil) determine the makeup air (HD or CD Mu). Both MFCs for HD and CD Mu are in the range of 0 to 5 lpm. If they are larger than 0 or larger than MFC’s noise such as 0.1 lpm, dilution ratios for PND1 and PND2 should be controllable. However a value close to ~2.5 lpm is recommended.

Note that the flow that SPCS sample flow is named Bypass Q (= Bypass + HD smp). The reference condition for this flow is 70 °F (21.1 °C) and 760 mmHg ambient air pressure. The user must ensure that correct flows are being used to correct the partial flow sampling system.



Figure D3: Main screen of the unit’s software and the analog input display.

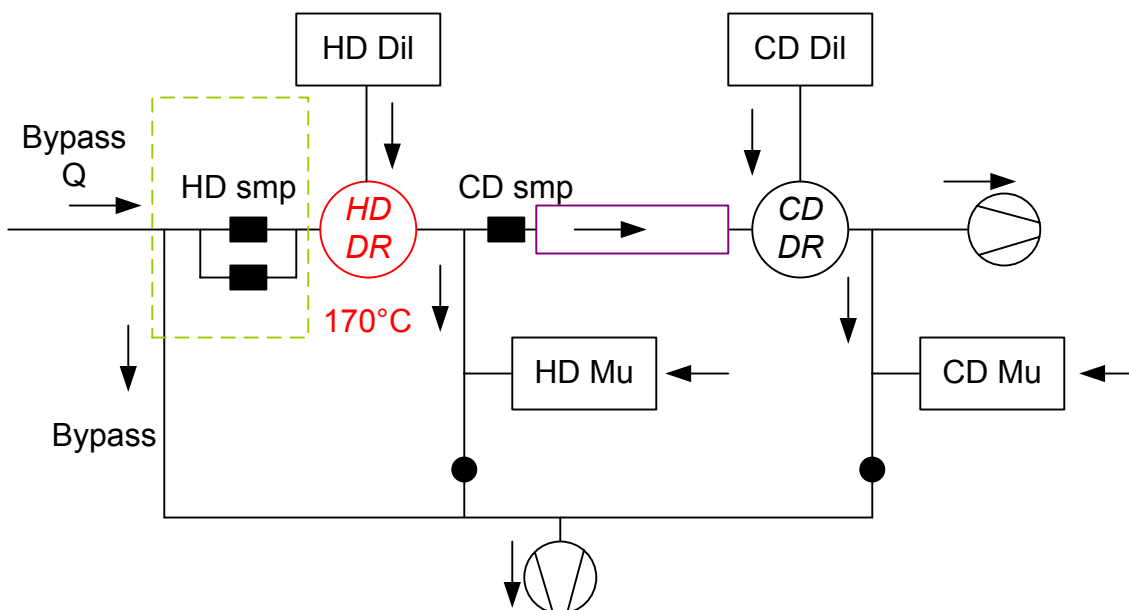


Figure D4: Flow rate measurements. The names correspond to the names used at the software (Figure C2). Note that Q_{air1} is HD Dil, Q_{s1} is HD smp in Eq. D1 and Q_{air2} is CD Dil, Q_{s2} is CD smp in Eq. 2.

Table D1: Typical flows and residence times in the SPCS.

<i>Typical set values are given below</i>		
HD DR [-]	10	10
HD Dil [lpm]	12.5	12.5
Bypass [lpm]	2	2
CD DR	8	15
CD Dil [lpm]	9.5	9.5
<i>Resulting values</i>		
Bypass Q [lpm]	3.4	3.4
HD smp [lpm]	1.4	1.4
HD Mu [lpm]	1.7	2.4
CD smp [lpm]	1.4	0.7
CD Mu [lpm]	2.4	3.1
<i>Estimated residence times</i>		
In the 4 m heated line (47°C) [s]	1.69	1.69
In the cabinet [s]	0.16	0.16
Total to HD [s] (must be <3 s)	1.85	1.85
From HD to ET [s]	0.10	0.19
In the ET [s]	0.09	0.18
To CPC [s] (must be <0.8 s)	0.37	0.37

Figure D5 shows the temperature measurements positions. These temperatures are different than those set by the user at the front panel of the unit, which are:

- Cabinet temperature (before primary dilution): 47°C
- Primary dilution air: 170°C
- Mixer: 170°C (same as primary dilution air)
- Evaporation tube: 350°C

Typical measured temperatures are:

CFO 1 = 50°C

CFO 2 = 50°C

CFO 6 = 55°C

Sample = 40°C

Cabinet = 45°C

HD = 135°C

Mixer = 100°C

EU = 270°C (at the coldest point)

CPC = 30°C

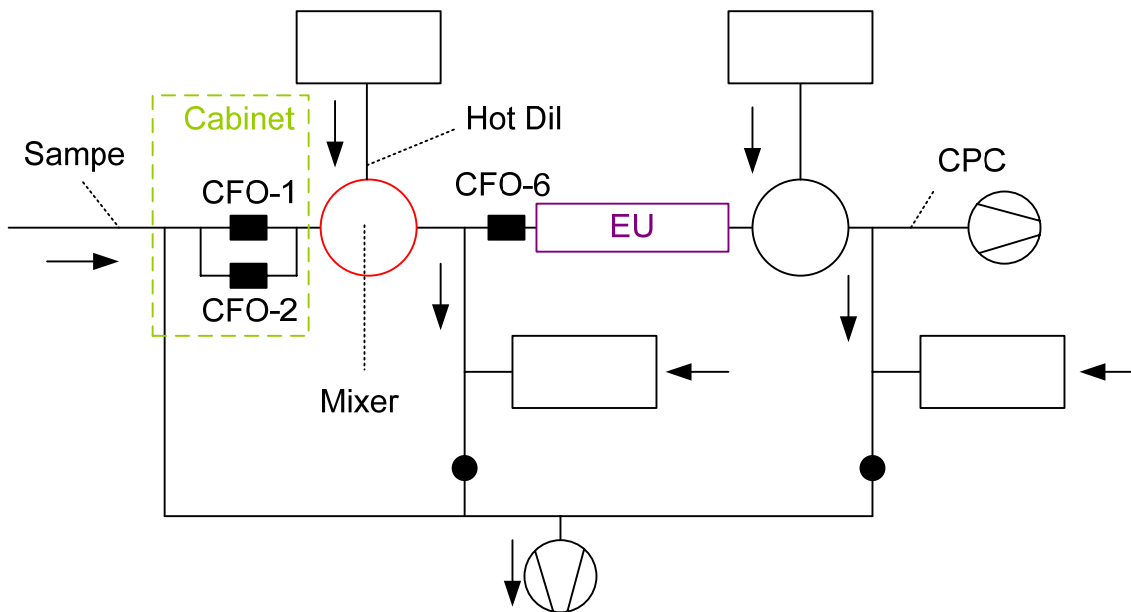


Figure D5: Temperature measurements. The names correspond to the names at the unit's software (Figure D2).

European Commission

EUR 23426 EN – Joint Research Centre – Institute for Environment and Sustainability

Title: Particle Measurement Programme (PMP) Heavy-Duty (HD) Inter-laboratory Exercise: Exploratory work at JRC (Oct 2007 – Feb 2008)

Author(s): B. Giechaskiel, S. Alessandrini, F. Forni, P. Martinez-Lozano, D. Lesueur, M. Carriero, G. Martini

Luxembourg: Office for Official Publications of the European Communities

2008 – 89 pp. – 21 x 29.9 cm

EUR – Scientific and Technical Research series – ISSN 1018-5593

ISBN 978-92-79-09485-9

DOI 10.2788/83175

Abstract

This document reports the results of the exploratory work during the PMP Heavy-Duty inter-laboratory exercise – from Oct. '07 to Feb. '08 - conducted at the Vehicles Emissions Laboratory (VELA-5) in the Transport and Air Quality Unit of the European Commission's Joint Research Centre (JRC, Ispra). This report presents the results of the work undertaken on an IVECO Cursor 8 Heavy-Duty engine equipped with a Continuous Regenerating Trap (CRT), i.e. the Golden Engine. Main objective of these tests were to finalize the measurement protocol that will be used in the validation exercise and the round robin. These tests included background tests, filter media effect, filter face velocity, preconditioning effect, comparisons of different particle number systems, and investigation of the golden instruments.

How to obtain EU publications

Our priced publications are available from EU Bookshop (<http://bookshop.europa.eu>), where you can place an order with the sales agent of your choice.

The Publications Office has a worldwide network of sales agents. You can obtain their contact details by sending a fax to (352) 29 29-42758.

The mission of the JRC is to provide customer-driven scientific and technical support for the conception, development, implementation and monitoring of EU policies. As a service of the European Commission, the JRC functions as a reference centre of science and technology for the Union. Close to the policy-making process, it serves the common interest of the Member States, while being independent of special interests, whether private or national.

LB-NA-23426-EN-C

